Transformations of Mercury in the Marine Water Column

By

Kathleen M. Munson

B. A., Vassar College, 2006

Submitted in partial fulfillment of the requirements for the degree of

Doctor of Philosophy

at the

MASSACHUSETTS INSTITUTE OF TECHNOLOGY

and the

WOODS HOLE OCEANOGRAPHIC INSTITUTION

February 2014

Signature of Author

_____

Joint Program in Oceanography
Massachusetts Institute of Technology
and Woods Hole Oceanographic Institution
10 December 2013

Certified by

_____

Dr. Carl H. Lamborg
Thesis Supervisor

Accepted by

_____

Dr. Elizabeth Kujawinski
Chair, Joint Committee for Chemical Oceanography
Woods Hole Oceanographic Institution

Abstract

Methylation of mercury (Hg) in the marine water column has been hypothesized to serve as the primary source of the bioaccumulating chemical species monomethylmercury (MMHg) to marine food webs. Despite decades of research describing mercury methylation in anoxic sediments by anaerobic bacteria, mechanistic studies of water column methylation are severely limited. These essential studies have faced analytical challenges associated with quantifying femtomolar concentrations of the methylated Hg species dimethylmercury (DMHg) and MMHg in marine systems. In addition, the complex biogeochemical cycling of Hg in natural systems require consideration of gaseous, dissolved, and particulate species of Hg in order to probe potential controls on its ultimate transfer into marine food webs.

The presented work provides a comprehensive study of Hg chemical speciation and transformations in Tropical Pacific waters. We developed an analytical method for MMHg determination from seawater that has the potential to ease measurements of MMHg distributions, as well as mechanistic studies of Hg species transformations.

We used this method, in addition to previously established methods, to measure dissolved and particulate Hg species distributions and fluxes along a transect of the Pacific Ocean. Over significant gradients in oxygen utilization and primary productivity, we observed a region of methylated Hg species focused in the Equatorial Pacific that appeared spatially separated from higher concentrations in North Pacific Intermediate Waters. From the first full water column depth profiles of this region, we also observed the intrusion of elevated Hg into deep waters of the Equatorial and South Pacific Ocean.

In addition we observed substantial potential rates of mercury methylation in subsurface and low oxygen waters along the Pacific transect as well as the Sargasso Sea using Hg isotope tracers. We observed dynamic production and decomposition of methylated Hg in low productivity waters, despite low ambient methylated Hg concentrations. From the addition of bulk organic matter as well as individual compounds important for methylation in anaerobic bacteria, we observe no simple limitation of Hg methylation in marine waters but highly dynamic conversion of Hg between methylated and inorganic species.

Thesis Supervisor: Carl H. Lamborg
Title: Assistant Scientist, Marine Chemistry and Geochemistry, Woods Hole Oceanographic Institution

Dedication

For
Prof. Roger Merritt
Prof. Carolyn Wetzel
Prof. Zachary Donhauser
Dr. Randy Peterson

and
Dr. Carl Lamborg

Table of Contents

List of Figures

List of Tables

Chapter 1
Introduction

Monomethylmercury (MMHg, chemically: CH_3Hg^+) bioaccumulates in marine food webs and has deleterious effects on upper trophic levels of marine life by reducing fertility and offspring survival [Scheuhammer et al, 2007]. In humans, MMHg acts a neurotoxin, capable of crossing both the blood-brain and placental barriers and thereby poses a specific threat to fetuses and children [Clarkson and Magos, 2006]. Due to its toxicity, the Environmental Protection Agency among other health organizations have recommended maximum consumption levels of fish with high MMHg concentrations for children and expectant mothers [US FDA-EPA, 2009]. Despite these guidelines, it is estimated that 0.6-11% of US women ages 16-49 have blood mercury (Hg) levels above the recommended limit for safe exposure [Mahaffey et al, 2004]. Estimates of fish sources suggest that up to 90% of fish consumed in the US are from marine and estuarine environments [Sunderland, 2007]. As a result, understanding the factors that control MMHg sources and transfer in marine environments is crucial for minimizing potential health threats to humans and marine life.

Mercury from Marine Waters to Biota

The need to quantify MMHg sources in natural waters is related to its uptake and transfer through marine trophic levels. Concentrations of dissolved MMHg in the open-ocean water column are typically <0.5 pM [Mason and Fitzgerald, 1990, 1993; Mason et al 1995, 1998; Sunderland et al, 2009; Cossa et al, 2011; Hammerschmidt and Bowman, 2012] but concentrations in fish tissue are in the range from 0.01 to >1000 μg/kg [Senn et al, 2010; Choy et al, 2009; Kraepiel et al, 2003]. Thus, Hg is bioaccumulated to a large degree through marine trophic levels. The most important step in the marine bioaccumulation of MMHg is related to the preferential retention of MMHg by phytoplankton [Mason et al, 1996]. In the example of Hg transfer between diatoms and the copepod grazers, Hg(II) was bound to the membrane of diatoms and is excreted rather than retained during feeding [Mason et al, 1996]. In copepods, the increased hydrophobicity of MMHg relative to Hg(II) that occurs upon the addition of the methyl group resulted in its preferential retention [Mason et al, 1996]. Bioaccumulation factors (BAF) measured in marine phytoplankton suggest that this initial step of trophic transfer is the most substantial, with BAF values of 10^4-10^7 [Baeyens, et al, 2003; Hammerschmidt and Fitzgerald, 2006; Szczebak et al, 2011; Hammerschmidt et al, 2013]. The large magnitude of transfer

between MMHg dissolved in the water column and the base of the marine food chain illustrates the importance of the initial production and partitioning of MMHg between dissolved and particulate pools.

Sources and Sinks of Marine Mercury

Marine cycling of Hg is linked to its behavior in the atmosphere. Mercury is highly volatile and also is found dissolved in water in its gaseous elemental form (Hg°). Emissions from coal burning, concrete production, gold amalgamation, and volcano outgassing are the primary sources of Hg° to the atmosphere [Streets et al, 2011]. Anthropogenic sources dominate the net release of Hg° by a factor of 3 since the beginning of the Industrial Revolution [Lamborg et al, 2002]. Hg° can enter marine systems directly via gas exchange, but is primarily delivered by wet and dry deposition after Hg° is oxidized to Hg(II) in the atmosphere, resulting in significant changes to its sorption properties. Once deposited in the surface ocean, large proportions of Hg are re-emitted to the atmosphere due to reduction of Hg(II) to reform Hg°, extending the residence time of Hg in the atmosphere [Mason et al 1994; Sørensen et al, 2010].

Other potential sources of Hg to the oceans are limited in magnitude. Modeling studies have proposed that riverine contributions of Hg to global oceans are low due to coastal deposition of riverine sediment [Sunderland and Mason, 2007] although warming Arctic rivers are thought to release large amounts of Hg on a basin scale [Fisher et al, 2012]. Submarine groundwater discharge has been identified as a possible source of Hg but is also limited in its spatial scale [Bone et al, 2007]. Hydrothermal sources of Hg are also small compared to atmospheric sources [Lamborg et al, 2006].

The primary sink for Hg from the ocean is evasion to the atmosphere in the surface ocean, which can remove up to 80 % of deposited Hg(II) as a result of photooxidation in the surface ocean via gas exchange [Mason et al, 1994; Sorensen et al, 2010]. For Hg that is not evaded from the surface ocean, sorption, removal on sinking particles, and eventual burial in sediments are the primary sinks.

Mercury that remains in the water column serves as the pool for methylation reactions to produce MMHg. However, the sorption of Hg, either as Hg(II) or MMHg, onto particles decreases the dissolved pool and potentially impacts the production of MMHg, either by removing Hg(II) substrate or by providing a surface for methylation. Once buried, porewater diffusion of Hg is a small flux, into deep waters [Hammerschmidt and Fitzgerald, 2006], although

the measurements of fluxes differ greatly between those measured by benthic flux chambers and those calculated from porewaters [Hammerschmidt and Fitzgerald, 2008] and have not been measured in sediments from the deep ocean.

Marine Mercury Distributions

Distributions of total Hg (THg) reveal the importance of atmospheric deposition as well as particle scavenging of Hg in the water column. Concentrations of THg are measurable in the surface ocean, generally < 1 pM in the Pacific [Laurier et al, 2004; Sunderland et al, 2009; Cossa et al, 2011; Hammerschmidt and Bowman, 2012], although substantially higher concentrations have been measured in the Atlantic [Mason et al, 1995; Mason and Sullivan, 1999]. Concentrations of THg generally increase with depth due to particle scavenging and release upon remineralization [Hammerschmidt and Bowman, 2012]. Deep waters, below 2000 m, often show substantial concentrations of THg that have been attributed to transport of THg via thermohaline circulation [Hammerschmidt and Bowman 2012].

Methylated Hg species, MMHg and DMHg, were first measured in the open ocean in 1990 [Mason and Fitzgerald, 1990, 1993]. However, high limits of detection (~50 fM) prevented MMHg determination in ~70% of water samples analyzed in this early study [Mason and Fitzgerald, 1993]. Similar high detection limits hindered full Hg speciation determination in early measurements in the Mediterranean and North Atlantic [Cossa et al, 1997; Mason et al, 1998].

Despite the analytical challenges associated with MMHg determination, marine distributions of MMHg, either as a distinct species or in combination with DMHg, are found to be low in marine surface waters and elevated at depths of low dissolved oxygen concentrations in the water column [Mason and Fitzgerald 1990, 1993; Mason and Sullivan, 1999; Cossa et al, 2009; Sunderland et al, 2009; Cossa et al, 2011; Hammerschmidt and Bowman, 2012]. These concentrations have been compared to rates of apparent oxygen utilization (AOU) in the water column, resulting in varied relationships between the two parameters [Mason and Sullivan, 1999; Sunderland et al, 2009; Cossa et al, 2011]. From these relationships a relatively simple model of Hg methylation has emerged. Hg methylation is thought to occur within the marine water column after the release of Hg(II) substrate from remineralized organic matter. This has been illustrated most clearly by the linear correlation between methylated Hg concentrations and organic carbon remineralization rate [Sunderand et al, 2009]. However, the mechanistic pathways of in situ methylation in marine environments have not been well characterized.

From a combination of limited DMHg and MMHg distribution data and supporting laboratory experiments, Mason et al, proposed that marine MMHg is produced from the breakdown of DMHg [Mason and Fitzgerald, 1993]. More recently, direct production of MMHg from Hg(II) has been proposed as a significant source of MMHg in Arctic waters [Lehnherr et al, 2011]. However, because many studies have not distinguished between the two organomercuric species, it is difficult to determine potential controls on the interconversion between DMHg and MMHg that results in MMHg availability for uptake through marine trophic webs.

The need for lower detection limits has been recognized as a significant hindrance to understanding MMHg production and breakdown in marine waters [Fitzgerald et al, 2007]. The recent development of a direct ethylation method for MMHg determination at sea [Bowman and Hammerschmidt, 2011] has improved the detection limit to ~5 fM but is not adaptable for preserving samples for shore-based analysis. Although methods with low femtomolar detection limits exist, including isotope dilution inductively coupled plasma mass spectrometry (ID-ICPMS) and cold vapor atomic fluorescence spectrometry (CVAFS), they have relied on tedious separation techniques such as organic extraction [Bloom, 1989; Horvat et al, 1993] or distillation [Horvat et al, 1993] to isolate MMHg from the seawater matrix, hindering MMHg species distribution data. In addition, the preservation of samples with acid for shore-based laboratory analysis result in the breakdown of DMHg to MMHg, yields combined methylated Hg ([DMHg] + [MMHg]) concentrations [Parker and Bloom, 2007] that hinder the mechanistic understanding of MMHg production.

Marine Mercury Methylation

Despite the importance of marine Hg cycling to resulting MMHg concentrations in marine fish and implications for human health, our mechanistic understanding of the biological and abiotic factors that might contribute to MMHg production are based on substantial work in coastal and freshwater systems. Theses studies have identified several potential targets for studies of marine MMHg production, but few established connections between anaerobic bacterial methylation and in situ methylation in marine waters.

Sulfate-reducing bacteria (SRB) were identified as Hg methylators in sediments in the 1980s [Choi et al, 1984a,b]. Subsequent work based on cultured organisms of SRB and iron-reducing bacteria, especially *Desulfovibrio* and *Geobacter* species have provided much of the current knowledge of Hg methylation. Long suspected of involving a reaction by

methylcobalamin (vitamin b12) in the acetyl-CoA pathway [Choi et al,1984b; Ekstrom and Morel, 2008], methylation in a variety of delta-proteobacteria, methanogens, and firmicutes has recently been attributed to the presence of two genes, *hgcA* and *hgcB* encoding a cobalamin-utilizing methyltransferase upstream of a ferrodoxin protein [Parks et al, 2013, Gilmour et al, 2013].

In addition, culture-based experiments have provided insight into mechanisms of cellular uptake of Hg(II) substrate for methylation by anaerobes, including the role of low molecular weight thiol ligands such as the amino acid cysteine and glutathione [Schaefer and Morel, 2009; Schaefer et al, 2011]. These experiments have revealed a role of active Hg(II) uptake by methylating bacteria, possibly via low-specificity metal uptake pathways [Schaefer et al, 2011].

MMHg production is also possible through abiotic mechanisms. Methylcobalamin, methyltin, and methyliodide are known to methylate Hg(II) in the absence of cells by the donation of their methyl groups [Maynard, 1932; Filippeli and Baldi, 1993]. Although laboratory-based and theoretical studies have suggested abiotic methyaltion pathways may be significant sources of MMHg in marine waters [Celo et al, 2006; Jimenez-Moreno et al, 2013], no field-based experiments have quantified their relative importance.

Isotope Tracers of Mercury Transformations

The seven stable isotopes of Hg (Table 1) provide a means of tracing Hg chemical species transformations in natural systems. Such experiments fall into two broad categories:

1. Measurements of mass dependent and mass independent Hg fractionation attributed to specific Hg species transformation, such as reduction, methylation, or ligand binding that are first characterized in controlled experiments and are then used to identify transformations from environmental samples [reviewed by Kritee et al, 2013].
2. Tracer addition experiments in which one or more well-characterized isotopically enriched Hg species are added to incubations of water or sediment and transformation reactions are quantified from changes in the isotopic ratio of a species of interest [Hintelmann et al, 1995; Hintelmann and Evans, 1997; Hintelmann and Ogrinc, 2003]

Stable Hg isotope signatures have been used to trace mechanisms of Hg transformations as a result of fractionation, both mass dependent fractionation and mass independent fractionation, that occur as a result of small differences in mass among Hg isotopes. Laboratory studies have been performed to measure fractionation during many abiotic and biotic Hg transformations, including photoreduction, photodemethylation, methylation by SRB, abiotic methylation and microbial reduction [Kritee et al, 2013]. However, these studies rely on well-characterized mechanisms that can be controlled in laboratory conditions to measure changes less than 5 per mil between isotopes.

Thus far, mass independent fractionation has been found to occur only during photodemethylation and photoreduction [Bergquist and Blum, 2007], which results in unique isotopic signatures of the odd isotopes, ^{199}Hg and ^{201}Hg. Mass dependent fractionation has been measured in microbial mediated methylation, demethylation, and reduction reactions [Kritee et al, 2007, 2008, 2009; Rodriguez-Gonzalez, 2009]. Fractionation has also been measured in abiotic transformations of Hg, including methylation by methylcobalamin at low pH [Jimenez-Martinez et al, 2013] and binding to ligands [Weiderhold, et al, 2010].

Blum et al, 2013 recently measured the isotopic composition of fish Hg from fish thought to feed at different depths in the water column. Measured δ^{202}Hg and Δ^{201}Hg values increased with feeding depth in nine fish tested [Blum et al, 2013]. The decreasing values of Δ^{201}Hg were interpreted to represent the uptake of less photochemically processed MMHg with increasing feeding depth in the ocean. The decreasing values of δ^{202}Hg were interpreted to represent a largely microbial process for methylation. Combined, these isotope signatures align with enhanced methylation of Hg by microbes at depth of net organic matter remineralization [Mason and Fitzgerald, 1993; Sunderland et al, 2009]. The use of isotope signatures to trace sources of Hg within food webs is intriguing. However, as Blum et al, 2013 note, the experimental values used to interpret the measured isotopic compositions have not been determined from marine systems. Furthermore, recent work has measured a similar extend of fractionation in abiotic Hg methylation by methylcobalamin as is seen in methylation by SRB [Jiminez-Martinez et al, 2013]. Therefore, measured stable isotope signatures of Hg from marine systems, either Hg species in the water column or in marine biota, cannot be fully interpreted until the fractionation factor associated with different marine mechanisms can be measured individually.

Isotope tracer studies allow quantification of Hg species transformations without the prior identification of the mechanisms involved. However, because they rely on the addition of

isotopically enriched spikes of Hg species, isotope tracer studies can only be used to quantify the potential for a transformation to take place in the tested system, typically seawater or sediment. These experiments rely on the assumption that additions of Hg species produce responses that mimic those that occur in situ, but this assumption is subject to scrutiny. For example, in the potential methylation rate measurements presented in this work, we investigated whether delivery of Hg(II) by organic matter remineralization is the primary limitation of Hg methylation. Since additions of isotoptically enriched Hg(II) are necessary to measure methylation rates in these dual tracer experiments, relief of Hg(II) limitation is implicit in all our presented measurements.

Tracer experiments quantify Hg species conversions by monitoring the isotopic changes of a single Hg species over the course of an incubation period. Such quantification hinges on the ability to accurately distinguish between Hg species. Mass balance of Hg species is not typically measured during these experiments and yields of MMHg are determined relative to internal standard recovery [Hintelmann and Evans, 1997]. The use of isotope tracer experiments therefore depends on the selection of appropriate experimental conditions to probe mechanisms of Hg transformations.

The work presented in the following chapters aimed to fill a variety of gaps in our knowledge of mercury biogeochemistry in marine systems. Our approach was to improve MMHg measurement techniques in order to allow for better coverage of Hg distributions in marine systems, use these techniques to analyze spatial and temporal variations in Hg species distributions, and determine which environmental factors control MMHg production in the open ocean water column by dual isotope tracer experiments testing potential limitations of methylation in marine waters. Together, our results provide important progress in determining both spatial variations in MMHg distributions as well as potential controls on their distributions.

Chapter 2 details a method for measurement of MMHg from small volumes of seawater. This method is adaptable to shipboard measurements as well shore-based determination of MMHg from preserved samples. When combined with purging of samples to remove DMHg from the sample volume, this method allows for easy distinction between these two Hg chemical species in open ocean environments. The method is also adaptable to hyphenated analysis, such as CVAFS-ICPMS methods for isotope tracer experiments presented in Chapters 3 and 5.

Chapter 3 presents potential methylation and demethylation rate measurements from the water colum of the Bermuda Atlantic Time Series (BATS) site in the Sargasso Sea. During two

cruises, we measured methylation and demethylation potential in oligotrophic waters from chlorophyll maximum and oxygen minimum depths. In our evaluation of measurements of transformations of isotopically enriched Hg species over the course of incubations, we discuss the relative importance of methylation and demethylation and the implied role of bacteria in water column methylation at this site.

Chapter 4 presents distributions of dissolved and particulate Hg between 17°N and 15°S in the Central Pacific Ocean along a transect of strong gradients in oxygen concentrations and utilization. In addition to providing information on potential sources and sinks of MMHg in these waters, the distribution data provide insight into the relative importance of spatial and temporal trends when viewed relative to the body open ocean Hg data currently available.

Chapter 5 presents Hg methylation potentials measured in waters collected from a subset of stations occupied for the speciation measurements shown in Chapter 4. In addition to methylation potentials in unamended waters, we also measured changes in methylation promoted by addition of organic matter. In measurements of methylation in both filtered and unfiltered water, we observe dynamic transformations between Hg(II) substrate and methylated Hg. The experiments described in this chapter are modeled after limitation measurements and are the first attempts to determine the controls on mercury methylation in the marine water column.

Appendix I provides explicit details of the analytical set up, data analysis, and example calculations for the linear matrix approach used in dual tracer CVAFS-ICPMS measurements of MMHg presented in Chapters 3 and 5.

References

Baeyens, W., M. Leermakers, T. Papina, A. Saprykin, N. Brion, J. Noyen, M. De Gieter, M. Elskens, and L. Goeyens (2003) Bioconcentraion and biomagnifications of mercury and methylmercury in North Sea and Scheldt Estuary fish. Arch. Environ. Contam. Toxicol. 45, 498-508.

Bergquist, B. A., and J. D. Blum (2007) Mass-dependent and mass-independent fractionation of Hg isotopes by photo-reduction in aquatic systems. Science, 318, 417-420.

Bloom, N. 1989 Determination of picogram levels of methylmercury by aqueous phase ethylation, followed by cryogenic gas chromatography with cold vapour atomic fluorescence detection. Can. J. Fish. Aquat. Sci., 46, 1131-1140.

Blum, J. D., B. N. Popp, J. C. Drazen, C. A. Choy, and M. W. Johnson (2013) Methylmercury production below the mixed layer in the North Pacific Ocean. Nat. Geosci., 6, 879-884.

Bone, S. E., M. A. Charette, C. H. Lamborg, and M. E. Gonneea (2007) Has submarine groundwater discharge been overlooked as a source of mercury to coastal waters? Environ. Sci. Technol., 41, 3090-3095.

Bowman, K. L., and C. R. Hammerschmidt (2011) Extraction of monomethylmercury from seawater for low-femtomolar determination. Limnol. Oceanogr. Methods 9:121-128.

Celo, V., D. R. S. Lean, S. L. Scott (2006) Abiotic methylation of mercury in the aquatic environment. Sci Tot. Environ., 328, 126-137.

Choi, S.-C., T. Chase Jr., R. Bartha (1994) Enzymatic catalysis of mercury methylation by Desulfovibrio desulfuricans LS, Appl. Environ. Microbiol. 60, 1432-1436.

Choi, S.-C., T. Chase Jr., R. Bartha (1994) Metabolic pathways leading to mercury methylation in Desulfovibrio desulfuricans LS Appl. Environ. Microbiol. 60, 4072-4077.

Choy, C. A., B. N. Bopp, J. J. Kenko, J. C. Drazen (2009) THe influence of depth on mercury levels in pelagic fishes and their prey. Proc. Natl. Acad. Sci. USA 106, 13865-13869.

Clarkson, T. W., and J. Magos (2006) The toxicology of mercury and its chemical compounds. Crit. Rev. Toxicol. 36, 609-662.

Cossa, D., B. Averty, N. Pirrone (2009) The origin of methylmercury in open Mediterranean waters. Limnol. Oceanogr. 54, 837-844.

Cossa, D., J.-M. Martin, K. Takayanagi, J. Sanjuan (1997) The distribution and cycling of mercury species in the western Mediterranean. Deep-Sea Res. II 44, 721-740.

Cossa, D., L. E. Heimburger, D. Lannuzel, R. S. Rintoul, E. C. V. Bulter, A. R. Bowie, B. Averty, R. J. Watson, and T. Remenyi (2011) Mercury in the Southern Ocean. Geochim. Cosmochim. Acta 75, 4037-4052.

Ekstrom, E. B., and F. M. M. Morel (2008) Cobalt limitation of growth and mercury methylation in sulfate-reducing bacteria. Environ. Sci. Technol. 42, 93-99.

Fisher, J. A., D. J. Jacob, A. L. Soerensen, A. L. Amos, A. Steffen, and E. M. Sunderland (2012) Riverine sources of Arctic Ocean mercury inferred from atmospheric observations. Nat. Geosci., 5, 499-504.

Fitzgerald, W. F., C. H. Lamborg, C. R. Hammerschmidt (2007) Marine biogeochemical cycling of mercury, Chem. Rev., 107, 641-662.

Filippelli, M., and F. Baldi (1993) Alkylation of ionic mercury to methylmercury and dimethylmercury by methylcobalamin: simultaneous determination by purge-and-trap GC in line with FTIR. Appl Organomet. Chem. 7, 487-493.

Hammerschmidt, C. R., and K. L. Bowman (2012) Vertical methylmercury distribution in the subtropical North Pacific Ocean. Mar. Chem., 132-133, 77-82.

Hammerschmidt, C. R., M. B. Finiguerra, R. L. Weller, and W. F. Fitzgerald (2013) Methylmercury accumulation in plankton on the continental margin of the Northwest Atlantic Ocean, Environ. Sci. Technol., 47, 3671-3677.

Hammerschmidt, C. R., and W. F. Fitzgerald (2006) Bioaccumulation and trophic transfer of methylmercury in Long Island Sound. Arch. Environ. Contam. Toxicol. 51, 416-424.

Hammerschmidt, C. R., and W. F. Fitzgerald (2006b) Methylmercury cyling in sediments on the continental shelf of southern New England. Geochim. Cosmochim. Acta 70, 918-930.

Hammerschmidt, C. R., and W. F. Fitzgerald (2008) Sediment-water exchange of methylmercury determined from shipboard benthic flux chambers. Mar. Chem. 109, 86-97.

Hintelmann, H., R. D. Evans, and J. Y. Villeneuve (1995) Measurement of mercury methylation in sediments by using enriched stable mercury isotopes combined with methylmercury determineaiton by gas chromatography-inductively coupled plasma mass spectrometry, J. Anal. Atom. Spectrom., 10, 619-624.

Hintelmann, H., and R. D. Evans (1997) Application of stable isotopes in environmental tracer studies – measurement of monomethylmercury (CH_3Hg^+) by isotope dilution ICP-MS and detection of species transformation, Fresenius J. Anal. Chem., 358, 378-385.

Hintelmann, H., and N. Ogrinc (2003) Determination of stable mercury isotopes by ICP/MS and their application in environmental studies, in Biogeochemistry of environmentally important trace elements, Eds: Cai, Y., and C. O. Braids, ACS Symp Ser Vol. 835, Washington, DC, p. 321-338.

Horvat, M., L. Liang, and N. S. Bloom (1993) Comparison of distillation with other current isolation methods for the determination of methyl mercury compounds in low level environmental samples Part II. Water. Anal. Chimica Acta 282, 153-168.

Jiménez-Moreno, M., V. Perrot, V. N. Epov, M. Monperrus, and D. Amouroux (2013) Chemical kinetic isotope fractionation of mercury during abiotic methylation of Hg(II) by methylcobalamin in aqueous chloride media. Chem. Geol. 336, 26-36.

Kraepiel, A. M. L., K. Keller, H. B. Chin, E. G. Malcolm, F. M. M. Morel (2003) Sources and variations of mercury in tuna. Environ. Sci. Technol., 37, 5551-5558.

Kritee, K., J. D. Blum, J. R. Reinfelder, T. Barkay (2013) Microbial stable isotope fractionation of mercury: a synthesis of present understanding and future directions. Chem. Geol., 336, 13-25.

Lamborg, C. H., W. F. Fitzgerald, J. O'Donnell, T. Torgersen (2002) An examination of global-scale mercury biogeochemistry using a non-steady state compartment model which features interhemispheric gradients in the atmosphere as constraints. Geochim. Cosmochim. Acta 66, 1105-1118.

Lamborg, C. H., K. L. Von Damm, W. F. Fitzgerald, C. R. Hammerschmidt, and R. Zierenberg (2006) Mercury and monomethylmercury in fluids from Sea Cliff submarine hydrothermal field, Gorda Ridge. Geophys. Res. Lett., 33, L17606.

Laurier, F. J. G., R. P. Mason, G. A. Gill, and L. Whalin (2004) Mercury distributions in the North Pacific Ocean—20 years of observations. Mar. Chem., 90, 3-19.

Lehnherr, I., V. L. St Louis, H. Hintelmann, and J. L. Kirk (2011) Methylation of inorganic mercury in polar marine waters. Nat. Geosci. 4, 298-302.

Mahaffey, K. R., R. P. Clickner, C. C. Bodurow (2004) Blood organic mercury and dietary mercury intake: National Health and Nutrition Examination Survey, 1999 and 2000. Environ. Health Perspec. 112, 562-570.

Mason, R. P., and W. F. Fitzgerald (1990) Alkylmercury species in the equatorial Pacific. Nature 347, 457-459.

Mason, R. P., and W. F. Fitzgerald (1993) The distribution and cycling of mercury in the equatorial Pacific Ocean. Deep Sea Res. Part I 40, 1897-1924.

Mason, R. P., J. R. Reinfelder, F. M. M. Morel (1996) Uptake, toxicity, and trophic transfer of mercury in a coastal diatom. Environ. Sci. Technol., 30, 1835-1845.

Mason, R. P., W. F. Fitzgerald, F. M. M. Morel (1994) The biogeochemical cycling of elemental mercury—anthropogenic influences. Geochim. Cosmochim. Acta 58, 3191-3198.

Mason, R. P., K. R. Rolfhus, W. F. Fitzgerald (1995) Methylated and elemental mercury cycling in surface and deep ocean waters of the North Atlantic. Water Air Soil Pollut. 80, 665-677.

Mason, R. P., K. R. Rolfhus, W. F. Fitzgerald (1998) Mercury in the North Atlantic. Mar. Chem. 61, 37-53.

Mason, R. P., K. A. Sullivan (1999) The distribution and speciation of mercury in the south and equatorial Atlantic. Deep Sea Res II, 46, 937-956.

Maynard, J. L. (1932) The action of mercury on organic iodides I: the formation of methylmercury iodide and benzylmercuric iodide. J. Am. Chem. Soc., 54: 2108-2112.

Monperrus, M., E. Tessier, D. Amouroux, A. Laynaert, P. Huonnic, O. F. X. Donard (2007) Mercury methylation, demethylation and reduction rates in coastal and marine surface waters of the Mediterranean Sea. Mar. Chem. 107, 49-63.

Parker, J. L., and N. S. Bloom (2007) Preservation and storage techniques for low-level aqueous mercury speciation. Sci. Tot. Environ., 337, 253-263.

Rodriguez-Gonzalez, P., V. N. Epov, R. Bridou, E. Tessier, R. Guyoneaud, M. Monperrus, and D. Amouroux (2009) Species-specific stable isotope fractionation of mercury during Hg(II)

methylation by an anaerobic bacteria (Desulfobulbus propionicus) under dark conditions. Environ. Sci. Technol., 43, 9183-9188.

Schaefer, J. K., and F. M. M. Morel (2009) High methylation rates of mercury bound to cysteine by Geobacter sulfurrducens Nat. Geosci. 2, 123-126.

Schaefer, J. K., S. S. Rocks, W. Zheng, L. Liang, B. Gu, and F. M. M. Morel (2011) Active transport, substrate specificity, and methylation of Hg(II) in anaerobic bacteria. Proc. Natl. Acad. Sci., 108, 8714-8719.

Scheuhammer, A. M., M. W. Meyer, M. B. Sandheinrich, M. W. Murray (2007) Effects of environmental methylmercury on the health of wild birds, mammals and fish. Amibo. 36, 12-18.

Senn, D. B., E. J. Chesney, J. D. Blum, M. S. Bank, A. Maage, J. P. Shine (2010) Stable isotope (N, C, Hg) study of methylmercury sources and trophic transfer in the northern Gulf of Mexico. Environ. Sci. Technol., 44, 1630-1637.

Sørensen, A. L., D. J. Jacob, D. G. Streets, M. L. I. Witt, R. Ebinghaus, R. P. Mason, M. Andersson, and E. M. Sunderland (2012) Multi-decadal decline of mercury in the North Atlantic atmosphere explained by changing subsurface seawater concentrations. Geophys. Res. Letts. 39, L21810.

Sørensen, A. L., E. M. Sunderland, C. D. Holmes, D. J. Jacob, R. M. Yantosca, H. Skov, J. H. Christensen, S. A. Strode, and R. P. Mason (2010) An improved global model for air-sea exchange of mercury: high concentrations over the North Atlantic. Environ. Sci. Technol. 44, 8574-8580.

Streets, D. G., M. K. Devane, Z. Lu, T. C. Bond, E. M. Sunderland, and D. J. Jacob (2011) All-time releases of mercury to the atmosphere from human activities. Environ. Sci. Technol. 54, 10485-10491.

Sunderland, E. M. (2007) Mercury exposure from domestic and imported estuarine and marine fish in the US seafood market. Environ. Health Perspec. 115, 235-242.

Sunderland, E. M., and R. P. Mason (2007) Human impacts on open ocean mercury concentrations, Global Biogeochem. Cy., 4, GB4002.

Sunderland, E. M., D. P. Krabbenhoft, J. W. Moreau, S. A. Strode, and W. M. Landing (2009) Mercury sources, distribution, and bioavailability in the North Pacific Ocean: insights from data and models. Gobal Biogeochem. Cy., 23, GB2010.

Szczebak, J. T., and D. L. Taylor (2011) Ontogenic patters in bluefish (Pomatomus sultatrix) feeding ecology and the effect on mercury biomagnifications. Environ. Toxicol. Chem., 30, 1447-1458.

United States Food and Drug Administration and Environmental Protection Agency (2009) What you need to know about mercury in fish and shellfish: advice for woman who might become pregnant, women who are pregnant, nursing mothers, young children. [Brochure].

Weiderhold, J. G., C. J. Cramer, K. Daniel, I. Ifante, B. Bourdon, and R. Kretzchmar (2010) Equilibrium mercury isotope fractionation between dissolved Hg(II) species and thiol-bound Hg. Environ. Sci. Technol., 44, 4191-4197.

Tables and Table Legends

Table 1: Mercury stable isotopes and their natural abundances

Isotope	Abundance (%)
^{196}Hg	0.15
^{198}Hg	9.97
^{199}Hg	16.87
^{200}Hg	23.10
^{201}Hg	13.18
^{202}Hg	29.86
^{204}Hg	6.87

Chapter 2
Determination of monomethylmercury from seawater with ascorbic acid-assisted direct ethylation

Kathleen M. Munson[1], Diana Babi[2], and Carl H. Lamborg[1]

[1]Marine Chemistry and Geochemistry Department, Woods Hole Oceanographic Institution, Woods Hole, Massachusetts, 02543.
[2]Tekran Instruments Corporation, 330 Nantucket Boulevard, Toronto, Ontario, M1P 2P4, Canada.

In revision for publication in *Limnology and Oceanography: Methods*

Abstract

We developed a technique to measure monomethylmercury (MMHg) concentrations from small volumes (180-mL) of seawater at low femtomolar concentrations using direct ethylation derivitization, decreasing the required volume by 90% from current methods while maintaining a <20 fM detection limit. In this method, addition of ascorbic acid prior to the derivitization of MMHg allows for full recovery of MMHg from the seawater matrix without the need for sample distillation or extraction. The small sample size and relative ease of detection is ideal both for shipboard as well as shore-based measurements of preserved MMHg samples. Combined with shipboard determination of dimethylmercury (DMHg) and elemental mercury (Hg(0)), this method can be used to determine full mercury speciation.

Introduction

Mercury (Hg) is a toxic metal with an organic monomethylmercury (MMHg) chemical form that bioaccumulates in aquatic food webs. At sufficiently high concentrations, MMHg toxicity can cause decreased fertility and offspring survival in the upper trophic levels of terrestrial and marine systems [Scheuhammer et al, 2007]. In humans, MMHg acts as a neurotoxin and can cause developmental defects to fetuses and small children [Clarkson and Magos, 2006]. Due to the importance of marine protein sources in human diets, efforts to improve our understanding of the production and distribution of MMHg in open-ocean systems have increased in recent decades. However, until recently, descriptions of Hg cycling in marine systems have relied heavily on studies of coastal and sedimentary systems, in which higher MMHg concentrations are more easily measured.

Determination of monomethylmercury concentrations is analytically challenging due to its femtamolar concentrations in much of the open ocean [Cossa et al, 2011; Hammerschmidt and Bowman, 2012; Mason and Fitzgerald, 1993; Sunderland et al, 2009]. Analytical methods, based on ethylation, to quantify MMHg, including the US EPA Standard Method 1630, require separation of MMHg from its environmental matrix. Either solvent extraction {Bloom 1989; Horvat et al, 1993] or distillation [Horvat et al, 1993] methods are commonly used to isolate MMHg for analysis. Following separation, MMHg is volatilized through derivitizaton, most commonly by addition of the ethylating agent sodium tetraethylborate (NaTEB) to form gaseous methylethylHg. Preconcentration of gaseous methylethylHg is achieved through trapping onto a Carbotrap [Bloom, 1989] or Tenax [Bowman and Hammerschmidt, 2011] column before analysis by GC separation of the methylethylHg and gaseous diethylmercury produced from Hg(II) substrate in solution. Once preconcentrated, sub-pM concentrations of MMHg can be quantified by atomic fluorescence spectrometry (AFS) or isotope dilution inductively-coupled plasma mass spectrometry (ID-ICPMS).

Initial attempts to avoid either MMHg distillation or extraction steps by direct ethylation of MMHg with NaTEB were inefficient, recovering 5-60% of added MMHg [Horvat et al 1993]. However, a method has recently been developed to detect MMHg from direct ethylation of 2-L volumes of seawater [Bowman and Hammerschmidt, 2011]. This method is advantageous for two reasons. First, it requires a minimal amount of sample processing compared to MMHg distillation or extraction, which makes the technique amenable for ship-based analyses. Second, the method allows for quantification of both dissolved MMHg and the gaseous dimethylmercury (DMHg)

organomercuric chemical species in seawater. The 2-L sample bottles can be purged with nitrogen (N_2) gas to measure DMHg concentrations in seawater prior to acidification and ethylation to volatilize MMHg. However, the 2-L sample volume can hinder shore-based analysis due to difficulties in sample transport and storage for high-resolution depth profiles. In addition, the efficiency of direct ethylation from seawater is variable, requiring careful consideration of appropriate standards for MMHg quantification [Bowman and Hammerschmidt, 2011].

Prior to the development of the direct ethylation method, preservation of samples with acid for shore-based MMHg determination using distillation or extraction methods prevented separate determination of DMHg and MMHg since DMHg decomposes to MMHg within a matter of hours in acidic conditions [Parker and Bloom, 2007]. As a result, profiles of acid-preserved samples cannot distinguish between the DMHg and MMHg organomercuric forms in their analyses and instead represent a combined ([DMHg + MMHg]) concentration [e.g., Sunderland et al, 2009].

Direct volatilization is also possible via hydride generation of mercury hydrides via the addition of sodium tetrahydridoborate (sodium borohydride) followed by collection on a cold-trap before analysis using AFS [Cossa et al, 2009]. Like other methods, hydride generation requires application at sea to distinguish between DMHg and MMHg. Otherwise, quantification of acid-preserved samples yields combined ([DMHg] + [MMHg]) concentrations. However, liquid N_2 is required to analyze the volatile mercury hydride compound. In addition, like the 2-L direct ethylation method, the mercury hydride method cannot be easily automated or adapted to in-line analysis for isotopic studies.

In order to address the limitations of current methods, we developed a method that improves the recently described direct ethylation method while simultaneously allowing for sample preservation. Ascorbic acid addition has been found to improve MMHg detection from distilled samples using US EPA Method 1630 [Tekran Instruments Corporation, 2011]. We therefore adapted the use of ascorbic acid to improve the low ethylation efficiency of MMHg from seawater samples observed using the direct ethylation method [Bowman and Hammerschmidt, 2011]. The method can be coupled with acidification and purging prior to MMHg derivatization to collect and quantify volatile DMHg as a distinct species [Lamborg et al., 2012].

Materials and Procedures

Plastic and Glassware

All plastic and glass bottles, tubing, and filter holders for water collection, reagents, and sample preparation were acid-washed in a class 100 clean room according to described protocols [Hammerschmidt et al., 2011]. Pre-filters for water filtration were combusted prior to use. Capsule filters were filled with 10% HCl, soaked for 24 hours, and rinsed with de-ionized water (>18 MΩ-cm; "MQ") until the rinse water pH was >6.

Either 42-mL amber glass vials (I-CHEM™, Fisher) or 250-mL amber glass bottles (I-CHEM™, Fisher) were used for MMHg analysis from 30-mL or 180-mL sample volumes, respectively. The sample volumes were chosen to maximize the MMHg signal detected from the purged sample while maintaining adequate headspace for appropriate positioning of the instrument's dual sample purge and analyte inlet needle (see below) above the height of the liquid. New Teflon backed septa (SunChem™) were soaked in Citranox™ (1%) overnight and 10% HCl for >24 hours, then rinsed with MQ prior to use. Previously pierced septa were reused after soaking in Citranox™ (1%) overnight and up to 6 days in 10% HCl and rinsed with MQ prior to use.

Seawater

Seawater used for method development was collected from the Equatorial Pacific Ocean in October 2011 on board the R/V Kilo Moana and from Vineyard Sound in Woods Hole, MA intermittently between November 2011 and March 2012. Open-ocean seawater was collected in acid-rinsed X-Niskin bottles on a dedicated trace-metal clean rosette deployed on Amsteel line. Seawater was filtered (47mm, Supor polycarbonate membrane, 0.2-μm pore size, Pall Corporation) from X-Niskin bottles that were pressurized with ultra high purity N_2 in a positive pressure, HEPA-filtered bubble constructed onboard the ship. Water was decanted into acid-clean 10-L polyethylene carboys and stored at room temperature until use. Vineyard Sound coastal seawater was collected in acid cleaned 2-L Teflon bottles mounted on a pole sampler from the shore at the Quissett Campus of the Woods Hole Oceanographic Institution. Water was filtered with a GF/A pre-filter (42-mm Whatman) and a 0.2-μm Sterivex-GV™ (Millipore) filter.

Monomethylmercury Determination

MMHg was determined by CVAFS gas chromatography with a Tekran 2700 Automated Methyl Mercury Analysis System (Tekran, Ontario, Canada). The system is designed to determine MMHg from 30-mL samples of freshwater. Samples are analyzed using an autosampler that features a septa-piercing needle equipped with a purge gas outlet and a sample inlet. After piercing the septum, Ar flow through the tip of the needle purges the sample and allows the loading of gaseous methylethylHg through the sample inlet until the needle withdraws from the sample vial. The dual purging and loading allows for in-line loading of the Tenax column (Supelco) and separation of derivitized Hg species through a GC column.

In the manufacturer set-up of the instrument, an event table file (ETF) is used to automate sample purging followed by loading and heating of the Tenax trap and GC column via a sequence of valve activation and deactivation. Gaseous species of Hg are purged from the sample at controlled flow rates (82, 120 or 152 mL/min) and loaded onto a Tenax trap at 31°C while bypassing the GC column, which has a separate continuous flow of Ar. During the desorption state, the valve between the Tenax trap and the GC column is opened, the Tenax trap is heated to 180°C, and the desorbed Hg derivatives are carried from the Tenax trap to the GC column (85°C). The chromatographically separated mercury species are fully combusted in a quartz pyrolysis column (720°C), combined with an Ar make up gas, and quantified by AFS. The Tenax trap and GC column are heated between sample loadings to avoid carryover between samples. The resulting chromatograph displays separate peaks of Hg(0), methylethylHg, and diethylHg, of which the methylethylHg peak can be quantitatively integrated to determine MMHg concentration.

Modifications of factory-installed software and hardware are necessary in order to detect MMHg from 180-mL of seawater using the Tekran 2700. The autosampler comes equipped with 3 trays that each hold 21 42-mL sample vials that correspond to pre-set autosampler positions. Although the autosampler has alternative settings for smaller sample vial sizes, there is no pre-installed set up for sufficiently large volume samples for seawater detection. Therefore, a custom foam and cardboard tray that accommodates 250-mL volume bottles was designed for bottle positions that correspond to vial positions that are pre-set for the autosampler configuration for 3 trays of 40 sample vials. In order to accommodate the differences in height between the 42-mL and 250-mL sample bottles, the z-axis height setting of the dual purge/inlet needle was adjusted

from 14700 mm to 13400 mm to keep the sampling inlet in the headspace during sample loading. In addition, the vial stopper was adjusted to allow clearance over the height of the bottles.

In order to maximize the signal, the flow rate of Ar gas for sample purging and the sample purging time were increased. The Ar gas flow was modified from manufacturer's installation by replacing the original 82-mL/min flow restrictor with a 152-mL/min flow restrictor. In addition, a new ETF was created that extended the sample purge time from 4 min to 8 min. As with the recommended configuration for analysis of 30-mL samples of freshwater, the gas stripping of MMHg from the 180-mL samples is not complete despite the extended purge time, but approaches 80% after 8 min. This extended purge time was chosen as a balance between maintaining the shortest possible analysis time, minimizing the amount of moisture that is forced onto the Tenax column, and maximizing the MMHg signal.

Standard and Sample Preparation

Acetate and citrate buffers, KOH, and sulfuric acid, were stored in acid-cleaned Teflon bottles. Solutions were remade as needed and to address any contaminants detected from reagent blanks.

For standard curve preparation, secondary stocks of 50 pM were prepared from dilution of concentrated MMHg primary stock (Alfa Aesar, 1000 ppm methylmercury chloride in water) in MQ and acidified to 0.25% HCl (concentrated, SEASTAR™ Chemical) to prevent loss of analyte to sides of the glass bottle. Standard curves ranging from 10 fM to 1000 fM were prepared daily from the secondary stock in MQ, filtered Equatorial Pacific seawater, and filtered Vineyard Sound seawater. MMHg was equilibrated with ambient ligands for at least 24 hours prior to further processing.

After equilibration, all samples and standards were acidified to a final concentration of 0.5% with concentrated sulfuric acid (Fisher, TM Grade) to extract MMHg from the seawater matrix and allowed to react for 24 hours prior to ethylation (Bowman and Hammerschmidt, 2011). Ascorbic acid (2.5% wt:vol in MQ, Fisher) was added to each sample prior to ethylation. Sample pH was then adjusted to 5 with KOH (45% wt:vol in MQ, Fisher). Sample pH was determined by testing 20 µL volumes of sample on pH strips (MColorpHast range 4.0-7.0, EMD Millipore). Neutralized samples were buffered with either acetate buffer (2M sodium acetate, Fisher; adjusted to pH 5 with H_2SO_4, conc. Fisher) or citrate buffer (1M sodium citrate Fisher; adjusted to pH 5 with H_2SO_4, conc. Fisher) according to sample size (Table 1). Sodium

tetraethylborate (NaTEB, Strem Chemical) was dissolved (1% final wt:vol) in pre-chilled 2% KOH in MQ and quickly aliquoted into 10-mL Teflon vials and kept frozen until use. For sample ethylation, an aliquot of NaTEB was thawed just until it formed a slush and was added to the buffered sample. Samples were then capped with Teflon-backed septa and inverted 10 times. The ethylation reaction was allowed to proceed for at least 20 minutes prior to initiating analysis.

Samples bottles were loaded into either the 42-mL vial tray provided by the manufacturer or the custom 250-mL bottle foam tray. Samples were analyzed after standards showed a linear relationship and peak area values for standards could be distinguished from those of reagent blanks (3x the standard deviation of triplicate regent blanks). Since the custom tray accommodates a maximum of 11 sample bottles, sets of 8-11 samples were typically prepared and all were analyzed within 4 hours of ethylation.

Assessment

The development of the presented method was focused on achieving two goals. First, we attempted to lower the detection limit of the automated method to adequately measure the low femtomolar concentrations of MMHg in open-ocean water. We did this by increasing the total sample volume from 30-mL to 180-mL as well as increasing total purge flow for larger sample volume by lengthening the purge time as well as increasing the Ar purge rate.

Second, we sought to improve the efficiency of MMHg extraction from the saltwater matrix. This was accomplished by the addition of ascorbic acid, which allowed for full extraction of added MMHg from seawater. We also replaced the acetate buffer commonly used in MMHg determination methods with citrate buffer in order to reduce signal inconsistencies that we observed after making alterations to the instrument method.

Sample Volume Adjustment

Using the instrument as designed with 30-mL sample volumes of seawater, the detection limit of 100 fM, as calculated from 3x the standard deviation of the blanks, was insufficient for low open-ocean MMHg concentrations, typically <100fM in the upper water column [Cossa et al, 2011; Hammerschmidt and Bowman, 2012; Mason and Fitzgerald, 1993; Sunderland et al, 2009]. The modification of the instrument to accommodate an increase in sample volume to 180-mL resulted in a daily detection limit of ~5 fM, from triplicate reagent blanks, which was sufficient for most depths within the open-ocean water column. This detection limit is on the same order of

magnitude as that of the recently described 2-L direct ethylation method [Bowman and Hammerschmidt, 2011] while decreasing the required volume by 90% and allowing the process to be automated.

Ar Purge Rate and Purge Volume

Unlike alternative analytical methods, the Tekran automated instrument used in this study does not completely purge MMHg from the sample. Instead, a purge time of up to 4 min is recommended for MMHg determination from freshwater samples for adequate mercury species separation. However, we observed a methylation artifact when using a 4 min purge time with 180-mL sample volumes. This artifact appeared after repeated analyses of individual acetate buffered samples and produced MMHg signals ranging between 73-477% (n=5) of the initial MMHg signal (Figure 1, A). The artifact was most pronounced in samples and standards with MMHg concentrations near 15 fM (Figure 1, B). We increased the purge time to 8 min in order to extract a higher proportion of the MMHg present in samples. The increased purge time resulted in a predictable decrease in measured MMHg from the first purge to the second but not in subsequent purges of an individual standard buffered with acetate (Figure 1, C). It is important to note that this artifact was not the result of MMHg carry over from previously analyzed samples. MMHg concentrations measured from blanks run between repeated purging of individual samples or standards were not elevated (<DL). Because acetate buffers are known to produce MMHg when exposed to light (e.g., Falter, 1999), we sought to avoid the apparent MMHg production in acetate buffered samples by using citrate buffer (see below).

Although we increased both the Ar purge rate and the Ar purging time, it is important to note that increasing the Ar purge rate from 80-mL/min to 120-mL/min produced only a modest increase in the MMHg sample signal of ~5% (n=5) from 30-60 mL sample volumes. However, the increase in total purge time from 1 min 45 sec to 4 min increased the MMHg sample signal by 25% (n=5). The difference between the effectiveness of changing the purge rate versus the total purge time may be attributed to the increase in gas pressure in the headspace above the aqueous sample and therefore a decrease in the volatilization of methylethylHg. While the MMHg signal was less sensitive to increases in the Ar purge rate than to increases in the sample volume, the increased purge rate combined with the increased length of the purge allowed for samples to be processed in a relatively high throughput manner while still retaining low femtamolar detection limits.

Determination of Reagent Blanks

Due to low MMHg concentrations present in open-ocean seawater, it is important to quantify the Hg species content of reagent blanks and take steps to minimize contamination. MQ in our laboratory often has measurable MMHg and Hg(II) concentrations that would hinder analysis of low seawater concentrations. As a result, we used two methods to quantify MMHg in the reagent blanks. First, MQ was exposed to ambient outdoor UV in 2-L Teflon bottles for 7-10 days until the concentration of MMHg in the water was negligible (<3 fM) and this water was then used to prepare reagent blanks. Alternatively, in order to check the MMHg contribution of the reagents to the total signal from blanks, the reagents prepared in lab MQ were added in increasing amounts (e.g., 1x, 2x and 3x above those values in Table 1) and were determined as the MMHg signal above the MQ water background (Figure 2).

The precision of the standard curves was determined daily to have an average relative standard deviation from 4 replicate standards of 6% (range: 4-9%) during method development. Generally, the slope of the standard curve was also consistent from day to day. Over a 14-day period, the average slope of daily standard curves of MMHg peak area versus the amount of MMHg added (fM) averaged 2.61 (± 0.31) area units per fM Hg for 180-mL volume standards. Differences in the slopes between standard curves prepared with MQ and those prepared with filtered seawater were similar, varying between -12% to +16% (n=3; Figure 5) for 180-mL volumes without the need to adjust for reduced ethylation efficiency due to the seawater matrix. As a result, standard curves prepared in MQ can be used for quantification of MMHg concentrations.

Ascorbic Acid Addition

The addition of ascorbic acid dramatically improved the extraction of MMHg from the seawater matrix. Extraction of MMHg standard from MQ averaged 34% (range: 2.7-81%, n=10) and improved to 97% (range: 86-109% n=7) when ascorbic acid was added (Figure 3). Although the mechanism by which MMHg recovery was improved is unknown, the function of ascorbic acid to overcome seawater matrix effects is affected by neither the order of reagent addition nor the length of time that ascorbic acid is allowed to react with the seawater sample. The increased extraction efficiency rendered by ascorbic acid yielded 98% recovery of equilibrated MMHg standard spikes from 30-mL volumes of filtered seawater within the 20-min reaction time allowed for the ethylation reaction (range: 81-128%, n=15). Exposing the sample to additional

manipulation by first adding ascorbic acid, resealing the sample bottle, incubating for 12 hrs, and then adding the remaining reagents yielded an average of 130% recovery (range: 104-155%, n=8) of added MMHg standard. In addition, recovery of MMHg from previously purged filtered seawater to which no ascorbic acid was added was enhanced, from 34% to 70% (range: 61-71%, n=2) compared to unpurged filtered seawater (Figure 3). This suggests that a volatile, oxidizing component of seawater may be the source of interference that inhibits extraction of MMHg from the seawater matrix.

Addition of ascorbic acid to samples prior to ethylation also greatly improved the effective lifespan of NaTEB. Previous studies have found that NaTEB quickly loses its ethylation ability in a matter of days, even when kept frozen in individual aliquots until use [USEPA, 2001; DeWild et al, 2002; Lamborg et al, 2012]. The addition of ascorbic acid extended the ethylation capacity of NaTEB. Individual aliquots of NaTEB were stable through several freeze and thaw cycles over weeks of analyses without noticeable changes in the ability to ethylate MMHg standards. Dissolved NaTEB stored frozen (-20°C) for > 2 months maintained its ability to ethylate MMHg equilibrated in filtered seawater (~88% recovery of added MMHg; n=2; Figure 4). This suggests that the perceived instability of NaTEB is not due to chemical breakdown from oxidation during storage, but is instead a result of interferences with the ethylation reaction by some component of either the seawater matrix or a breakdown product of NaTEB itself.

Citrate Buffering

Contamination from reagents can be minimized through the use of trace metal grade acids and bases. However, the organic acid buffers can contribute a significant amount of MMHg contamination to sample signals. In initial attempts to reduce this contamination, NaTEB was added to the acetate buffer, allowed to react at room temperature for 20 min, and purged with Hg-free N_2 at 0.5-L/min for 30 min to remove MMHg and inorganic Hg species. However, upon analysis, it was discovered that this daily addition of NaTEB and purging of the acetate buffer contributed to an in-growth of MMHg observed with subsequent purges of individual samples/standards (Figure 1). As a result, we replaced the acetate buffer with citrate buffer to avoid similar production of MMHg during analysis. Although the citrate buffer has a higher concentration of MMHg contamination, ranging between 5 and 73 fM (n=15) compared to less than 5 fM in acetate buffer, the contamination from the citrate buffer did not appear to increase with time or exposure to light. Repeated purging of citrate buffered samples for 8 minutes also

resulted in a predictable decrease in the MMHg peak area averaging 77% of its previous value (range: 74-82%, n=6) without the MMHg in-growth observed with acetate buffered MMHg concentrations <15 fM.

In addition to the greater MMHg contamination found with citrate buffer, its use decreased the sensitivity of the MMHg detection, calculated from the slope of the MMHg peak area versus concentration of added MMHg standard, to 45% that of acetate buffered standards at a flow rate of 82-mL/min. However, at the higher 152-mL/min flow rate, the slope of the citrate buffered standards is 77% that of acetate buffered standards (Figure 2).

Discussion

Direct ethylation of MMHg has provided a means to vastly improve the understanding of Hg speciation in marine systems, especially the organomercuric species DMHg and MMHg, which are present in low femtomolar concentrations in the open-ocean water column [Cossa et al, 2011; Hammerschmidt and Bowman, 2012; Mason and Fitzgerald, 1993; Sunderland et al, 2009]. Because sample preservation with acid leads to the demethylation of DMHg to MMHg [Parker and Bloom, 2005], a method capable of distinguishing between these two organomercuric species is essential to understand the partitioning of Hg species. Although the direct ethylation method provides a promising alternative to sample distillation, the seawater matrix presents interferences that can lower ethylation efficiency.

Although the addition of ascorbic acid does not lower the detection limit (~5 fM) compared to the current method of direct ethylation of MMHg from sweater (Bowman and Hammerschmidt 2011), complete recovery of MMHg from the seawater matrix is advantageous for two reasons. First, the ethylation enhancement observed using ascorbic acid, presumably due to its function as a mild reductant, may occur to unknown degrees in seawater samples, depending on their concentrations of naturally occurring reductants. As a result, without complete MMHg extraction, relative concentrations between seawater samples may reflect differences in ethylation efficiency due to the composition of the seawater matrices rather than differences in MMHg concentrations. Second, the increased ethylation efficiency observed in pre-purged seawater (Figure 3) can potentially overestimate the assumed ethylation efficiency when MMHg standard curves are prepared in purged samples [Bowman and Hammerschmidt, 2011].

Preservation of open-ocean seawater samples can be essential for mechanistic studies of mercury species cycling in ocean environments. Thus, the presented ascorbic acid-assisted direct

ethylation method has been developed to allow for both ship-based and lab-based MMHg measurement. In combination with ship-based measurement of DMHg from untreated seawater prior to preservation with H_2SO_4, this method overcomes major restrictions faced while using many of the current methods used for MMHg analysis. In addition, our semi-automated method can improve throughput for linked anaylsis, such as CVAFS-ICPMS for mechanistic studies using additions of stable Hg isotopes [Monperrus et al, 2007; Lehnherr et al, 2011].

Comments and Recommendations

We developed the described method specifically to reduce the required volume needed to measure MMHg from seawater while maintaining a minimal amount of sample manipulation. The addition of ascorbic acid enables complete extraction of low open-ocean concentrations of MMHg from seawater matrices. Complete extraction is important for avoiding potential biases in MMHg determination that may result from changes in ethylation efficiency caused by differences in seawater matrix composition between samples.

Direct methylation from Hg(II) has recently been revealed as a potentially significant source of MMHg in the marine water column [Lehnherr et al, 2011; Sunderland et al, 2009]. However, MMHg may also be produced from the abiotic degradation of highly photolabile DMHg [Mason et al, 1995]. Since we developed this method to measure MMHg from acid-preserved samples that were stripped of DMHg before preservation, we have not run standard curves to quantify the DMHg detected by the Tekran 2700. Thus, we recommend that the described method be used in conjunction with ship-based measurements of DMHg for full dissolved Hg speciation analysis [Bowman and Hammerschmidt 2011; Lamborg et al, 2012].

Although our method was developed using one of two commonly used commercially available MMHg auto analyzers, the addition of ascorbic acid can be adapted to existing manual methods in order to minimize matrix effects during analysis.

Acknowledgements

This research was supported by the National Science Foundation (OCE-1031271). K. M. M. was supported by a Graduate Research Fellowship from the National Science Foundation.

References

Bloom, N. 1989 Determination of picogram levels of methylmercury by aqueous phase ethylation, followed by cryogenic gas chromatography with cold vapour atomic fluorescence detection. Can. J. Fish. Aquat. Sci., 46, 1131-1140.

Bowman, K. L., and C. R. Hammerschmidt (2011) Extraction of monomethylmercury from seawater for low-femtomolar determination. Limnol. Oceanogr. Methods 9, 121-128.

Clarkson, T.W. and L. Magos (2006) The toxicology of mercury and its chemical compounds. Crit. Rev. Toxicol. 36, 609-662.

Cossa, D., B. Averty, and N. Pirrone (2009) The origin of methylmercury in open Mediterranean waters. Limnol. Oceanogr. 54, 837-844.

Cossa, D., L. E. Heimburger, D. Lannuzel, S. R. Rintoul, E. C. V. Bulter, A. R. Bowie, B. Averty, R. J. Watson, and T. Remenyi (2011) Mercury in the Southern Ocean. Geochim. Cosmochim. Acta 75, 4037-4052.

DeWild, J., M. Olson, and S. Olund (2002) Determination of methylmercury by aqueous phase ethylation, followed by gas chromatographic separation with cold vapor atomic fluorescence detection. U. S. Geol Surv. Open File Rep 01-445, 19 pp.

Falter, R. (1999) Experimental study on the unintentional abiotic methylation of inorganic mercury during analysis: Part 2: Controlled laboratory experiments to elucidate the mechanism and critical discussion of the species specific isotope addition correction method. Chemosphere 39, 1075-1091.

Hammerschmidt, C. R., and K. L. Bowman (2012) Vertical methylmercury distribution in the subtropical North Pacific Ocean. Mar. Chem. 132-133, 77-82.

Hammerschmidt, C.R., Bowman, K.L., Tabatchnick, M.D., and C. H. Lamborg (2011) Storage bottle material and cleaning for determination of total mercury in seawater. Limnology and Oceanography-Methods, 9, 426-431.

Horvat, M., L. Liang, and N. S. Bloom (1993) Comparison of distillation with other current isolation methods for the determination of methyl mercury compounds in low level environmental samples Part II. Water. Anal Chimica Acta 282, 153-168.

Lamborg, C.H., Hammerschmidt, C.R., Gill, G.A., Mason, R.P. and S. Gichuki (2012) An Intercomparison of Procedures for the Determination of Total Mercury in Seawater and Recommendations Regarding Mercury Speciation during GEOTRACES Cruises. Limnology and Oceanography-Methods, 10, 90-100.

Lehnherr, I., V. L. St. Louis, H. Hintelmann, and J. L. Kirk. (2011) Methylation of inorganic mercury in polar marine waters. Nat. Geo. 4, 298-302.

Mason, R. P. and W. F. Fitzgerald (1993) The distribution and biogeochemical cycling of mercury in the equatorial Pacific Ocean. Deep-Sea Res. I 40, 1897-1924.

Mason, R. P., K. P. Rolfhus., and W. F. Fitzgerald (1995) Methylated and elemental mercury cycling in surface and deep ocean waters of the North Atlantic. Water, Air, Soil, Pollut. 80, 665-677.

Monperrus, M., E. Tessier, D. Amouroux, A. Leynaert, P. Huonnic, and O. F. X. Donard (2007) Mercury methylation, demethylation and reduction rates in coastal and marine surface waters of the Mediterranean Sea. Mar. Chem. 107, 49-63.

Parker, J. L. and N. S. Bloom (2005) Preservation and storage techniques for low-level aqueous mercury speciation. Sci. Total. Environ. 337, 253-363.

Sunderland, E. M., D. P. Krabbenhoft, J. W. Moreau, S. A. Strode, and W. M. Landing (2009) Mercury sources, distribution, and bioavailability in the North Pacific Ocean: Insights from data and models. Global Biogeochem. Cy. 23, GB2010.

Tekran Instruments Corporation (2011) Series 2700 Methyl Mercury Analysis System: Analytical Guides. Rev: 1.10.

US EPA (USEPA) (2001) Method 1630: methyl mercury in water by distillation, aqueous ethylation, purge and trap, and cold vapor atomic spectrometry. Washington, DC.

Figures and Figure Legends

Figure 1: Increases in measured MMHg, relative to the initial MMHg measured, was observed during repeated analysis of individual seawater samples buffered with acetate buffer (180-mL) (A). Similar variability was observed in acetate-buffered standards of 25 fM MMHg added to filtered seawater using a 4-minute Ar purge in the analytical method (B). Extending the Ar purge time of acetate-buffered standard to 8 minutes failed to alleviate this variability (C). Quantitative stripping of MMHg was observed from citrate-buffered standards using an 8-minute Ar purge (D).

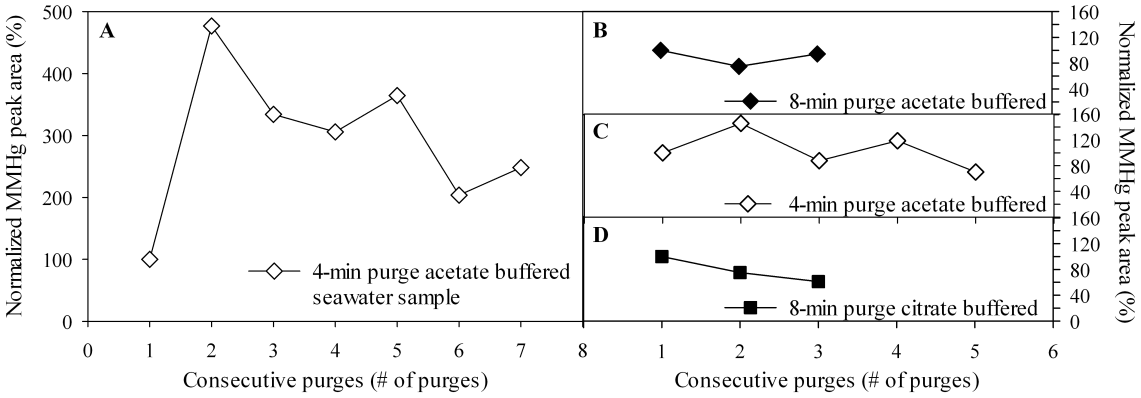

Figure 2: Comparison of standard curves of instrument MMHg peak area versus added MMHg standard (5-100 fM) prepared with acetate buffer and citrate buffer. Citrate buffered standards yield less sensitivity as observed from the lower slope of the standard curve. By increasing the rate of the Ar purging during sample analysis by replacing the 82-mL/min flow restrictor with a 152-mL/min flow restrictor, the sensitivity of the citrate-buffered standard curve approaches that of the acetate-buffered standard curve.

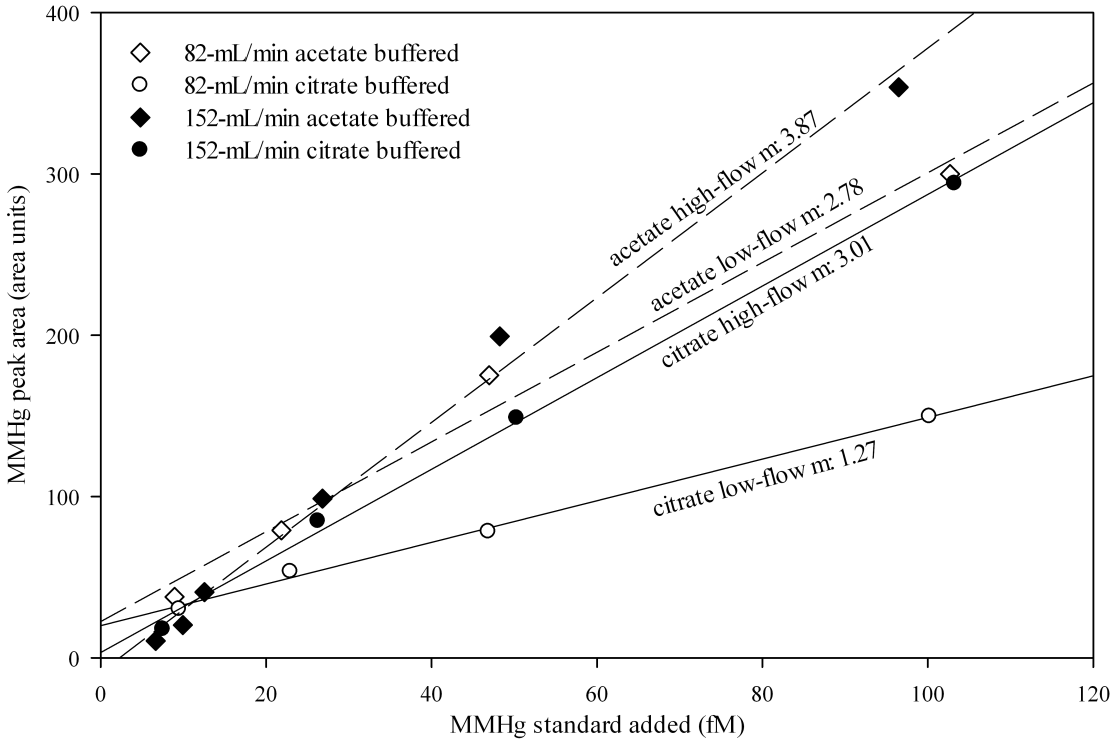

Figure 3: Percent recovery of added MMHg standard (0.02-1ppt) equilibrated for 24 hours in filtered Vineyard Sound seawater measured by direct ethylation. In the absence of ascorbic acid (left) the recovery of MMHg is generally less than 40%. Purging of filtered seawater prior to MMHg standard addition (center) may increase the recovery. The addition of ascorbic acid (right) yields significantly greater recovery from seawater not purged before standard addition ($p < 0.005$).

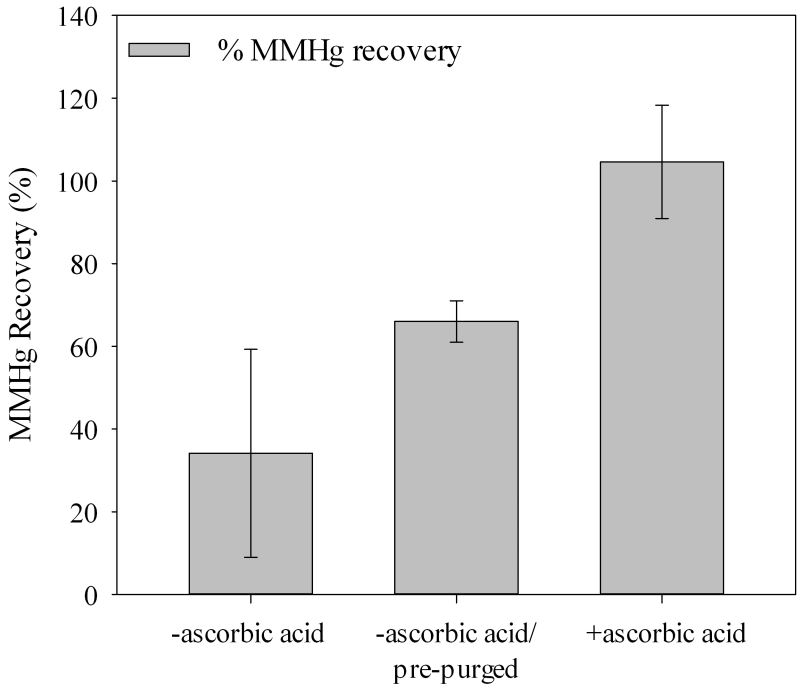

Figure 4: Representative standard curve of instrument MMHg peak area versus added MMHg standard (15-250 fM) from 180-mLvolumes used to quantify seawater samples. Four replicates of 25 fM are shown and are used to calculate standard variability. Inset: MMHg blank in reagents is calculated from the slope of the linear fit obtained from the instrument MMHg peak area versus stepwise increases in reagent concentrations

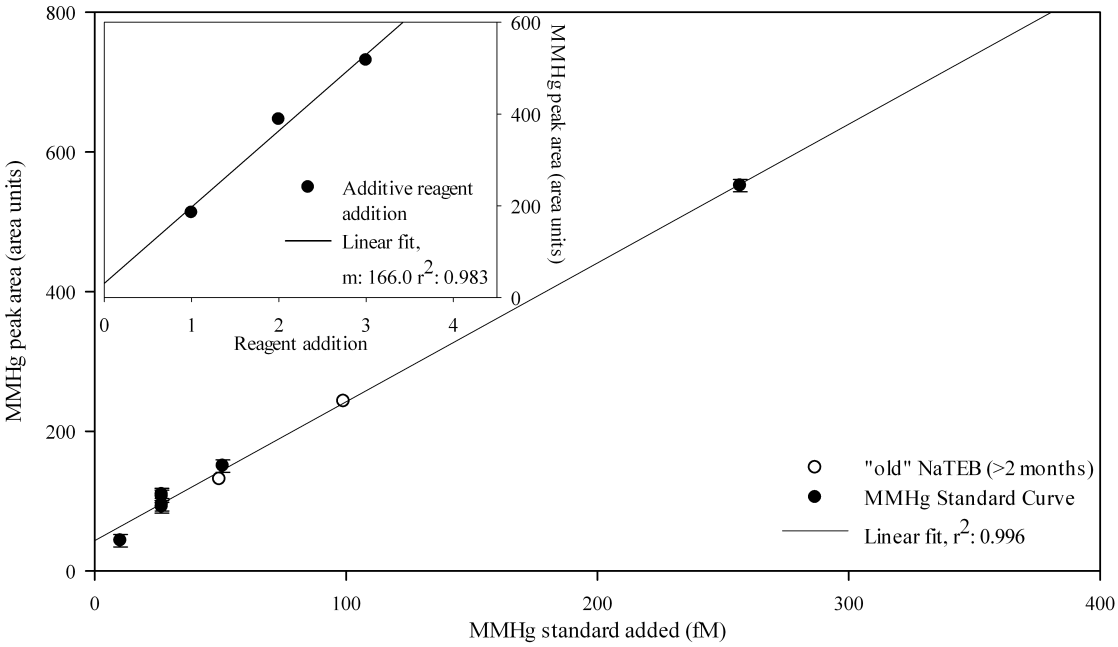

Figure 5: Recovery of added MMHg standard from de-ionized water (MQ) and filtered Vineyard Sound seawater (FSW) using ascorbic acid assisted direct ethylation. Instrument MMHg peak areas are corrected for reagent blanks measuring from each of the corresponding sample matrices. The addition of ascorbic acid to the FSW prevents the need for correcting for low ethylation efficiency from direct ethylation of seawater. Although open-ocean concentrations of MMHg are generally well below 1000 fM, standards show similar recovery from FSW and MQ beyond the range required for determining ocean MMHg concentrations.

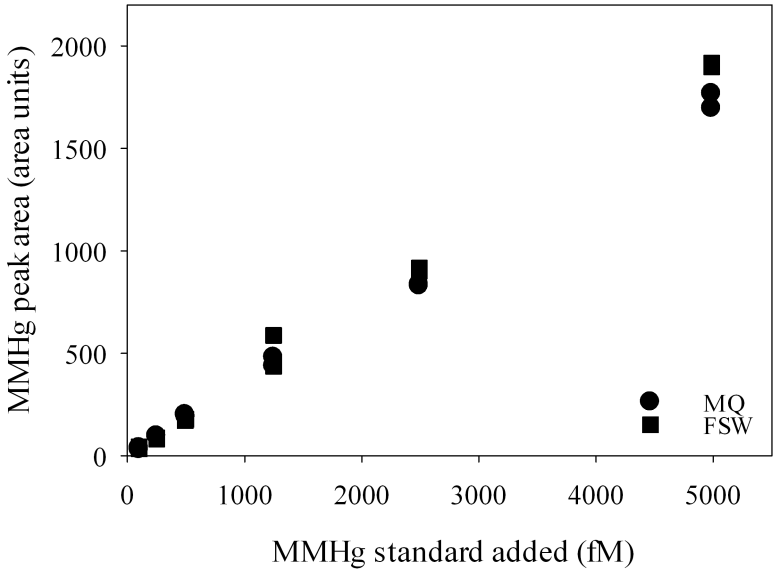

Tables and Table Legends

Table 1: Reagents optimized for 30-mL and 180-mL sample volumes. Acetate buffer (2M) was used initially as outlined in USEPA Standard Method 1630. However, citrate buffer (1M) replaced acetate buffer for low concentration seawater samples to eliminate ingrowth of MMHg in samples upon repeated analytical runs of the same samples.

Final Sample Volume (mL)	Detection Limit (fM)	Ascorbic Acid (μL)	2M Acetate Buffer (mL)	1M Citrate Buffer (mL)	NaTEB (μL)
30	100	50	0.225	0.55	30
180	5	300	1.0	2.0	85

Chapter 3
Methylation and Demethylation of Mercury in the Sargasso Sea

Abstract

We measured potential rates of mercury methylation and demethylation at the Bermuda Atlantic Time-series Study (BATS) site during the spring bloom and fall within a single calendar year. Bottle incubations of filtered and unfiltered seawater reveal active methylation and demethylation within the chlorophyll maximum and the oxygen minimum zone at the BATS site, resulting in specific methylation rate constant (k_m) values between 4.58-5.17 (% d^{-1}) in April and 0.22-0.61 (% d^{-1}) in October. We observed no clear enhancement of methylation in unfiltered waters during 24-hour incubations in April compared to filtered controls. Higher resolution measurements over the 24-hour incubation period in October revealed highly dynamic methylation and demethylation despite small net changes over the total incubation period. In waters from the chlorophyll maximum depth, concentrations of methylated mercury (MeHg) produced from inorganic mercury (Hg(II)) spike additions reached a maximum within 4 hours and decreased throughout the remainder of the incubation period. The transition from net methylation to net demethylation was enhanced by the presence of particles. In contrast, unfiltered waters from the oxygen minimum depth showed continual methylation over the course of 24-hour incubations.

Demethylation measured during April show enhanced demethylation in unfiltered water compared to filtered water. Overall rates were comparable to those measured in marine Arctic and Mediterranean waters. Demethylation rates were enhanced within the oxygen minimum region. However, we could not make quantitative comparisons of demethylation rates between April and October because of rapid demethylation of the monomethylmercury (MMHg) spike that occurred at the beginning of the October incubation.

These results show that methylation does take place in oligotrophic marine waters despite low standing concentrations of methylated mercury species. In addition, methylated mercury concentrations in marine waters may be largely controlled by rates of demethylation, rather than methylation in the open-ocean water column.

Introduction

Despite the importance of marine fish for human consumption [Sunderland, 2007] and the potential health risks posed by exposure to high concentrations of mercury (Hg) [Clarkson and Magos, 2006], little is known about the potential for Hg methylation in the marine water column. This is important to explore as monomethlymercury (MMHg) is the chemical species of Hg that bioaccumulates in marine food webs. Measurements of methylation within the marine water column have been performed in a limited number of marine sites, largely limited to coastal and semi-coastal locations within the Canadian Arctic Archipelago [Lehnherr et al, 2011] and the Mediterranean Sea [Monperrus et al, 2007]. Experiments at these sites have found significant production of MMHg in seawater and have suggested that observed methylation may be driven by microbial processes [Monperrus et al, 2007].

The impact of changing anthropogenic emissions of Hg on ocean Hg distributions and resulting bioaccumulation is the central question for potential mitigation strategies [Krabbenhoft and Sunderland, 2013]. A decreasing trend in total Hg (THg) concentrations has been suggested for North Atlantic water due to decreases in European and North American Hg emissions [Mason et al, 2012]. Recent compilations of atmospheric and surface ocean Hg measurements and model results have proposed the net evasion of anthropogenic mercury from the North Atlantic surface ocean [Sørensen, et al 2010, Sørensen et al, 2012], which might enhance surface water depletion of THg. However, few water column measurements of Hg species concentrations have been made repeatedly at open ocean sites in the North Atlantic over the past 3 decades. In addition early measurements of Hg may be subject to contamination [e. g. Gill and Mason (2005) as shown in Mason et al, 2012] and recent intercalibration for total Hg (THg) determination show that modern analyses have low consistency, ~40%, among participating laboratories [Lamborg et al, 2012]. Despite the difficulty in determining temporal trends in THg distributions, concentrations of the bioaccumulating MMHg in the North Atlantic depend on the dynamic cycling of Hg species within the water column. At any depth, measured MMHg concentrations can potentially result from Hg(II) substrate delivery via sinking particulate matter to zones of net remineralization, advective transport from sedimentary sources, in situ production within the water column, and loss processes such as demethylation and particle scavenging [reviewed by Mason et al, 2012]. In North Atlantic waters, MMHg composes a small percentage, generally <10%, of THg and is often decoupled from THg concentrations [Bowman et al, 2013]. As a result, in order to determine whether North Atlantic MMHg concentrations are decreasing with lowered regional emissions,

and, as a result, whether MMHg available for bioaccumulation in marine food webs is changing over time, it is important to determine the controls on methylation in these marine waters.

Early studies of MMHg distributions and stability in marine waters proposed that MMHg is produced from the breakdown dimethylmercury (DMHg) that is directly formed from microbial methylation of Hg(II) [Mason and Fitzgerald, 1993]. Subsequent measurements of dissolved Hg species in surface and intermediate waters have observed correlations between concentrations of methylated Hg species (DMHg and/or MMHg) and rates of oxygen utilization [Sunderland, et al, 2009; Cossa et al, 2011]. As a result of these observations, methylation rates are thought to be limited by the rate of Hg(II) substrate delivery from remineralization of sinking organic matter [Sunderland et al, 2009]. Potential Hg methylation and demethylation rates from the sites in the Mediterranean and the Canadian Arctic Archipelago have demonstrated the complexity of MMHg and DMHg formation and degradation in marine waters. Methylation rates appear significant not only in waters of net remineralization, but also in euphotic waters where methylated Hg concentrations are typically lower [Monperrus et al, 2007; Lehnherr et al, 2011]. In these upper water column depths, methylated Hg species may be controlled by demethylation processes that are absent deeper in the water column, such as photodemethylation [Whalin et al, 2007; Monperrus et al, 2007; Lehnherr et al, 2011].

However, methylation rates in surface waters may also be influenced by primary productivity. Coastal waters of the Mediterranean Sea yield both higher rates of methylation than more open-ocean waters as well as larger seasonal signals, with enhanced methylation during the spring bloom and lower methylation in the late fall [Monperrus et al, 2007]. Demethylation rates measured at the same locations are more consistent between coastal and more open-ocean sites but show a contrasting seasonal signal, with enhancement of demethylation during late fall months only in more open-ocean waters [Monperrus et al, 2007]. Methylated Hg concentrations result from the net balance between methylation and demethylation. Thus, seasonal differences between these two processes may result in seasonal variations in dissolved concentrations of MMHg and its availability for uptake and eventual transfer to marine fish.

We measured potential methylation and demethylation rates at the Bermuda Atlantic Time-series Study (BATS) site during the spring bloom and in the fall in order to assess seasonal changes in methylation and demethylation potential within oligotrophic marine waters. We compared potential methylation and demethylation rates at the base of the euphotic zone, where phytoplankton abundance is highest but methylated Hg concentrations are generally low, to those

at the depth of highest net organic matter remineralization, where marine methylated Hg concentrations are typically greatest. By comparing unfiltered waters to 0.2 μm filtered controls, we aimed to determine the potential for methylation and demethylation driven by heterotrophic bacteria from dark incubations.

Materials and Methods

Incubations were performed on board the *R/V Atlantic Explorer* with water collected from the BATS site (31° 40'N, 64° 10'W) between 25-27 April 2012 and 7-13 October 2012. During the April 2012 cruise two sets of incubations were performed. Water for one set was collected from acid-cleaned GO-Flo bottles deployed on Kevlar line and triggered with Teflon messengers. For the second set of incubations water was collected from Niskin bottles deployed on the ship's rosette. In order to avoid contamination due to sampling water through which the rosette and line had previously travelled, water collection was triggered during the downcast. Concentrations of MMHg of water collected from Niskins and GO-Flo bottles were within 5% of each other, suggesting little contamination from the Niskin bottles. As a result, water for October incubations was collected from the rosette Niskin bottles.

Water was decanted from all bottles within a "bubble" constructed from plastic sheeting and filled with HEPA-filtered air under positive pressure provided by an AirClean 3000 flow bench. Water from GO-Flo bottles or Niskin bottles was decanted into acid-cleaned 9-L polycarbonate carboys (Nalgene). Bottles for filtered incubations were filled with water pumped through a 0.2 μm capsule filter (47 mm, Supor polycarbonate membrane, Pall Corporation) through acid-washed Teflon tubing linked by a short piece of silicon tubing (Masterflex 25) by a peristaltic pump (Masterflex). Bottles for unfiltered incubations were filled by pumping water though the tubing without the capsule filter in line.

Isotopically enriched ^{198}MMHg and ^{202}Hg(II) spikes were pre-equilibrated at 4°C with natural ligands in 0.2 μm filtered seawater for 24 hours prior to addition to incubation bottles. Seawater for pre-equilibration was collected from the BATS site in casts prior to those for incubation water and filtered through the capsule filter as noted above. The equilibrated spikes were added to triplicate bottles for each time point using dedicated gas-tight syringes (Hamilton).

During the April incubations, spike concentrations were: 700 fM ^{198}MMHg and 2200 fM ^{202}Hg(II). Bottles were fixed to 0.5% (final) with H_2SO_4 (conc., J. T. Baker) after addition of Hg

spikes for the t0 time point and after 24-hour incubations in the dark in a cooler at 20°C for the t24 time point.

During the October incubations, added spike concentrations were increased to: 1346 fM ^{198}MMHg and 7000 fM ^{202}Hg(II). In order to prevent rapid methylation and demethylation observed in the April incubations, t0 bottles were fixed to 0.5% (final) with H_2SO_4 prior to addition of Hg isotope spikes. Bottles were incubated for 0, 0.5, 2, 4, 8, 12, and 24 hours in the dark in a cooler at 20°C after which they were fixed to 0.5% (final) with H_2SO_4.

Hg species-specific isotope abundances were analyzed in the WHOI Plasma Facility. The cell vent of a Tekran 2700 Automated Methyl Mercury Analyzer was linked via a polyethylene y-connector to the sample Ar gas of a Thermo Element 2. MMHg was derivitized to methylethylHg using ascorbic-acid assisted direct ethylation [Munson—this work, Chapter 2]. Acidified bottles were buffered to 0.01% with citric acid buffer (1M, Fisher, pH 5) and neutralized to pH 5 with KOH (45%, Fisher) prior to the addition of ice-cold 1% sodium tetraethylborate (2% KOH, Fisher). Ascorbic acid (300 μL of 2.5%, Fisher) was added to ensure full extraction of MMHg. All reagents were prepared in de-ionized water (>18 MΩ-cm). Samples processing was performed within a class 100-grade clean room at WHOI and were transported to the plasma lab for analysis.

After at least 20-min reaction time for ethylation, the MeHg (DMHg + MMHg) in the incubation bottles was quantified as MMHg by GC separation prior to pyrolysis to Hg(0) with the Tekran 2700. All 7 Hg isotopes were quantified in the resulting Hg(0), MMHg (as methylethylHg), and Hg(II) (as diethylHg) peaks using the Thermo Element 2.

Methylation and demethylation were determined from changes in the isotopic composition of the MMHg peak using a linear matrix approach using ^{200}Hg as the tracer of ambient Hg [Hintelmann and Ogrinc, 2003; in detail Munson—this work, Appendix I]. The results of these calculations distinguished between ambient Me^{200}Hg, MM^{198}Hg remaining from the MM^{198}Hg spike, and Me^{202}Hg produced from the ^{202}Hg(II) spike for each sample. Determinations of MM^{198}Hg lost and Me^{202}Hg produced in at each time point, including t0, were made by comparing the ratios of MM^{198}Hg and Me^{202}Hg to the reference isotope ^{200}Hg observed in the measured methylethyl Hg peak to the ratios in the equilibrated spike [Hintelmann and Evans, 1997].

Potential methylation rate constants (k_m) were measured in a similar manner to those of Lehnherr et al, 2011 as the change in MM^{202}Hg(II) produced relative to available ^{202}Hg(II)

substrate divided by the incubation time. However, unlike Lehnherr et al, 2011, we did not assume a general loss of ^{202}Hg(II) substrate over time. Instead, we used the observed response in the diethylHg peak of the Tekran 2700 to track the change of ^{202}Hg(II) substrate for each incubation time point. This approach is validated by the linear response to additions of Hg(II) standards in the diethylmercury peak (Figure 1). Although we did not determine ethylation efficiencies for Hg(II) conversion to diethylHg, the linear response of the diethylHg to added Hg(II) allowed us to approximate available ^{202}Hg(II) in each sample bottle as the ^{202}Hg spike component of the diethylHg peak quantified by CVAFS-GC-ICPMS. Values for the ^{202}Hg spike component were calculated from the isotopic composition of the chromatographically separated diethylHg peaks using a similar linear matrix approach as was used to trace MM^{198}Hg and Me^{202}Hg in the methylethylHg peak [Munson—this work, Appendix I]. Potential demethylation rate constants (k_d) were calculated from the slope of the linear best fit line of ln(MM^{198}Hg) vs. time.

The k_m values presented in this work represent the combined production of methylated Hg species from Hg(II). Thus, our reported k_m values do not differentiate between different mechanisms of MeHg production measured by Lehnherr et al, 2011. No distinction was made between the production of MMHg from Hg(II), the production of DMHg from Hg(II), and the production of DMHg from MMHg. Instead, the acid preservation of samples produced a combined measurement of methylated Hg ([DMHg] + [MMHg]) at each time point. As a result, the presented k_m values represent the overall conversion of Hg(II) to either DMHg or MMHg, or varying relative proportions of the two species.

Results

Potential Methylation Rates

Previous measurements of potential methylation rates have observed "instantaneous" methylation within ~30 minutes of adding enriched Hg(II) to seawater incubations [Lehnherr et al, 2011]. Consistent with these observations, we observed significant methylation in t0 sample bottles that occurred within the ~ 2 hours that elapsed between ^{202}Hg(II) spike addition and sample preservation with acid during the April incubation experiments (black bars, Figure 2). This pre-t0 methylation was indicated by the difference in the isotopic composition of the produced MeHg relative to the composition of added Hg(II) substrate in the equilibrated spike. Although rapid methylation has been attributed to abiotic mechanisms or methylation by inactive

cells [Lehnherr et al, 2011], incubations of cultured sulfate- and iron-reducing bacteria have demonstrated both a time-lag of ~10 min between Hg(II) addition and MMHg production [Schaefer et al, 2011] and immediate methylation of Hg(II) substrate with ~1 min sampling resolution [Graham et al, 2012]. The reasons for such inconsistencies are unknown, but may be due to differences in experimental conditions that influence Hg(II) substrate uptake, including Hg(II)-ligand interactions and cell density [Graham et al, 2012]. Regardless of the cause, the 2 hour time period between Hg(II) spike addition and t0 sample preservation during the April incubations likely provided sufficient time for a wide range of potential methylation pathways, including intracellular methylation by microbes, extracellular processes, or abiotic transformations. As a result, we define "initial" methylation as methylation observed in t0 samples rather than "instantaneous" methylation due to our inability to determine the exact pathway and time scale of the observed methylation.

During the April cruise, initial methylation was sufficient to account for all methylation observed over the 24-hour incubation, ranging from 5.62-7.09 % of the available ^{202}Hg(II) substrate for all samples (Figure 2). During the October cruise, t0 samples were fixed with acid prior to addition of the ^{202}Hg(II) spike in order to limit initial methylation to the timescale of ^{202}Hg(II) spike mixing in the sample bottle, and thus more accurately represent "instantaneous" methylation. These t0 samples produced less initial methylation than seen in April, ranging between 0.03-0.27 % of available ^{202}Hg(II), as well as a varied contribution of initial methylation to the total methylation after 24 hours (Figure 3). However, subsequent methylation in the 24-hour incubation period was significantly lower in October than April (Figures 2 and 3). Therefore, we cannot determine to what extent the high initial methylation observed in April was due to truly "instantaneous" methylation versus methylation over the 2 hour experiment set up before t0 sample preservation.

Perhaps due to the magnitude of initial methylation, values of k_m calculated from the methylation of ^{202}Hg(II) over the 24-hour incubation period measured during the April cruise showed no significant difference by depth or between filtered and unfiltered water (Figure 2, Table 3). In contrast, during the October cruise, k_m values reflect the continued production of Me^{202}Hg within the 24-hour incubation (Figure 3, Table 3).

More frequent sampling over the 24-hour incubation period during the October cruise revealed highly dynamic changes in methylation rates within the 24-hour incubation. Maximum percentages of Me^{202}Hg produced from available ^{202}Hg(II) were reached after 4 hours of

incubation in both filtered and unfiltered water collected from the chlorophyll maximum depth (0.2 μm: 0.47 ± 0.00 %; unfiltered: 0.67 ± 0.06 %; Figure 3). This newly formed $Me^{202}Hg$ was lost to subsequent demethylation over the remainder of the incubation period, with enhanced demethylation in unfiltered water compared to filtered water (Figure 3).

In water collected from the oxygen minimum depth, initial methylation was similar between filtered and unfiltered water (0.2μm: 0.27 ± 0.01 %; unfiltered: 0.27 ± 0.04 %). Indications of rapid methylation and subsequent demethylation in unfiltered is indicated by the maximum in $Me^{202}Hg$ at 0.5 hours that is rapidly lost (Figure 3). However, a more robust signal appears to be the gradual increase in $Me^{202}Hg$ produced over the course of the 24-hour incubation (Figure 3). In contrast to the influence of particles on methylated Hg in waters from the chlorophyll maximum, where $Me^{202}Hg$ production and demethylation both appeared to be enhanced within the incubation period, the presence of particles in the low oxygen waters appear to enhance continual production of $Me^{202}Hg$ and yield the highest values of k_m measured in October (Table 2).

Potential Demethylation Rates

During the spring bloom, potential demethylation rates were higher in unfiltered water (0.32 d^{-1}) compared to 0.2 μm-filtered water (0.05 d^{-1}) at the chlorophyll maximum depth (Table 3). In contrast, values of k_d measured at the oxygen minimum depth were similar between filtered (0.39 d^{-1}) and unfiltered (0.44 d^{-1}) water (Table 3).

The reported values for k_d from the April experiments were calculated from the net loss of $MM^{198}Hg$ from t0 to t24-hours. However, rapid demethylation was observed in all bottles, and t0 $MM^{198}Hg$ concentrations ranged from 177 fM in water from the chorophyll maximum depth to between 214-218 fM in water from the oxygen minimum depth. These values represent 25-31% of the 700 fM concentration of each bottle after $MM^{198}Hg$ spike addition, suggesting that although measurable over the 24 hour incubation period, demethylation was occurred quickly after addition of the enriched $MM^{198}Hg$ spike.

Demethylation was more difficult to quantify in the October incubations. Despite nearly doubling the initial concentration of $MM^{198}Hg$ spike in each bottle (from 2200 to 7000 fM final concentration) rapid demethylation was rapid in waters from both the chlorophyll maximum and oxygen minimum depths. Concentrations of $MM^{198}Hg$ in t0 bottles ranged between 41-44 fM in water from the chlorophyll maximum depth and only 11-23 fM in water from the oxygen

minimum depth, or 1-3% of the 1346 fM added $MM^{198}Hg$ spike. The values for k_d shown in Table 3 from October incubations therefore are not directly comparable to those measured in April because they are not integrated over the entire incubation period. Instead, they represent demethylation from secondary methylation of newly produced $MM^{198}Hg$ that may have a distinct k_d value compared to that of demethylation of $MM^{198}Hg$ from the pre-equilibrated spike.

The rapid demethylation of $MM^{198}Hg$ in the October incubations presumably produced $^{198}Hg(II)$ (as well as $^{198}Hg(0)$) that could serve as a substrate for methylation, which may account for the slight increases observed in measured $MM^{198}Hg$ observed over time, most notably in water from the oxygen minimum depth (Figure 4). However, the substantial variations in measured $MM^{198}Hg$ between bottles, resulted in non-significant differences between time points (Figure 4).

Discussion

In these incubations of marine waters, environmentally relevant concentrations of added $MM^{198}Hg$ and $^{202}Hg(II)$ were pre-equilibrated with natural ligands in filtered seawater prior to addition to incubation bottles in order to more closely mimic conditions by which methylation and demethylation occur in situ. Although we quantify conversion between Hg(II) and methylated Hg from spike additions, large values of initial methylation in 0.2 μm filtered samples suggests that methylation potential remains heavily influenced by interactions between Hg(II) and pools of natural ligands in seawater. The initial methylation observed in 0.2 μm filtered seawater samples was not observed in the pre-equilibrated spike solutions, which differed from incubation water primarily in the relative concentrations of Hg(II) to natural ligands. Assuming ligand binding sites occur at maximum concentrations of 0.3 nN in marine waters [Lamborg et al, 2004], the ratio of Hg(II) to equilibrated ligand binding sites is 124 in the equilibrated spike and decreases to 0.007 in the incubation bottles. Ligands may therefore play an important role in influencing methylation reactions. We observed initial methylation in 0.2 μm filtered water from both depths in both sets of incubations, which may indicate a role of dissolved ligands in the process.

We observed higher percentages of initial methylation in April than was found in previous measurements in Arctic waters. Lehnherr et al, 2011 observed methylation of 0.03-0.25% of added Hg(II) substrate in t0 bottles. We observed significantly higher initial percentages, >5%, in April incubation (Figure 1), although, as noted above, this occurred over the

relatively long period of time between spike addition and t0 sample preservation (2 hours vs 30 minutes). Because Lehnherr et al, 2011 added significantly higher concentrations of Hg(II) substrate, 380 pM compared to the 2.2 pM used in our experiments, the larger percentages of methylated Hg observed in our April incubations represent similar total methylted Hg produced in Arctic waters. The methylated Hg produced in Arctic waters due to initial methylation represents 29-240 fmole methylated Hg [Lehnherr et al, 2011]. Despite the much larger percentages of methylated Hg from our April incubations, the total methylated Hg produced during these experiments represents ~28 fmole, similar to those observed in the Artic. In contrast, although we observed similar percentages, 0.03-0.27 % (Figure 3), of methylayed Hg(II) substrate in October incubations to those of Lehnherr et al, 2011, these represent ~3 fmole methylated Hg because of the much lower concentrations of Hg(II) that we added.

Unlike previous reports, the initial methylation we observed in April incubations was sufficient to result in a net loss of $Me^{202}Hg$ over the course of 24-hour incubations (Figure 1). Lehnherr et al, noted demethylation between 12 and 24 hours of incubation of MeHg that was produced from isotopically enriched Hg(II) substrate between 0 and 12 hours at 2 sites within the Canadian Arctic Archipelago [Figure 2a, Lehnherr et al, 2011]. The net loss of $Me^{202}Hg$ during the 24-hour incubation period indicates not only a similar transition from net methylation to net demethylation in the Sargasso Sea as was seen in some Arctic waters but also that the time scale of this transition is faster in the North Atlantic than the Arctic. However, since methylation in the April incubations was only measured at two time points, we cannot determine whether and for how long net methylation continued beyond the ~2 hour period over which initial methylation occurred. As a result, higher temporal resolution sampling over the course of 24-hour incubations is needed for water column methylation rate measurements.

Although we observed a decreased capacity for Hg(II) methylation during October incubations, the higher resolution sampling during the incubation time course show that the transition from net methylation to net demethylation of $Me^{202}Hg(II)$ took place between 4 and 8 hours of incubation in waters from the chlorophyll maximum as well as filtered water from the oxygen minimum (Figure 3). This suggests faster cycling of Hg between Hg(II) and MeHg pools in the Sargasso Sea compared to the Arctic, despite lower productivity.

Values of k_d measured in April from unfiltered waters are comparable to those measured in the Canadian Arctic Archipelago [Lehnherr et al, 2011], including a slight enhancement in k_d in the oxygen minimum depth (Table 3). The large enhancement in k_d in unfiltered relative to

filtered waters from the chlorophyll maximum depth (Table 3) demonstrates the importance of particles in demethylation, perhaps due to the high abundance of phytoplankton at this depth. Photodemethylation is also a potentially important process in surface waters (0.003-0.43 d^{-1}) [Whalin et al, 2007; Monperrus et al, 2007; Lehnherr et al, 2011]. Since our experiments were performed in the dark, we can only speculate as to the relative importance of photodemethylation and demethylation by particles, either abiotic or biotic in origin. However, the low concentrations of methylated Hg species observed in the upper ocean in the Sargasso Sea [Lamborg et al, 2012; Bowman et al, 2013] support photodemethylation as the dominant process in these waters.

Potential demethylation rates were more difficult to quantify during the October cruise compared to the April cruise, with time course measurements suggesting that essentially all of the added $MM^{198}Hg$ spike was lost immediately upon addition to bottle incubations despite remaining stable in filtered seawater during the 24-hour spike pre-equilibration. Although demethylation measured as the disappearance of isotopically enriched MMHg has been successfully measured in marine waters [Lehnherr et al, 2011], a more reliable measurement may be the monitoring of production of isotope specific Hg(II) formed from the breakdown of the enriched MMHg spike [Monperrus et al, 2007].

Analysis of $MM^{198}Hg$, especially in waters from the chlorophyll maximum depth, over the October incubation time course more closely resembles that of methylation than predicted demethylation (Figures 3, 4). The increase in $MM^{198}Hg$ from t0 to t2-hr for both unfiltered and filtered water as well as the subsequent decrease in $MM^{198}Hg$ within 8 hours of incubation (Figure 4) are similar to those observed in time course measurements of $Me^{202}Hg$ production from $^{202}Hg(II)$ substrate (Figure 3).

Because methylation in sedimentary systems is known to occur by bacterial processes, a significant aim of the present study was to determine whether marine Hg methylation is likewise a cellular process. In order to address this question, we compared potential methylation rates in water filtered through a 0.2 μm pore size capsule filter to unfiltered water and incubated in the dark to determine the methylation potential of heterotrophic bacteria. The clearest indication of heterotrophic methylation is the sustained methylation in unfiltered waters from the oxygen minimum depth during October sampling (Figure 3).

Together these data suggest that oligotrophic marine waters have the capacity to methylate available Hg(II) substrate. Despite the inconsistencies in results between the 2 sets of incubations, measureable initial methylation in both filtered and unfiltered water suggests that

although the yet unidentified compounds in marine water responsible for methyl donation to Hg(II) might be of biological origin, they do not require intact cells for methylation to take place. However, this MeHg that is rapidly produced appears to be short-lived in marine waters, especially in the presence of particles, based on the rapid transition from net methylation to net demethylation. Whether or not this MeHg is available for uptake and bioaccumulation is unknown but has the potential to greatly impact human health as THg concentrations change in marine waters.

Alternatively, the enhancement of methylation in unfiltered water relative to filtered water in the October incubations is consistent with previous assumptions that heterotrophic bacteria contribute to Hg methylation in oxic marine waters [Mason and Fitzgerald, 1993; Monperrus et al, 2007]. Furthermore, in low oxygen waters of the Sargasso Sea, heterotrophic bacteria appear to be able to sustain MeHg production over the course of 24-hour incubations and may therefore supply MMHg for accumulation through marine food webs.

Acknowledgements

We thank Rod Johnson, Steve Bell, Gwyn Evans, Kristen Buck, and Mike Lomas for providing ship time, assistance with water sampling, and generous use of lab space and equipment. We also thank Jane Burrows at the Bermuda Institute of Ocean Sciences and Ronni Schwartz at the Massachusetts Institute of Technology for administrative help. This research was funded by the Scurlock Fund from the Massachusetts Institute of Technology, a Graduate Research Fellowship from the National Science Foundation awarded to K. M. Munson, and grant OCE-1031271 from the National Science Foundation awarded to C. H. Lamborg and M. A. Saito.

References

Bowman, K. R., C. R. Hammerschmidt, C. H. Lamborg, and G. Swarr (2013) New insights on mercury speciation with fully resolved high-resolution profiles across a zonal section of the North Atlantic Ocean. Presentation at the Aquatic Sciences Meeting, New Orleans, LA.

Clarkson, T. W., and J. Magos (2006) The toxicology of mercury and its chemical compounds. Crit. Rev. Toxicol. 36, 609-662.

Cossa, D., L. E. Heimburger, D. Lannuzel, R. S. Rintoul, E. C. V. Bulter, A. R. Bowie, B. Averty, R. J. Watson, and T. Remenyi (2011) Mercury in the Southern Ocean. Geochim. Cosmochim. Acta 75, 4037-4052.

Graham, A. M., A. L. Bullock, A. C. Maizel, D. A. Elias, C. C. Gilmour (2012) Detailed assessment of the kinetics of Hg-cell association, Hg methylation, and methylmercury degredation in several Desulfovibrio species, Appl. Environ. Microbiol. 78, 7337-7346.

Hintelmann, H., and R. D. Evans (1997) Application of stable isotopes in environmental tracer studies – measurement of monomethylmercury (CH_3Hg^+) by isotope dilution ICP-MS and detection of species transformation, Fresenius J. Anal. Chem., 358, 378-385.

Hintelmann, H., and N. Ogrinc (2003) Determination of stable mercury isotopes by ICP/MS and their application in environmental studies, in Biogeochemistry of environmentally important trace elements, Eds: Cai, Y., and C. O. Braids, ACS Symp Ser Vol. 835, Washington, DC, p. 321-338.

Krabbenhoft, D. P., and E. M. Sunderland (2013) Global change and mercury. Science, 341, 1457-1458

Lamborg, C. H., C. R. Hammerschmidt, G. A. Gill, R. P. Mason, and S. Gichuki (2012) An intercomparison of procedures for the determination of total mercury in seawater and recommendations regarding mercury speciation during GEOTRACES cruises, Limnol. Oceanogr.: Methods 10, 90-100.

Laurier, F. J. G., R. P. Mason, G. A. Gill, and L. Whalin (2004) Mercury distributions in the North Pacific Ocean—20 years of observations, Mar. Chem., 90, 3-19.

Lehnherr, I., V. L. St Louis, H. Hintelmann, and J. L. Kirk (2011) Metyhlation of inorganic mercury in polar marine waters, Nature Geosci. 4, 298-302.

Mason, R. P., A. L. Choi, W. F. Fitzgerald, C. R. Hammerschmidt, C. H. Lamborg, A. L. Sørensen, and E. M. Sunderland (2012) Mercury biogeochemical cycling in the ocean and policy implications, Environ. Res.,119, 101-117.

Mason, R. P., and W. F. Fitzgerald (1993) The distribution and cycling of mercury in the equatorial Pacific Ocean. Deep Sea Res. Part I 40, 1897-1924.

Monperrus, M., E. Tessier, D. Amouroux, A. Leynaert, P. Huonnic, and O. F. X. Donard (2007) Mercury methylation, demethylation and reduction rates in coastal and marine surface waters of the Mediterranean Sea, Mar. Chem., 107, 49-63.

Schaefer, J. K., S. S. Rocks, W. Zheng, L. Liang, B. Gu, and F. M. M. Morel (2011) Active transport, substrate specificity, and methylation of Hg(II) in anaerobic bacteria. Proc. Natl. Acad. Sci., 108, 8714-8719.

Sørensen, A. L., D. J. Jacobs, D. G. Streets, M. L. I. Witt, R. Ebinghaus, R. P. Mason, M. Andersson, and E. M. Sunderland (2012) Multi-decadal decline of mercury in the North Atlantic atmosphere explained by changing subsurface seawater concentrations. Geophys. Res. Lett., 39, L21810.

Sørensen, A. L., E. M. Sunderland, C. D. Holmes, D. J. Jacob, R. M. Tantosca, H. Skov, J. H. Christensen, S. H. Strode, and R. P. Mason (2010) An improved global model for air-sea

exchange of mercury: High concentrations over the North Atlantic, Enivron. Sci. Technol., 44, 8574-8580.

Sunderland, E. M. (2007) Mercury exposure from domestic and imported estuarine and marine fish in the US seafood market. Environ. Health Perspec. 115, 235-242.

Sunderland, E. M., D. P. Krabbenhoft, J. W. Moreau, S. A. Strode, and W. M. Landing (2009) Mercury sources, distribution, and bioavailability in the North Pacific Ocean: insights from data and models. Gobal Biogeochem. Cy., 23, GB2010.

Whalin, L., E.-H. Kim, and R. P. Mason (2007) Factors influencing the oxidation, reduction, methylation and demethylation of mercury species in coastal waters. Mar. Chem., 107, 278-294.

Figures and Figure Legends

Figure 1: Quantification of Hg(II) standard. Integrations of the diethylHg peak area from chromatographic separation of Hg species detected after direct ethylation with the Tekran 2700 methylmercury analyzer show a strong linear relationship with concentrations of added Hg(II) standard. Although ethylation efficiency for Hg(II) was not determined, the linear response suggests ethylation was consistent across a range of Hg(II) concentrations. As a result, the diethylHg peaks can be used as minimum estimates of available Hg(II) substrate for normalization of methylated Hg production.

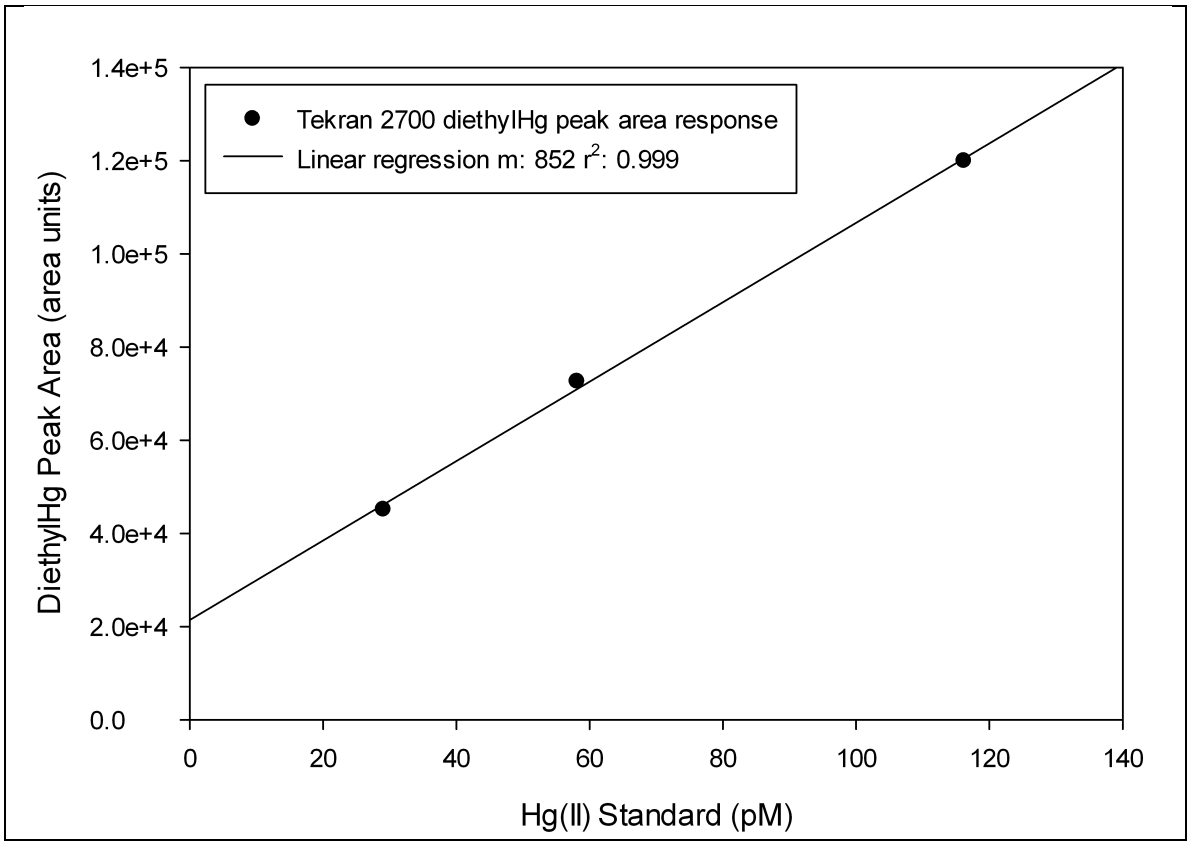

Figure 2: Methylated mercury production from the BATS site during the April spring bloom. $Me^{202}Hg$ produced from $^{202}Hg(II)$ added to water collected from the chlorophyll maximum (CMX, 105 m) and oxygen minimum zone (OMZ, 800 m) depths at the BATS site in April 2012. Initial methylation (black bars) was measured as a percentage of available $^{202}Hg(II)$ converted to $Me^{202}Hg$ at the t0 time point. 24-hour methylation (grey bars) was measured as the percentage of available $^{202}Hg(II)$ converted to $MM^{202}Hg$ after 24 hours of incubation. High initial methylation was observed in all samples and was sufficient to account for the total MeHg production over the course of 24-hour incubations. The error bars represent 1 standard deviation from triplicate incubation bottles.

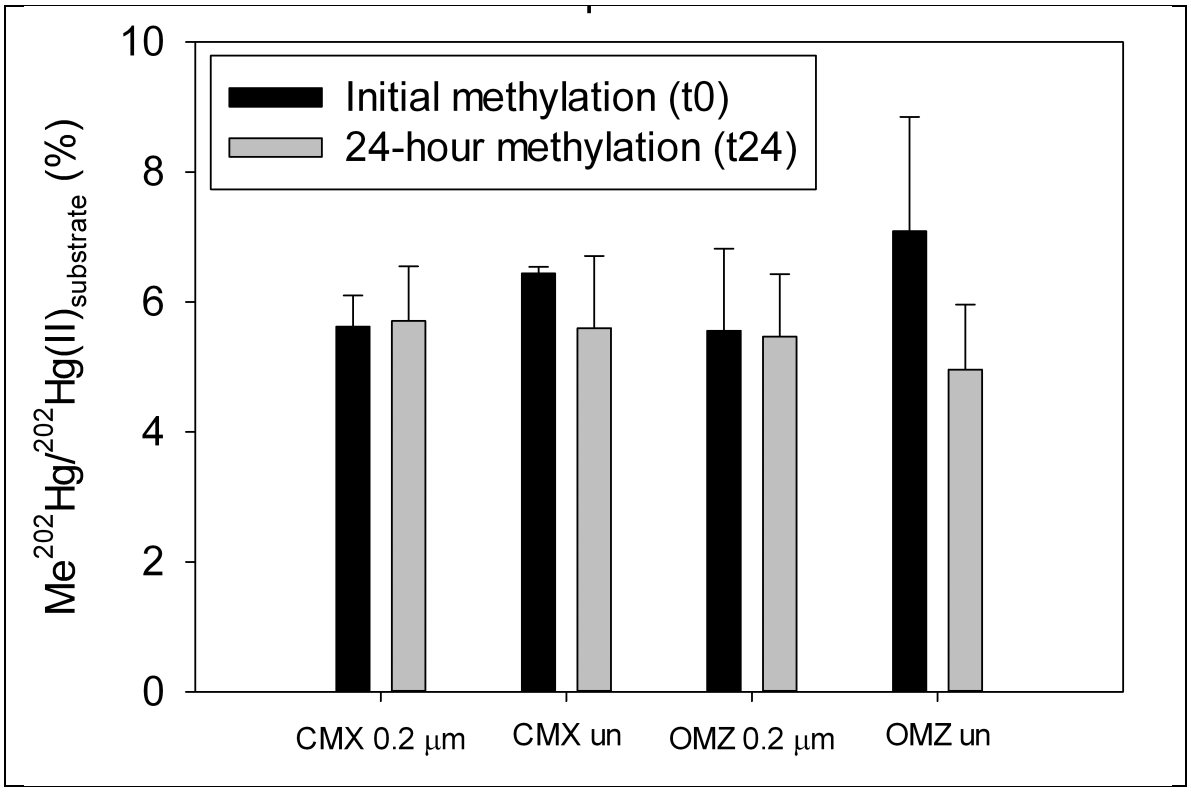

Figure 3: Methylated mercury production during 24-hour time course in the fall. Production of $Me^{202}Hg$ relative to $^{202}Hg(II)$ substrate over a 24-hour time course incubation of water from the chlorophyll maximum (CMX, 120 m, circles) and the oxygen minimum depth (OMZ, 800 m, triangles) at the BATS site. Initial methylation was observed in both 0.2 μm filtered (black symbols) and unfiltered (white symbols) seawater from both depths at the BATS site in October 2012. Methylation continues through the first 4 hours for 0.2 μm filtered seawater at both depths before demethylation of newly synthesized $Me^{202}Hg$ begins. The presence of particulate matter in unfiltered waters from the chlorophyll maximum appears to enhance demethylation. In contrast, with the exception of a spike in both methylation and demethylation at t0.5 hr, the presence of particulate matter, which likely includes heterotrophic bacteria sustains methylation throughout the 24-hour incubation. The error bars represent 1 standard deviation from triplicate incubation bottles.

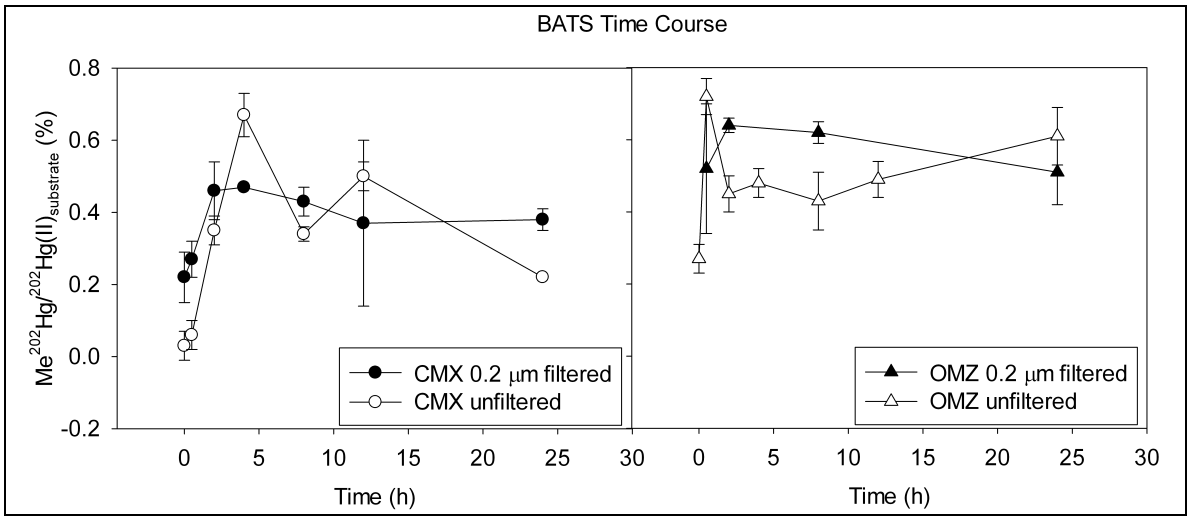

Figure 4: Methylmercury degradation during 24-hour time course incubation in the fall. Total changes in $MM^{198}Hg$ concentration with time in 0.2 um filtered (black symbols) and unfiltered (white symbols) from the depths of the chlorophyll maximum and oxygen minimum at the BATS site in October 2012. Triplicate bottles show large variability that result in no significant change in waters from the chlorophyll maximum and oxygen minimum depths at the BATS site. Concentrations of $MM^{198}Hg$ are a small percentage, 1-3 %, of the total 1230 fM added in the $MM^{198}Hg$ spike even in by the t0 time point. The $^{198}Hg(II)$ produced from this demethylation appears available for subsequent methylation between t0 and t2-t4 hr in waters from the chlorophyll maximum depth. Secondary demethylation, occurs after t2-t4 hr and indicates that methylation and demethylation cycles are dynamic within the euphotic zone of oligotrophic waters. The error bars represent 1 standard deviation from triplicate incubation bottles.

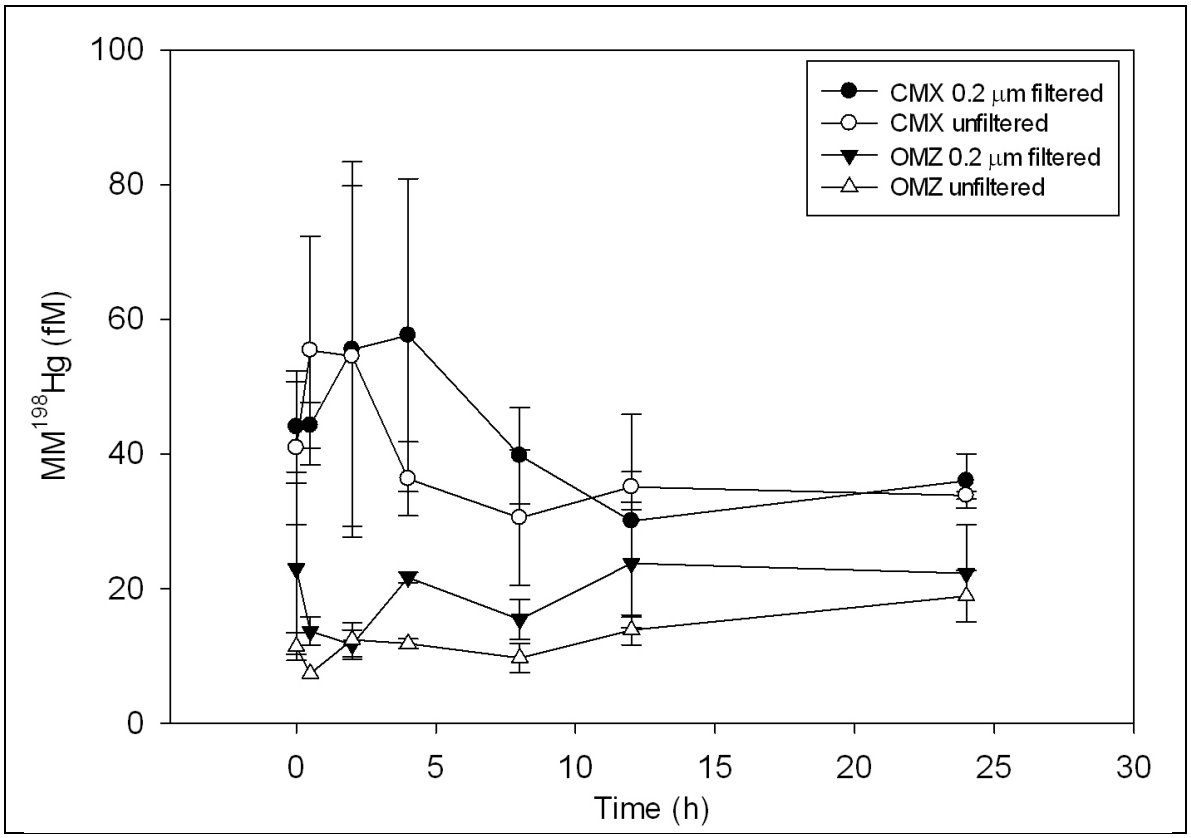

Tables and Table Legends

Table 1: Experimental details for measurements of mercury methylation and demethylation potential in waters from the BATS site.

Cruise	Depth (m)	MMHg (fM)	Hg(II) (pM)	O_2 (µmol/kg)	$MM^{198}Hg$ (fmol)	$^{202}Hg(II)$ (fmol)
April	120	15.8 ± 1.6	0.41	220	126	396
	800	54.7 ± 1.0	0.40	148	126	396
October	105	22.9 ± 1.5	2.06	215	242	1260
	800	26.2 ± 0.9	1.52	148	242	1260

Table 2: Potential demethylation rates from water collected from the BATS site. Potential demethylation rates were measured from the loss of $MM^{198}Hg$ in incubations of water from the chlorophyll maximum and oxygen minimum depths at the BATS site in April and October 2012. are greater in unfiltered water compared

Sample	April k_d (d^{-1})	October k_d (d^{-1})*
CMX 0.2 µm filtered	**0.05**	**1.6**
CMX unfiltered	**0.32**	**2.1**
OMZ 0.2 µm filtered	**0.39**	**nd****
OMZ unfiltered	**0.44**	**nd****

*k_d for October were calculated over the time period where $MM^{198}Hg$ decreased, between t4 hr-t12 hr for CMX 0.2 µm filtered, t0.5 hr-t8 hr for CMX unfiltered. April k_d values were calculated over 24-hours.

**nd showed no significant decrease in $MM^{198}Hg$ over the incubation time course

Table 3: Potential methylation rates for water collected from the BATS site. Methylation rates (k_m) calculated from total methylated mercury production over 24 hours of dark incubation in filtered and unfiltered water from the chlorophyll maximum (CMX) and oxygen minimum (OMZ) depths during the April bloom cruise and the October cruise.

Sample	April total k_m ($x10^{-2}$ d^{-1})	October total k_m ($x10^{-2}$ d^{-1})
CMX 0.2 µm filtered	**5.00 ± 0.90**	**0.38 ± 0.03**
CMX unfiltered	**5.17 ± 1.03**	**0.22 ± 0.00**
OMZ 0.2 µm filtered	**5.05 ± 1.46**	**0.51 ± 0.09**
OMZ unfiltered	**4.58 ± 1.87**	**0.61 ± 0.08**

Chapter 4
Mercury Species Concentrations and Fluxes in the Central Tropical Pacific Ocean

Kathleen M. Munson,[1,2] Carl H. Lamborg,[1] Gretchen J. Swarr,[1] Mak A. Saito[1]

1. Department of Marine Chemistry and Geochemistry, Woods Hole Oceanographic Institution, Woods Hole, MA 02543
2. MIT/WHOI Joint Program in Chemical Oceanography

Preparation for submission to *Global Biogeochemical Cycles*

Abstract:

Consumption of marine fish exposes humans to potentially harmful concentrations of monomethylmercury (MMHg). The complex cycling of mercury (Hg) in marine environments poses analytical challenges that limit our understanding of the temporal trends in mercury cycling and its potential for entering marine foods webs. We present dissolved mercury speciation data from 10 stations in the North and South Equatorial Pacific. In addition, we compare the mercury content in suspended particles from 6 stations and sinking particles from 3 stations to constrain the sources and sinks of mercury along large water mass differences and gradients in oxygen utilization. In general, concentrations of methylated Hg are low with maximum concentrations, ~0.18 pM for both MMHg and dimethylmercury (DMHg) species, observed in the equatorial Pacific. South of the Equator, concentrations of MMHg and DMHg fall to 0.1 pM. Notably, both THg and methylated Hg species in the upper 1000 m show a significant decrease from those measured in the North Pacific Intermediate Water (Sunderland et al, 2009). Combined, THg and methylated Hg concentrations in the surface and intermediate waters suggest Hg cycling distinct from that of the North Pacific gyre. Suspended particulate THg and MMHg comprise a small percentage of the dissolved concentrations but show distinct trends, increasing in importance with depth. Sinking fluxes of THg can reasonably explain the shape of dissolved THg profiles, but those of MMHg are far too low to account for dissolved MMHg profiles. In contrast to the upper ocean full depth profiles reveal, for the first time, elevated concentrations of THg extending into deep waters of the North Pacific and tapering off in the South Pacific. These deep water data reveal the contrast between anthropogenically impacted and unimpacted waters. Despite higher THg concentrations at depth, concentrations measured between the surface-1000 m compared to those observed in previous cruises in the North and Equatorial Pacific suggest minimal temporal changes in this region on decadal time scales.

Introduction

The exposure of humans to the toxic element mercury is linked to its chemical speciation in marine environments. Humans are exposed to the bioaccumulating organic monomethylmercury (MMHg) through consumption of fish. Despite its elevated concentrations in a variety of piscivorous fish, MMHg is often found at concentrations composing <15% of total mercury (THg) in the water column of the Atlantic and Pacific Oceans [Hammerschmidt and Bowman, 2012; Cossa et al, 1997; Mason and Sullivan, 1999; Sunderland et al, 2009; Mason and Fitzgerald 1991; Mason and Fitzgerald, 1993]. Unlike freshwater systems, marine environments can also contain significant concentrations of the dissolved gaseous organic form dimethylmercury, DMHg [Cossa et al, 1997; Mason and Fitzgerald, 1990; 1993; Mason and Sullivan, 1999; Hammerschmidt and Bowman, 2012].

Water column methylation of inorganic divalent Hg(II) has long been invoked to account for elevated MMHg and DMHg concentrations observed in the marine water column [Mason and Fitzgerald, 1993; Sunderland et al, 2009; Hammerschmidt and Bowman, 2012; Cossa et al, 2011]. Although resulting MMHg concentrations depend on the availability of the Hg(II) substrate for methylation, prediction of methylation is complicated by the redox chemistry of Hg(II), which can be reduced to gaseous elemental Hg (Hg(0)). As a result of its multiple identities in marine environments, the bioaccumulation of Hg in marine foods webs and ultimate exposure of humans to mercury depends on the transformations between Hg pools.

Despite the importance of quantifying the speciation of Hg to understand its potential for entering marine food webs, measurements of all four methylated and inorganic Hg chemical species are limited to a few areas in the open ocean. Mason and Fitzgerald (1993) first measured MMHg and DMHg in the Pacific. However, their relatively high detection limits of 50 fM resulted in measurable concentrations of MMHg in only~30% of water depths analyzed [Mason and Fitzgerald, 1993]. Hammerschmidt and Bowman, 2012, provided dissolved speciation of methylated and total Hg as well as particulate THg and MMHg at a single site in the North Pacific. However, recent efforts to determine sources of MMHg are hampered by analytical challenges in preserving Hg speciation. Due to its instability in acidic conditions, DMHg cannot be easily preserved for shore-based determination. As a result, studies of MMHg production have relied on total methylated Hg concentrations ([DMHg]+[MMHg]) [Sunderland et al, 2009; Cossa et al, 2011].

The long-standing model for MMHg production attributes marine MMHg to the breakdown of DMHg, which in turn is produced directly from Hg(II) [Mason and Fitzgerald, 1993]. More recently, measurements of water column methylation have suggested that direct production of MMHg from Hg(II) dominates in the Arctic water column [Lehnherr et al, 2011]. MMHg, but not DMHg, bioaccumulates in marine phytoplankton. As a result, distinguishing between distributions and production of these methylated Hg species has the potential to provide important insight into the link between dissolved Hg concentrations and resulting fish MMHg concentrations.

Even less frequently reported than full speciation data sets are studies that include particulate concentrations and sinking fluxes of Hg species. Including such measurements can help resolve potential movement and in situ generation of Hg species within the ocean. From a site in the North Pacific. Hammerschmidt and Bowman, 2012 observed increases in the ratio of particulate MMHg to particulate carbon that indicate either the preferential retention of MMHg on particles, particle scavenging of MMHg win the water column, or production of MMHg on sinking particles [Hammerschmidt and Bowman, 2012].

A recent analysis of North Pacific water found that increased Asian emissions, roughly a doubling over the past 25 years [Pacyna et al, 2006], had resulted in increased methylated Hg concentrations in the North Pacific Intermediate Waters (NPIW) due to water column in situ methylation [Sunderland et al, 2009]. While not overlapping, the stations occupied in the presented work extend the transect of Sunderland et al, 2009 as well sample waters measured two decades prior by Mason and Fitzgerald [1990; 1993] in 1990. As a result, we are able to evaluate whether those increases observed by Sunderland et al, 2009 extend throughout the North Atlantic or are limited in geographic range.

In the present study, we explore the full dissolved and particulate speciation of Hg across significant biogeochemical gradients in the Central Tropical North and South Pacific. We use these measurements to evaluate the fluxes of mercury species from the surface to the intermediate waters, explore potential sources of methylated Hg, and assess the impact of anthropogenic emissions on the North and Tropical Pacific Ocean.

Materials and Methods

Dissolved and particulate mercury speciation was measured from a subset of stations (Table 1) occupied in the North and South Central Pacific Ocean between 3-24 October 2011 on

board the *R/V Kilo Moana* (Figure 1). These stations were occupied as part of the Metzyme cruise (Lamborg and Saito, chief scientists), whose goal was to explore the distribution and activity of micronutrients and metalloproteins in the ocean across a gradient of primary productivity and subsurface respiration. Water for dissolved Hg determination was sampled from 8 stations roughly following a North to Southwest transect beginning southeast of Hawaii at 17°N 154°W and ending at 12°S 168°W and 2 stations heading west along 15°S south of Samoa. Suspended particles for Hg and MMHg determination were collected by deployment of large volume in situ pumps at various depths at 6 stations spanning the North to Southwest cruise transect. Sinking particles for THg and MMHg determination were collected in sediment traps deployed at 3 stations between 17°N and the Equator.

Water for dissolved mercury speciation measurements was collected in acid-rinsed 8-L X-Niskin bottles attached to a dedicated epoxy-coated trace-metal sampling rosette (SeaBird) and deployed on Amsteel line. Bottle sampling was triggered by a SeaBird Autofiring Module programmed to activate bottles by pressure during up-casts. Niskin bottles were decanted in a positive pressure, HEPA-filtered water sampling bubble constructed from plastic sheeting. Decanting took place under ultra-clean N_2 pressure through 0.2 μm polyethersulfone filters (Supor).

Suspended particles were sampled from between 4-14 depths at 6 stations along the cruise track (Table 1) using in situ pumps (McLane Research Laboratories, Inc.). Sampling of suspended particles was biased towards stations north of the equator. Suspended particles were collected on combusted, acid-cleaned quartz microfiber filters (1-μm, Whatman QMA) after an in-line acid-cleaned polyester mesh pre-filters (51-μm, Sefar Petex 07-51/33) to provide particles of two particulate size fractions. Subsamples of the large size fraction (> 51-μm) were not available for Hg analysis, thus we present particulate Hg data for the < 51-μm size fraction. The pumps were deployed for up to 3 hours in order to pump ~1000 L of seawater through the filters. Filters that were installed and deployed but through which no water was pumped, were processed as blanks.

Sinking particles were collected in acid-cleaned polycarbonate particle collection tubes with removable 250-mL low density polyethylene bottles as collection cups arranged in PVC frames at depths of 60 m, 150 m, and 500 m at stations 1, 3, and 5 using a surface-tethered system [Lamborg et al, 2008]. Twelve tubes at each depth were deployed containing a layer of 250mL of borate-buffered (pH = 8.2) seawater brine prepared from freezing filtered seawater and collecting

the concentrated seawater as it melts. Above the brine, each tube was filled with borate buffered filtered seawater (pH 8.2) [Lamborg et al, 2008]. Three capped tubes were deployed in the trap array as process blanks. Upon recovery, the tubes were allowed to sit for 1 hour to allow any particles in the tube to finish sinking. The bottles were then removed and portions of the contents filtered on either pre-weighed polycarbonate membranes (1 μm, Nuclepore) or combusted quartz fiber filters (QMA). The membranes were used to determine mass and Hg species fluxes. The QMA filtered were used for C and N flux determinations.

Hydrographic Data

Depth, salinity, conductivity, and dissolved oxygen were measured by a SeaBird Electronics deployed on the trace metal rosette. Nutrient samples were filled with filtered seawater during Niskin decanting, frozen on board, and measured by the laboratory of Joe Jennings at Oregon State University.

From dissolved nitrate (NO_3^-) concentrations measured along the cruise transect, we calculated the parameter N* [Gruber and Sarmiento, 1997, Deutsch et al, 2001] to investigate the potential influences of nitrogen cycling on Hg speciation. The parameter is calculated by the following equation:

$$N^* = [NO_3^-] - ([PO_4^{3-}]*16) + 2.9 \text{ mmol } m^{-3}$$

Comparing the observed NO_3^- to the expected dissolved nutrient ratio according to Redfield stoichiometry can account for additions or absence of NO_3^-. As a result, N_2 fixation increases N* values while denitrification decreases N* values [Gruber and Sarmiento, 1997].

Total Mercury Determination

Filtered water for dissolved mercury speciation was decanted from the X-Niskin bottles into acid-cleaned 2-L Teflon bottles. Subsamples for total mercury (THg) were poured off into acid-cleaned 250-mL glass bottles (I-Chem) and oxidized with 0.1mL bromine monochloride (%) for >12 hours and pre-reduced with NH_2OH (1mL 30% wt:vol). Samples were then reduced with $SnCl_2$ and total mercury concentrations were determined by dual Au-amalgamation cold vapor atomic fluorescence spectrometry (CVAFS) with a Tekran 2600 against both gaseous Hg and aqueous Hg(II) standards.

Gaseous Mercury Determination

Gaseous elemental (Hg°) and dimethylmercury (DMHg) were purged directly from the remaining seawater in the 2-L Teflon bottles using a multi-port cap (Omnifit Q-series; Danbury, CT) and impinger with a fine pore frit that extends to the bottom of the bottle. Hg° and DMHg were purged from the seawater sample using ultra-pure N_2 gas (0.5 L min^{-1}) for 1 hour. The gaseous species were separated and pre-concentrated onto a gold-coated sand trap attached downstream of a Tenax trap in outlet of the purge cap [Lamborg et al, 2008]. After purging, traps were dried with Ar gas flow for 2 min. Hg° was determined using a Tekran 2600, while DMHg was determined using a Tekran 2500 following isothermal GC separation and pyrolysis to Hg°. Both analytical systems were calibrated with Hg° standard addition.

Methylmercury Determination

Following purging of gaseous mercury species, ~200mL subsamples for monomethylmercury (MMHg) determination were poured from the 2-L Teflon bottles into acid-cleaned 250-mL glass bottles (I-Chem) and acidified to 0.5% with concentrated H_2SO_4 (trace metal grade, Fisher Scientific). Samples were stored at -40°C and analyzed at the Woods Hole Oceanographic Institution using ascorbic acid-assisted direct ethylation [Munson—this work, Chapter 2]. Samples were buffered with either 2 M acetic acid or 1 M citric acid buffer (pH 5) and neutralized with KOH (45%) to pH 5. The addition of ascorbic acid (0.167% final v/v) allowed for enhanced MMHg determination from seawater after direct derivitization with sodium tetraethylborate (1%, in 2% KOH).

Sample bottles were fitted with Teflon backed silicon septa caps (I-Chem) and run on a Tekran 2700 Automated Methylmercury Analyzer equipped with a custom autosampler tray. MMHg concentrations were determined versus linear standard curves prepared daily with MMHg standards solution.

Suspended and Sinking Particulate Mercury

MMHg and THg in suspended and sinking particles were determined by digesting weighed filter portions in HNO_3 (2N, trace metal grade, Fisher) for 4 hours at 60°C with intermittent sonication. Digests were either oxidized with BrCl and processed as described above for THg determination or processed as described above for MMHg determination with direct

ethylation. Suspended particulate Hg species are presented as concentrations representing the measured Hg or MMHg collected on filters from known volumes of filtered seawater. Total filtered mass was not determined.

Results

Hydrographic Parameters

Salinity profiles of the cruise transect reveal a sharp transition between Station 1 (17°N) and Station 2 (12°N) (Figure 2). Station 1 displays the southern extent of the North Pacific Intermediate Waters in intermediate waters and high salinity surface waters. However, Stations 2 and 3 reveal lower salinity surface water at the surface, representing the convergence of the North Equatorial Current and the North Equatorial Counter Current. Waters with salinity values ~34.5 reach the surface at Stations 2 and 3 (12°N and 8°N, respectively) appears to segregate shallow waters (< 400 m) of the North Pacific from the Equatorial Pacific. Shoaling of nutrients and seasonal thermocline is observed at the edge of the North Pacific Subtropical Gyre. Upwelling of dissolved nutrients is apparent in the upper 150 m at Station 5 (0°N), where concentrations of H_3PO_4, > 0.6 µmol/L, and HNO_3, > 6 µmol/L persist (Figure 2). South of the Equator, high salinity waters are observed above a seasonal thermocline that extends deeper in the water column moving south.

Dissolved Mercury Speciation

Total Mercury

Surface concentrations of THg are low, < 0.5 pM, for all stations (Figure 5). These low concentrations extend through the mixed layer, ~75 m north of the Equator and to depths ~125 m south of the Equator. Below the mixed layer, THg concentrations approach ~1 pM reaching a maximum of ~1.5 pM in regions of the intermediate waters (<1000m in depth).

Elevated concentrations of THg (1.5-2 pM) are observed in deep waters (bellow 2000 m) at the northern end of the transect (17°N) and decrease (1.25-1.5 pM) moving south in deep waters south of the equator (5°S) (Figures 4, 8). These relatively high THg concentrations result from North Pacific Bottom Water moving south until they are replaced at depth (>4500 m) with Antarctic Bottom Water (S = 34.7, P15 WOCE, Jan-Mar 1996 S section, Sept/Oct 1994 N section). The resulting lower THg concentrations (~1 pM) in deep water south of 5 S fall within the range of those measured in the AABW (0.98-1.99 pM) [Cossa et al, 2011].

Elemental Mercury

Concentrations of Hg°, like those of THg, are low in the mixed layer with highest surface concentrations at Stations 1 and 2 where Hg° approaches 0.1 pM (Figure 5). Concentrations of Hg° generally increase below the mixed layer, reaching maximum concentrations in the upper water column immediately below the thermocline.

Two features are noted within this region immediately below the thermocline in the upper ocean profiles of Hg°. At Station 2 (12°N), a large Hg° maximum of 0.2-0.4 pM is focused at depths between 200-400 m (Figure 8). This maximum also extends to Stations 1 and 3. A second maximum of 0.2-0.35 pM Hg° was measured between 150 and 350 m at Station 10 (Figure 8).

Minimum concentrations of Hg° are generally observed immediately beneath the maximum concentrations at the base of the mixed layer (Figures 5, 8). In the South Pacific, this minimum is broad and extends to depths of 1000m. In the North Atlantic, this minimum in narrow and concentrations quickly increase from ~0.1 pM to 0.2 pM. In addition, at several depths within the region of the deep North Pacific where elevated THg was measured, Hg° concentrations increase to 0.2-0.3 pM.

With the exception of the two features noted above, Hg° concentrations appear to be controlled largely by temperature. Distributions of % Hg° saturation (Figure 9) are similar to those of Hg° concentrations (Figure 8) and do not appear to be influenced by THg, as % Hg° saturation normalized to THg (Figure 9) are similar to those of % Hg° saturation (Figure 8).

Monomethylmercury

Concentrations of MMHg approach detection limits in much of the surface ocean, with the exception of the Equator, where concentrations vary between 15-70 fM in the upper 200 m (Figure 7).

In the upper 1000 m of the ocean, MMHg appears to be distributed slightly asymmetrically around the equator, with elevated MMHg concentrations north of the Equator relative to south (Figure 8). The highest concentrations of MMHg observed along the cruise transect, 150-165 fM, are seen at the depths of the oxygen minimum at the equatorial station.

MMHg concentrations in the deep equatorial region are also elevated with respect to adjacent stations. MMHg concentrations increase from ~50 fM to 85-155 fM between 2000-3500 m at the equator (Figure 6).

Dimethylmercury

Concentrations of DMHg are generally higher than those of MMHg. In contrast to MMHg, DMHg in the surface ocean (>20m) was often above our detection limit, generally ~0.2 pM (Figure 7). DMHg, like MMHg, reaches its maximum concentrations, 0.12-0.16 pM, at depths with low oxygen concentrations. However, it is important to note that the highest DMHg concentrations are found at depths with intermediate dissolved O_2 concentrations (~60 μmol/kg) rather than minimum dissolved O_2 concentrations. Like MMHg, DMHg is distributed asymmetrically with the maximum concentrations measured north of the Equator at Station 4 (4°N) (Figure 8).

Beneath the mixed layer, DMHg concentrations average ~0.075 pM with slightly lower concentrations in south of the Equator.

In the deep ocean, elevated DMHg concentrations of ~0.1 pM were measured at several depths within waters with elevated THg concentrations, most notably at Station 3 (8°N) (Figure 6).

Suspended Particulate Mercury Speciation

Suspended particles collected from in situ pumps have low concentrations of both THg (THg_{susp}) and MMHg ($MMHg_{susp}$). THg_{susp} ranged from 0.01-0.05 pM from all stations and averaged 5.3 % (range: 1.0-27.4 %) of dissolved THg concentrations (Figure 11). $MMHg_{susp}$ ranged from 0.1-3.1 fM and averaged 3.7 % (range: 0.2-12.8 %) of dissolved MMHg concentrations (Figure 11). Previous measurements of Hg species in the Pacific have not distinguished between dissolved and particulate species [Mason and Fitzgerald, 1993; Laurier et al, 2004; Sunderland et al, 2009]. However, the low percentages of THg_{susp} and $MMHg_{susp}$ allow us to compare our measured values to those previously determined in the Pacific. Such comparisons are least accurate in surface waters, where suspended particles make up a greater percentage of total Hg species because of low dissolved species concentrations.

Concentrations of THg_{susp}, decrease slightly from the northern to southern ends of the cruise transect. THg_{susp} concentrations average 0.03 ± 0.001 pM at Stations 1 (n=8), 3 (n=14), 5 (n=13). South of the Equator, the concentration falls to 0.02 ± 0.002 pM at stations 6 (n=4), 8 (n=4), 9 (n=3).

Average $MMHg_{susp}$ concentrations, with the exception of Station 1 (0.7 fM, n=8), roughly decrease from Station 3 (1.6 fM, n=14) to Station 9 (0.4 fM, n=2).

Although the concentrations of THg_{susp} and $MMHg_{susp}$ are negligible compared to the dissolved species concentrations, the depth distributions of each suggest differences in the cycling of difference Hg species. THg_{susp} concentrations are generally highest within the upper 50 m of the water column (Figure 11). In contrast, $MMHg_{susp}$ concentrations are highest within 100 m of the depth of minimum dissolved O_2 concentration at each station measured (Figure 11). The only exception to these trends are at Station 1, where THg_{susp} could not be measured within the upper 50m and Station 9, where $MMHg_{susp}$ was not measured at 400m, where the dissolved O_2 concentration was lowest.

Sinking Particulate Mercury Speciation

Sinking particulate Hg fluxes attenuate with depth at each station, approaching 31.3 pmol/m^2/d (± 12.0) at 500 m for all three stations (Figure 13). Fluxes from the mixed layer were highest (156.6 pmol/m^2/d) at Station 5 and lowest (36.7 pmol/m^2/d) at Station 1. Assuming 80 % of wet and dry Hg deposition is rapidly evaded in the surface ocean [Mason and Sheu, 2002; Strode et al, 2007; Sørensen, et al 2010], measured particulate fluxes at all stations exceed deposited Hg, modeled by GEOS-Chem [Sørensen et al, 2012; Anne Sørensen, personal communication] (Figure 13). The observed fluxes therefore require additional inputs of Hg to Tropical Pacific waters, most notably at the Equator, where upwelling and lateral transport likely entrain THg.

Measured values of sinking particulate MMHg fluxes ranged between 0-1.63 pmol/m^2/d. A relatively high detection limit of 1.52 pmol/m^2/d prevents quantitative analysis of measured values. However, particle fluxes of MMHg appear to be small throughout the upper water column.

Apparent Oxygen Utilization

Elevated concentrations of methylated Hg species have commonly been measured in low oxygen regions of the open ocean water column [Mason and Fitzgerald, 1993; Sunderland et al, 2009; Hammerschmidt and Bowman, 2012; Cossa et al, 2011]. Possible explanations for in situ methylation in these regions include distinct microbial communities, release of Hg(II) substrate for methylation from organic matter during remineralization, or a combination of these factors.

The cruise transect bisected a variety of oxygen regimes (Figure 3). Beginning at Station 1, North Pacific Subtropical Gyre circulation distributes O_2 in the upper 200m of the water column. At this southern limit of the Gyre, we observed dissolved O_2 concentrations, ~20 μmol/kg between 400-800 m. Moving to the edge of the Gyre, at Station 2 is the strongest oxygen minimum zone of the cruise, with dissolved O_2 concentrations < 2 μmol/kg extending broadly between 200-900 m. At Station 3, the oxygen minimum zone remains broad 150-700 m but has dissolved O_2 concentrations again in the range of 20 μmol/kg. From Station 4 southward, the oxygen minimum zones weaken, with dissolved O_2 concentrations never falling below 50 μmol/kg.

Beginning at Station 8, elevated O_2 concentrations (> 80 μmol/kg) persist in the upper water column, increasing southward.

Apparent oxygen utilization ($[O_2]_{sat}$-$[O_2]_{meas}$) can be used to estimate the extent of dissolved O_2 utilization for means of organic matter remineralization [Garcia and Gordon, 1992 as modified by Sarmiento and Gruber, 2006]. Highest concentrations of methylated Hg were seen at intermediate values of apparent oxygen utilization (Figure 14)

As has been seen in previous studies, concentrations of methylated Hg ([DMHg] + [MMHg]) increases to a degree with AOU. However we observe an overall linear relationship between ([DMHg] + [MMHg]) versus AOU rather than the parabolic relationship observed by Sunderland et al, 2009. In addition, the relationship appears to differ significantly depending on station. Measurements from the CLIVAR P16N cruise found clustering of methylated Hg versus AOU by depth, perhaps due to largely sampling a single water mass of North Pacific Intermediate Water [Sunderland et al, 2009]. In contrast, we observe a tighter clustering of all depths by station, with wider ranges of AOU waters sampled in southern stations (Figure 14).

Relative Concentrations of Monomethylmercury and Dimethylmercury

Generally, at northern stations (Station 2-6), MMHg concentrations are similar to those of DMHg, with the exception of Station 4 (Figure 7). South of Station 6, MMHg concentrations fall more rapidly than DMHg, resulting in significantly higher DMHg concentrations compared to MMHg. At Station 12, MMHg concentrations are once again comparable to those of DMHg.

From their Hg speciation analysis at the SAFe station in the North Atlantic, Hammerschmidt and Bowman reported MMHg:DMHg molar ratios that they used to distinguish between a steady-state exchange of CH_3-groups between DMHg and MMHg throughout the

water column in contrast to the oxygen minimum zone, where an elevated MMHg:DMHg molar ratio was interpreted to suggest a different mechanism of CH_3-group transfer during in situ methylation [Hammerschmidt and Bowman, 2012]. They reported a MMHg:DMHg molar ratio ~2 throughout the water column, with the exception of the oxygen minimum zone, where the ratio increased to ~5 [Hammerschmidt and Bowman, 2012]. We observed MMHg:DMHg molar ratios that varied between stations, but were generally lower than those observed at the SAFe station. MMHg:DMHg molar ratio varied between 0.2-1, with maximum values near 3.5 (Figure 15, Station 3, 600 m). The ratio values generally decrease along the cruise track.

Discussion

Factors Controlling Mercury Speciation

Salinity contours of the cruise track show that the Station 1 sampled the southern boundary of North Pacific Intermediate Water, while Stations 2 and 3 show the influence of the North Pacific Subtropical Gyre in the upper 200 m of the water column.

The maximum of Hg° observed at Station 2 at the edge of gyre circulation occurs at a minimum of dissolved O_2, <2 μm/kg, a region of potential alternative metabolisms that might influence the production of Hg(0). From the distribution of N*, we see that the maximum in Hg° at Station 2 between 100-400m corresponds with a deficit in [NO_3^-], N*: range -6 to -8 mmol m^{-3} (Figure 10), which suggests denitrification at this depth. Analysis of δO and δN from these waters also reveal fractionation signals indicative of denitrification [P. Rafter, personal communication].

No direct link between marine denitrification and Hg reduction has been noted previously in the literature, although microbial mediated Hg reduction has observed in marine systems [Mason et al, 1995; Rolfhus and Fitzgerald, 2004; Poulain et al, 2007], Denitrification has been implicated as a pathway of Hg(II) reduction by *mer* operon-mediated reduction in bacteria [Schaefer et al, 2002; Kritee et al, 2008]. Therefore, it is plausible that the observed peak in Hg(0) at Station 2 is induced by the strong denitrification signal represented by the values of N* at this location. However, calculations of N* in waters across the transect show no additional regions where denitrification occurs to the extent that it does at Station 2. As a result, the potential for denitrification to influence Hg speciation on basin scales will rely on future measurements of Hg(0) in regions of denitrification.

In contrast to the maximum of Hg(0) at Station 2, the maximum at Station 10 (15°S) appears in waters of relatively high dissolved O_2 concentrations, 164 μM/kg, and no decreases in

N* value, indicated Hg(II) reduction that is independent of denitrification. This Hg(0) maximum in the South Pacific co-occurs with local maxima in both dissolved PO_4 and NO_3 (Figure 10). This maximum in Hg(0) occurs at a depth of 250 m, deeper than light penetration to drive photodemethylation and subsequent Hg(II) reduction. However, abiotic reduction mechanisms have also been found to dominate in some systems [Monperrus et al, 2007; Whalin et al, 2007; Qureshi et al, 2010].

The elevated concentrations of THg observed at depth demonstrate the clear distinction between waters extending from the North Pacific, where elevated concentrations of THg have been attributed to anthropogenic influences [Sunderland et al, 2009] and those in the Equatorial and South Pacific. However, these high THg concentrations are surprising given previous observations that tracers of entrainment of anthropogenic activity have not yet penetrated below 1000 m in the North Pacific [Mason et al, 2012].

The salinity data suggest that the observed attenuation of the elevated THg seen in depth profiles is likely the displacement of waters moving south from North Pacific with more dense Antarctic Bottom Water (AABW, S 34.65-34.75). Likewise, the concentration of THg in these higher salinity waters (<1.3 pM from Station 8, 4500-5000 m southward) is within the range measured recently in AABW [Cossa et al, 2011].

Fluxes of Mercury in the Central Pacific

Particulate THg fluxes closely agree with modeled fluxes from the mixed layer and are greater than regional wet and dry deposition [Sørensen et al, 2012; Anne Sørensen, personal communication] (Figure 13). Particulate THg fluxes are influential for both removal of Hg species through sorption onto sinking organic matter as well as Hg(II) delivery to intermediate waters for methylation [Sunderland et al, 2009]. However, the particulate fluxes of THg are surprising given the methylated Hg concentrations. Despite low particulate THg delivery at Station 1 (17°N, Figure 13), intermediate waters in the North Pacific have substantially higher methylated Hg species concentrations [Sunderland et al, 2009; Munson—this work, Chapter 5] than those measured in Equatorial and South Pacific stations (Figure 18). Conversely, higher particulate THg fluxes were measured at Station 3 (8°N) compared to Station 1 but did not result in higher methylated Hg concentrations (Figure 7). This indicates additional requirements, beyond Hg(II) substrate delivery, for Hg methylation in intermediate waters.

Temporal Trends in Dissolved Mercury Speciation

Despite the fact that it was one of the first regions where full Hg speciation was measured [Kim and Fitzgerald, 1986; 1988; Gill and Fitzgerald, 1988; Mason and Fitzgerald 1990, 1991, 1993], there have been no subsequent measurements of Hg in the Equatorial and South Pacific in the past two decades.

Comparisons of the closest stations sampled in 1990 to those sampled in 2011 show a decrease in THg concentrations both in the thermocline and in oxygen deficient waters. Above the thermocline (200 m), we observed a decrease from 1.72 pM THg (1.45 pM excluding St 4 outlier) to 0.24 pM (Figure 16). Below the thermocline, we observed a decrease of 1.23 pM (1.17 pM excluding St 4 outlier) to 0.66 pM (Figure 16).

Overall comparisons of profiles from the two cruises (Figure 16) shows that our measured THg concentrations in the upper water column are significantly lower than those in nearest stations of Mason and Fitzgerald, 1993. Deeper in the water column, however, some concentrations are similar, resulting in changes in both the shapes and the overall concentrations of mercury in 2011 compared to 1990. A clear maximum in THg at 500m was observed by Mason and Fitzgerald in the South Pacific waters between 0 and 10°S and 140°W and 170°E [Mason and Fitzgerald, 1993, Stations 4, 6, 8, 9]. This feature is absent from the depth profiles of THg from Stations 7 or 8, which fall within the area sampled by Mason and Fitzgerald (Figure 16). Instead, the shape of the profiles measured by Mason and Fitzgerald most closely resemble our profiles from Station 1-5 (Figure 5). However, even in the stations where the shape of the profiles resemble those of Mason and Fitzgerald, our data show a much lower THg concentrations in the upper 200 m (< 2 pM).

Sunderland et al, 2009 calculated a significant increase in THg concentrations measured during the North Pacific Intergovernmental Oceanographic Commission (IOC) cruise in 2002 [Laurier et al, 2004] and those measured from similar latitudes during the CLIVAR 2006 [Sunderland et al, 2009]. The THg concentrations from our Station 1 fall between those measured during IOC (Station 9) and CLIVAR P16N (Figure 18), suggesting that the temporal increase observed between 2002 and 2006 either did not penetrate to 17°N, the northernmost station along our transect, or has not continued in the subsequent period between measurements in this region. Similarities in the shape of the total mercury profile at Station 1 and Station 45 of the CLIVAR P16N cruise (Figure 18) suggest that similar processes determine the mercury distributions at both locations. North Pacific THg concentrations have been found to vary by up to factor of 2 at

open ocean stations separated by ~1000 km [Hammerschmidt and Bowman, 2012]. Since the IOC, CLIVAR, and Metzyme stations are separated from each other by ~750 km, it is possible that the differences in THg concentrations reflect spatial rather then temporal differences in North Pacific THg.

In addition, Sunderland et al, 2009 characterized the temporal increase in THg concentrations within the North Pacific Intermediate Water, a specific water mass that extends southward at ~155°W only to ~20°N [Talley, 1993]. As a result, we would not expect to see the impact of high THg or methylated Hg from NPIW to persist southward along the Metzyme cruise track. Instead the Central and Equatorial Pacific appears to be a region with distinct Hg cycling than the North Pacific (Figure 18).

Full Hg speciation from this transect of the Tropical Pacific Ocean reveals a region of low THg and methylated Hg relative to previous reports from the North Pacific [Sunderland et al, 2009]. The general decrease in THg, DMHg, and MMHg from the North Pacific toward the South Pacific follow increasing trends in dissolved oxygen concentrations. However, from sinking particulate THg fluxes, we observe that low concentrations, most notably of DMHg and MMHg, are not the result of limited THg supply to low oxygen regions of the ocean. Instead, THg availability to methylation appears to be limited. Indeed, in extremely low oxygen waters, denitrification appears to decrease DMHg and MMHg concentrations either by reduction of Hg(II) substrate or by demethylation and subsequent reduction of methylated Hg. Such processes must be taken into account when considering how changes in Hg emissions and ocean chemistry will ultimately impact MMHg bioaccumulation over time.

Acknowledgements

Financial support for this study was provided by the National Science Foundation in a grant from the Chemical Oceanography Program (OCE-1031271) to C. H. Lamborg and M. A. Saito and a Graduate Student Fellowship to K. M. Munson. We thank Erin Bertrand, Rene Boiteau, Tyler Goepfert, Nick Hawco, Dawn Moran, and David Wang for their assistance in water sampling, filtration, and pump deployment. We also thank Vic Polidoro, Trevor Young, Captain Drewry, and crew of the *R/V Kilo Moana* for making sample collection possible. We thank Anne Sørensen and Elsie Sunderland for providing electronic versions of published data.

We thank Bill Jenkins and John Bullister for advice and assistance with water mass age calculations.

References

Cossa, D., J.-M. Martin, K. Takayanagi, and J. Sanjuan (1997) The distribution and cycling of mercury species in the western Mediterranean. Deep Sea Res. II, 44, 721-740.

Cossa, D., L.-E. Heimburger, D. Lannuzel, S. R. Rintoul, E. C. V. Butler, A. R. Bowie, B. Averty, R. J. Watson, and T. Remenyi (2011) Mercury in the Southern Ocean. Geochim. Cosmochim. Acta 75, 4037-4052.

Deutsch, C., N. Gruber, R. M. Key, and J. L. Sarmiento (2001) Denitrification and N_2 fixation in the Pacific Ocean, Global Biogeochem. Cycles, 18, GB4012.

Garcia, H. E., and L. I. Gordon (1992) Oxygen solubility in seawater: better fitting equations, Limnol. Oceanogr., 37(6), 1307-1312.

Gill, G. A., and W. F. Fitzgerald (1988) Vertical mercury distributions in the oceans. Geochim, Cosmochim. Acta 52, 1719-1728.

Gruber, N., and J. L. Sarmiento (1997) Global patterns of marine nitrogen fixation and denitrification, Global Biogeochem. Cycles, 11, 235-266.

Hammerschmidt, C. R., and K. L. Bowman (2012) Vertical methylmercury distributions in the subtropical North Pacific Ocean, Mar. Chem., 132-133, 77-82.

Kim, J. P., and W. F. Fitzgerald (1986) Sea-air partitioning of mercury in the equatorial Pacific Ocean. Science 231, 1131-1133.

Kritee, K., J. D. Blum, M. W. Johnson, B. A. Bergquist, and T. Barkay (2007) Mercury stable isotope fractionation during reduction of Hg(II) to Hg° by mercury resistant microorganisms, Environ. Sci. Technol., 41, 1889-1895.

Lamborg, C. H., K. O. Buesseler, and P. J. Lam (2008),Sinking fluxes of minor and trace elements in the North Pacific Ocean measured during the VERTIGO program. Deep-Sea Res. II, 55, 1564-1577.

Laurier, F. J. G., R. P. Mason, G. A. Gill, and L. Whalin (2004) Mercury distributions in the North Pacific Ocean—20 years of observations, Mar. Chem., 90, 3-19.

Lehnherr, I., V. L. St. Louis, H. Hintelmann, and J. L. Kirk (2011) Methylation of inorganic mercury in polar marine waters, Nat. Geosci., 4, 298-302.

Mason, R. P., and W. F. Fitzgerald (1990) Alkylmercury species in the equatorial Pacific. Nature 347, 457-459.

Mason, R. P., and W. F. Fitzgerald (1991) Mercury speciation in open ocean waters. Water, Air, Soil Pollut., 56, 779-789.

Mason, R. P., and W. F. Fitzgerald (1993) The distribution and cycling of mercury in the equatorial Pacific Ocean, Deep Sea Res., Part I, 40(9), 1897-1924.

Mason, R. P., F. M. M. Morel, and H. F. Hemond (1995) The role of microorganisms in elemental mercury formation in natural waters, Air Water Soil Pollut., 80, 775-787.

Mason, R. P., and G.-R. Sheu (2002) Role of the ocean in the global mercury cycle. Global Biogeochem. Cy., 4, 1093.

Mason, R. P., K. A. Sullivan (1999) The distribution and speciation of mercury in the south and equatorial Atlantic. Deep Sea Res II, 46, 937-956.

Munson, K. M., D. Babi, C. H. Lamborg, (in review) Monomethylmercury determination from seawater using ascorbic-acid assisted direct ethylation.

Pacyna, E. G., J. M. Pacyna, F. Steenhuisen, and S. Wilson (2006) Anthropogenic mercury emission inventory for 2000. Atmos. Environ., 22, 4048-4063.

Poulain, A. J., S. M. Ni Chadhain, P. A. Ariya, M. Amyot, E. Garcia, P. G. C. Campbell, G. J. Zylstra, and T. Barkay (2007) Potential for mercury reduction by microbes in the high Arctic. Appl. Environ. Microbiol., 73, 2230-2238.

Qureshi, A., N. J. O'Driscoll, M. Macleod, Y.-M. Neuhold, and K. Hungerbuhler (2010) Photoreactions of mercury in surface ocean water: gross reaction kinetics and possible pathways. Environ. Sci. Technol. 44, 644-649.

Rolfhus, K. R., and W. F. Fitzgerald (2004) Mechanisms and temporal variability of dissolved gaseous mercury production in coastal seawater, Mar. Chem., 90, 125-136.

Sarmiento, J. L., and N. Gruber (2006) Ocean Biogeochemical Dynamics, 526pp., Princeton University Press, Princeton, New Jersey.

Schaefer, J. K., J. Letowski, T. Barkay (2002) mer-mediated resistance and volatilization of Hg(II) under anaerobic conditions, Geomicrobiol. J. 12, 8-102.

Schlitzer, R. (2004) Ocean Data View, http://odv.awi-bremerhaven.de.

Sørensen, A. L., D. J. Jacob, D. G. Streets, M. L. I. Witt, R. Ebinghaus, R. P. Mason, M. Andersson, and E. M. Sunderland (2012) Multi-decadal decline of mercury in the North Atlantic atmosphere explained by changing subsurface seawater concentrations. Geophys. Res. Letts. 39, L21810.

Sunderland, E. M., D. P. Krabbenhoft, J. W. Moreau, S. A. Strode, and W. M. Landing (2009) Mercury sources, distribution, and bioavailability in the North Pacific Ocean: Insights from data and models, Global Biogeochem. Cycles, 23, GB2010, doi: 10.1029/2008GB003425.

Talley, L. D. (1993) Distribution and formation of North Pacific Intermediate Water, J. Phys. Oceanogr., 23, 517-537.

Whalin, L., E.-H. Kim, and R. P. Mason (2007) Factors influenced the oxidation, reduction, methylation, and demethylation of mercury species in coastal waters. Mar. Chem., 107: 278-294.

Figures and Figure Legends

Figure 1: Map of Metzyme cruise stations. The Metzyme cruise left Honolulu, Hawai'i 1 October and arrived in Apia, Samoa 25 October, 2011. Dissolved, suspended particulate, and sinking particulate Hg species were collected at various stations along the cruise track (Table 1).

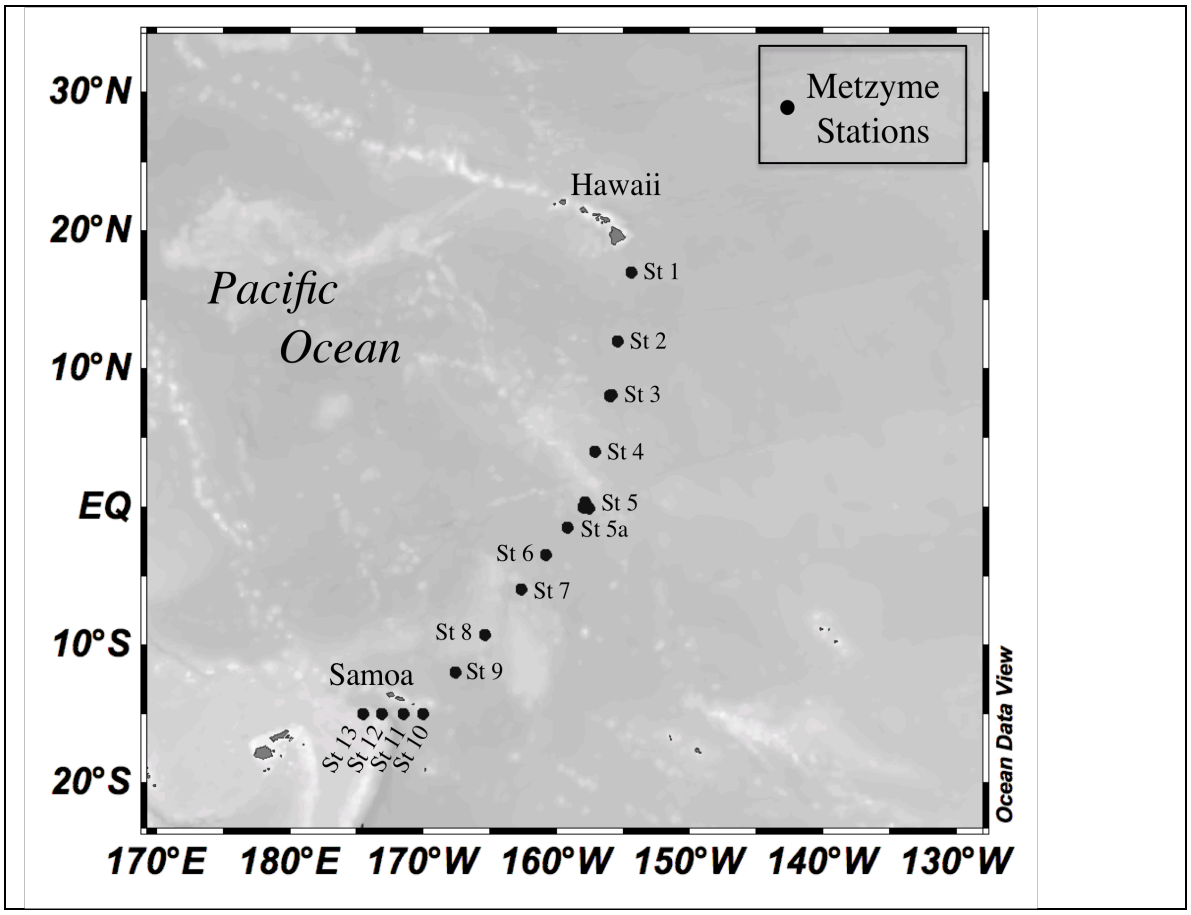

Figure 2: Hydrographic characteristics of the North to South transect of the Metzyme cruise. Temperature, salinity, and major nutrients phosphate and nitrate concentrations at Stations 1-10 for the upper 1000 m (upper panel) and full water column (bottom panel).

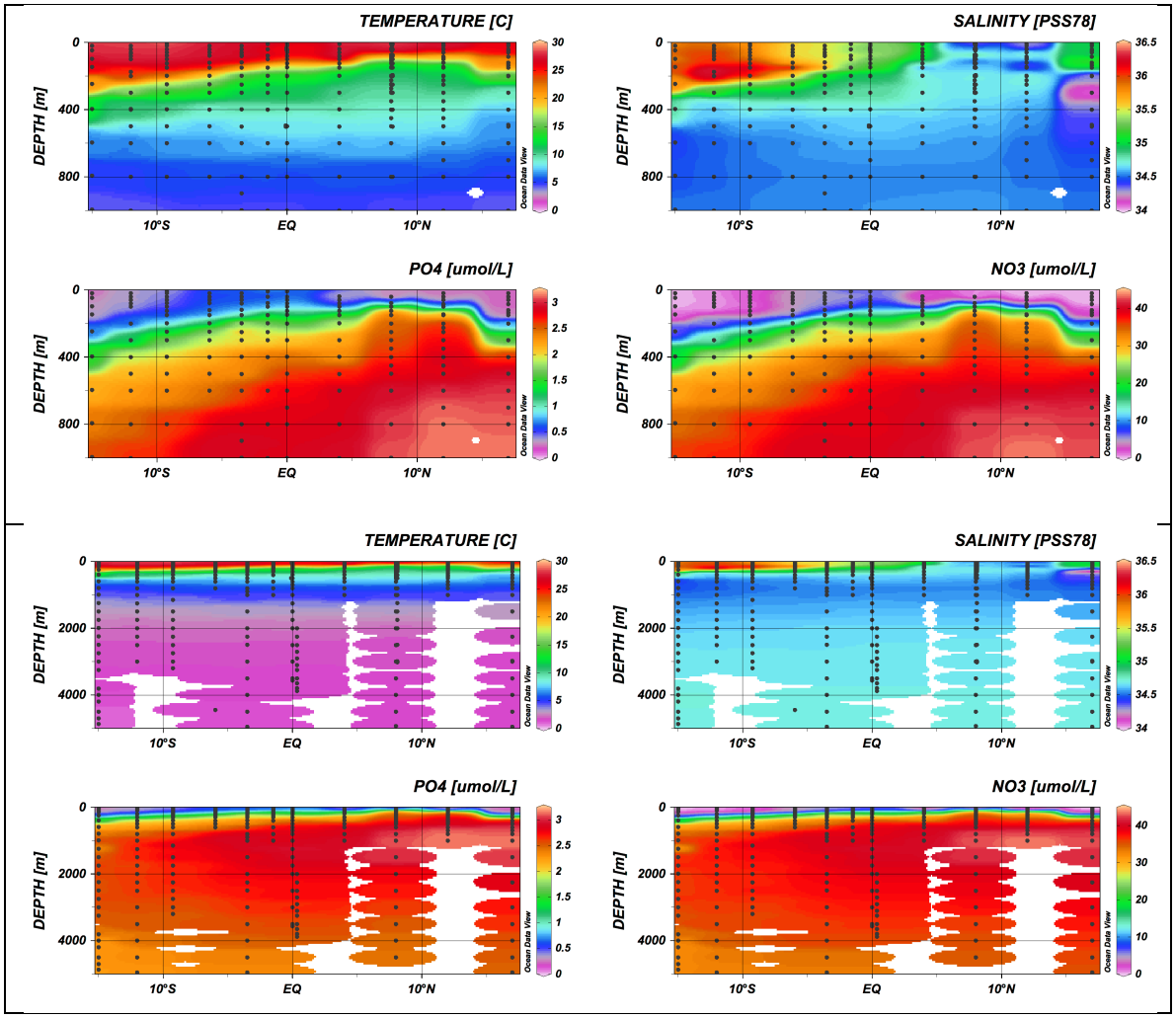

Figure 3: Oxygen and apparent oxygen utilization along the North to South transect of the Metzyme cruise. Dissolved oxygen and calculated AOU for upper 1000 m of Stations 1-10. Values of AOU are closely related to dissolved oxygen concentrations, with highest oxygen utilization centered at Station 2 (12°N) and extends to below the North Pacific Subtropical Gyre at Station 1 (17°N) and beneath the sharp oxycline at Station 3 (8°N). South of the Equator, gradients of both dissolved oxygen concentrations and AOU are weak throughout intermediate waters.

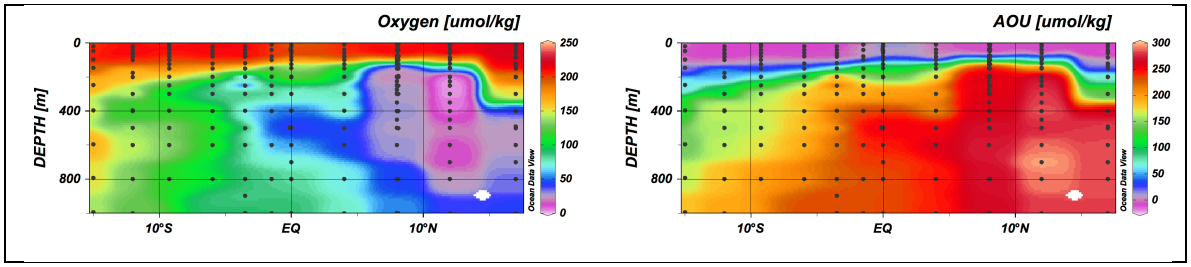

Figure 4: Full water column depth profiles of total mercury and elemental mercury at all stations along the Metzyme cruise track. Total Hg concentrations (black circles) are low at the surface and increase with depth. Hg° concentrations (white circles) often exhibit subsurface maxima as well as increasing concentrations in deep waters (> 2000 m).

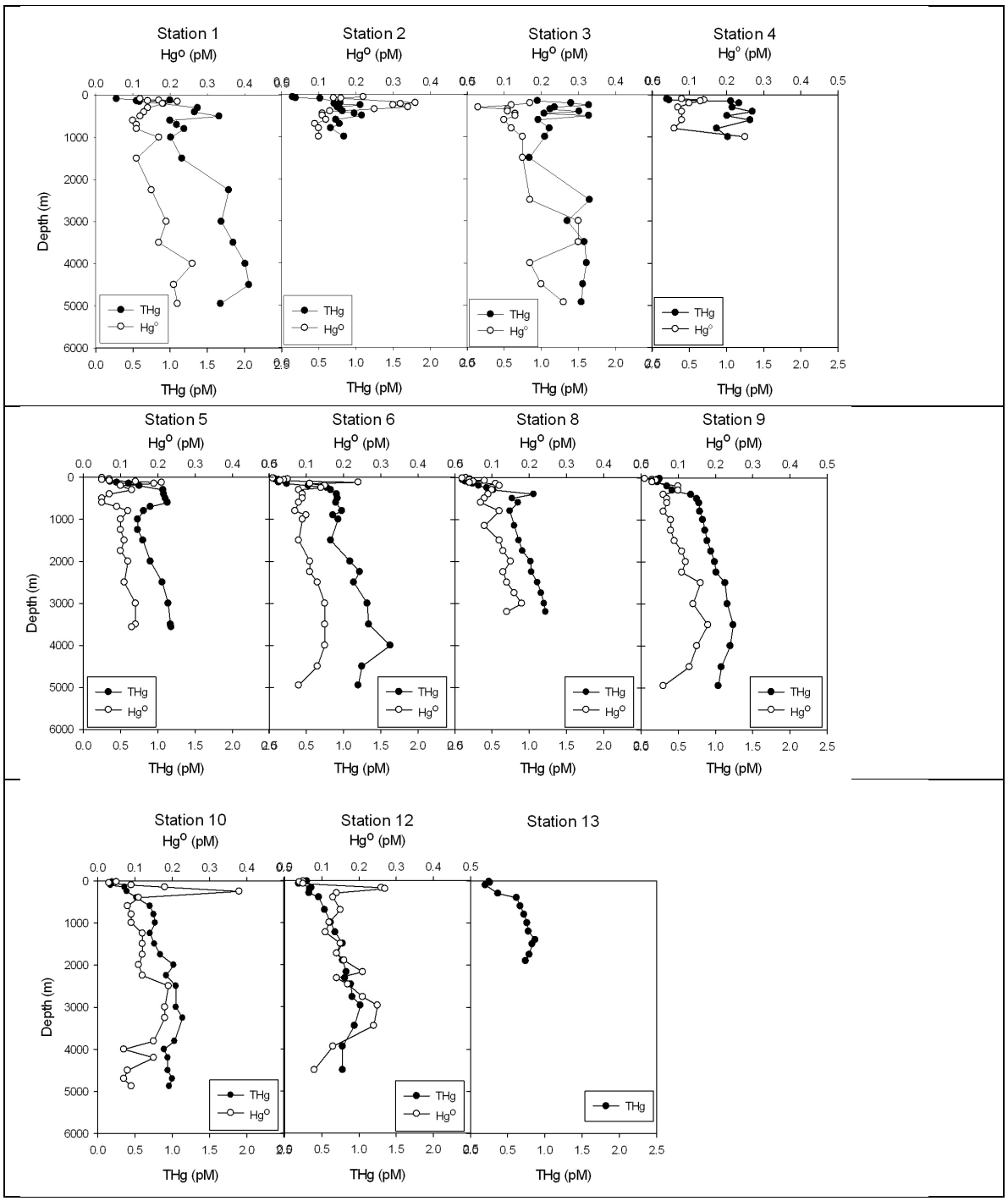

Figure 5: Upper 1500 m water column profiles of total mercury and elemental mercury at all stations along the Metzyme cruise track. Total Hg concentrations (black circles) are low at the surface and increase with depth. Surface THg concentrations are low and Hg° concentrations (white circles) often subsurface maxima in both the North and South Pacific away.

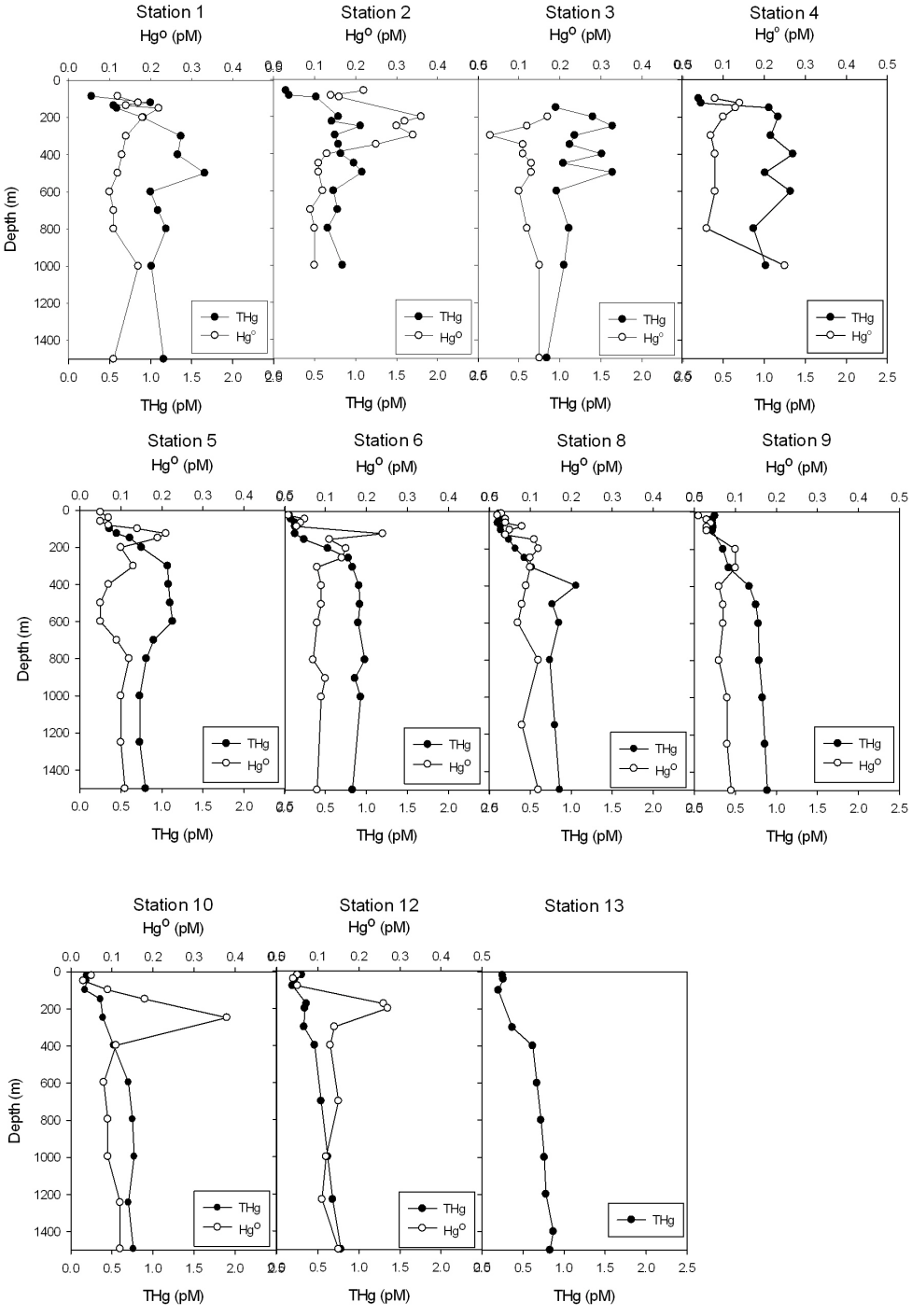

Figure 6: Full water column depth profiles of monomethylmercury and dimethylmercury at all stations along the Metzyme cruise track. MMHg concentrations (black circles) are highest at the Equatorial station and exhibit maxima in low oxygen waters primarily in the North Pacific. DMHg concentrations (white circles) are comparable or higher than those of MMHg and exhibit maxima in low oxygen waters in the North Pacific.

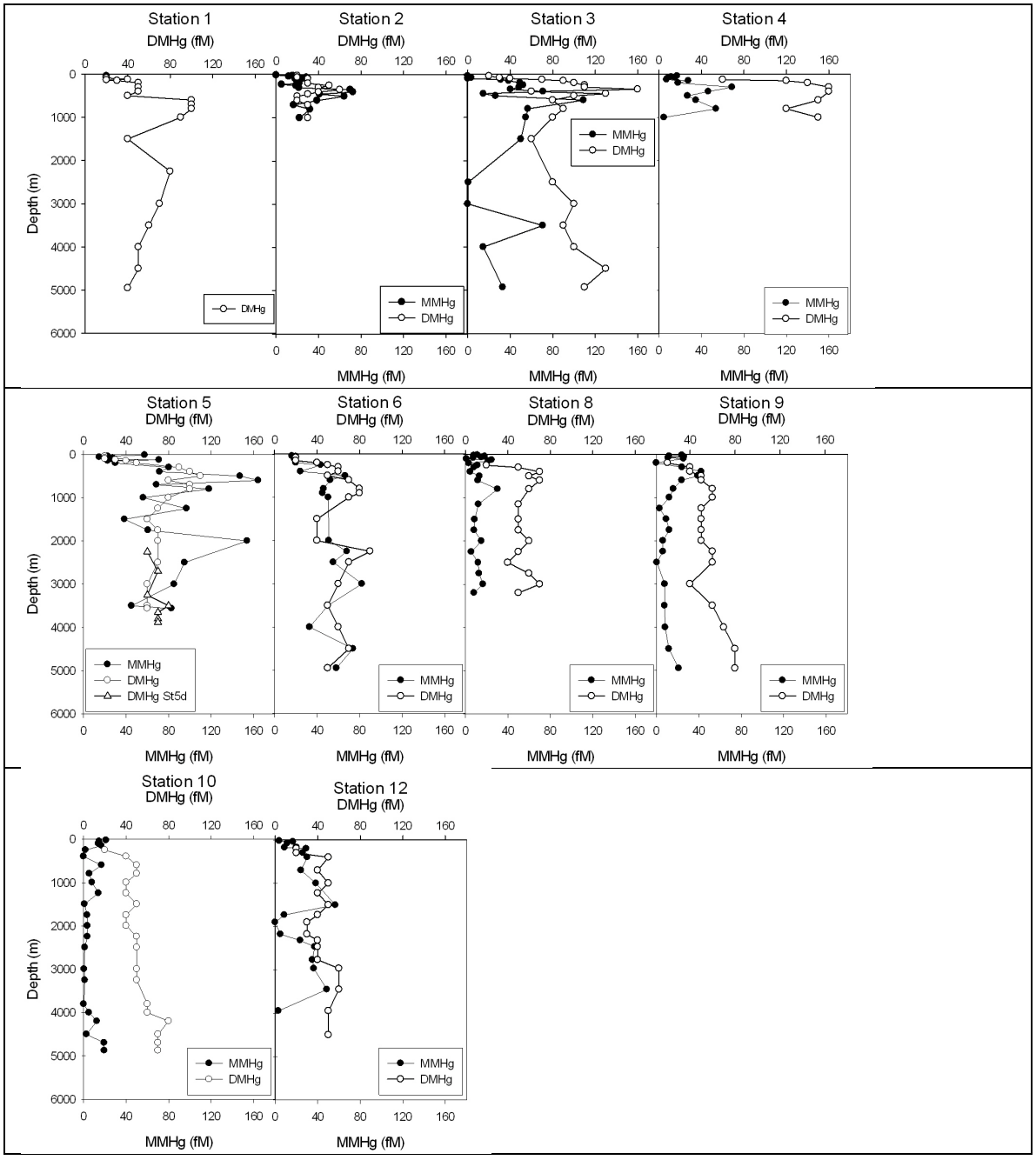

Figure 7: Upper water column depth profiles of monomethylmercury and dimethylmercury at all stations along the Metzyme cruise track. Both MMHg (black circles) and DMHg (white circles) concentrations are low in surface waters and increase in intermediate waters, most notably in North Pacific and Equatorial waters and are low in South Pacific waters.

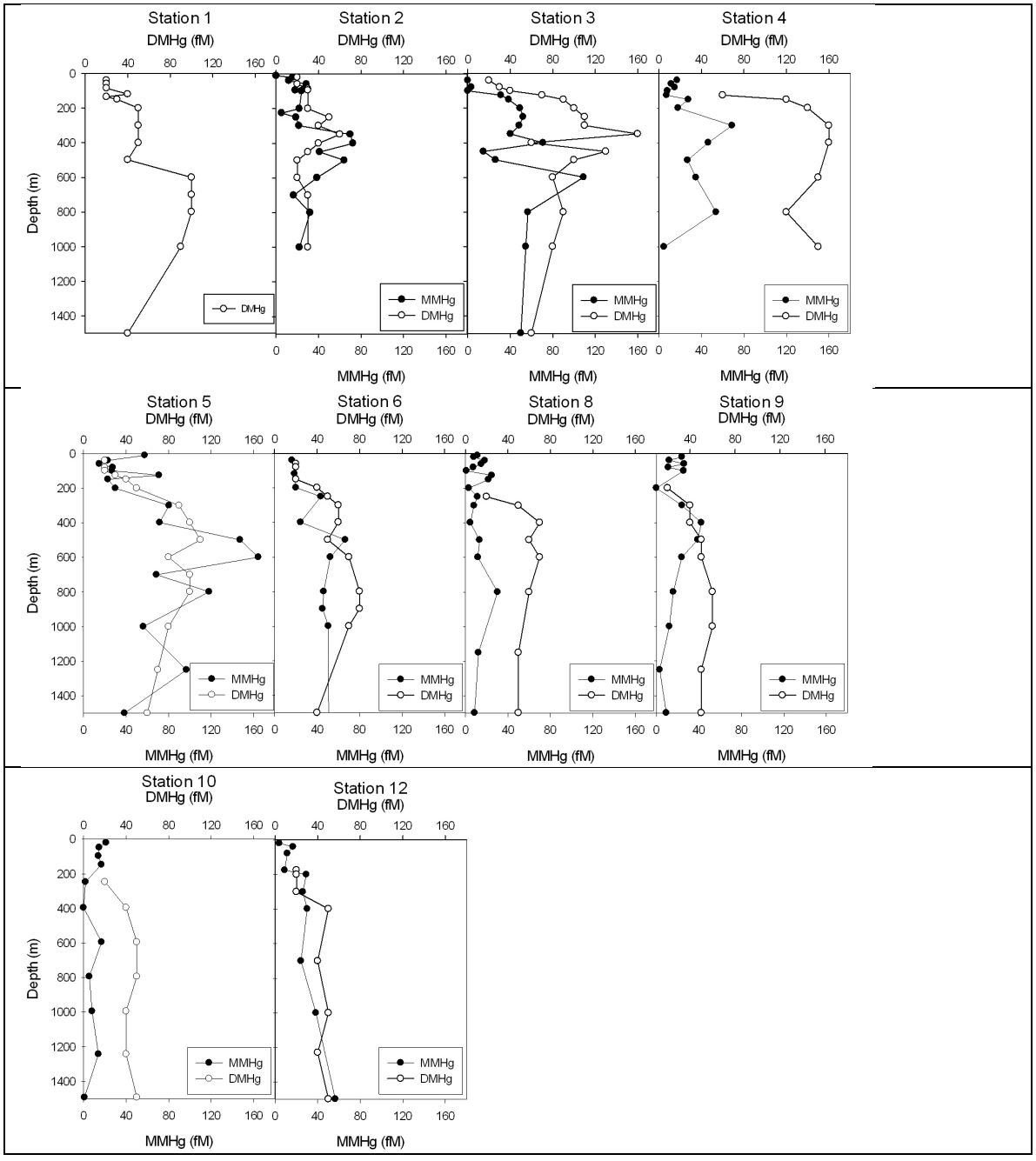

Figure 8: Ocean Data View gridded sections of mercury species concentrations along North to South transect of the Metzyme cruise. Upper water column (surface-1000 m; top panel) and full water column (bottom panel) of the Metzyme North to South transect (17°N to 15°S). Methylated species, DMHg and MMHg, have patterns that are distinct from THg. Hg(0) distributions reveal localized maxima of reduction at Station 2 (12°N) and Station 10 (15°S). The full depth section of THg reveals the relatively high concentrations in the North Pacific.

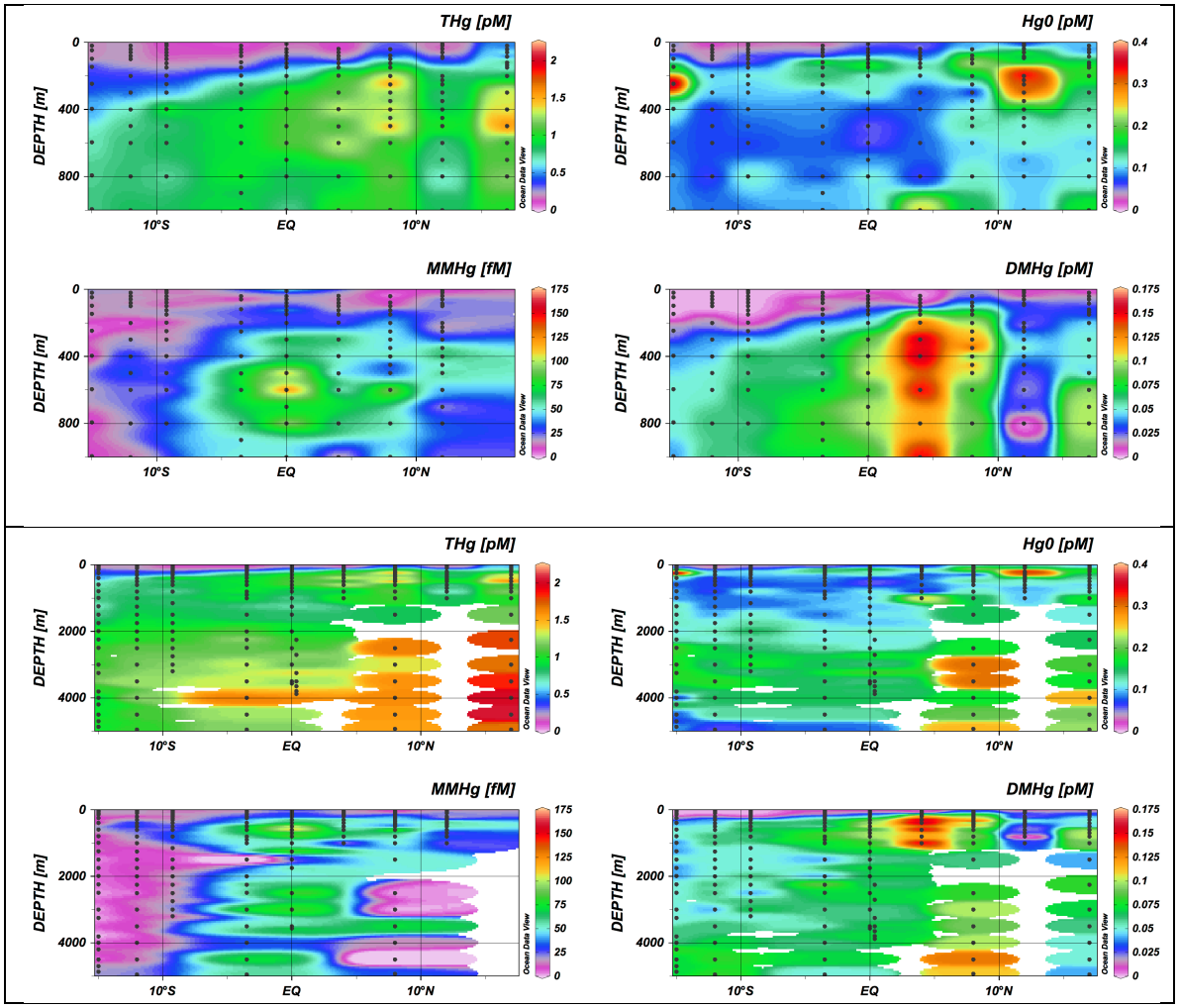

Figure 9: Percent saturation of Hg° in the water column of the Tropical Pacific Ocean. Percent saturation of Hg(0) in the upper 1000 m (top panel) and the full water column (middle panel). The distribution patters are similar to that of Hg(0) (Figure 8). Normalization to THg (bottom panel), reveals that percent saturation of Hg(0) is independent of THg distributions.

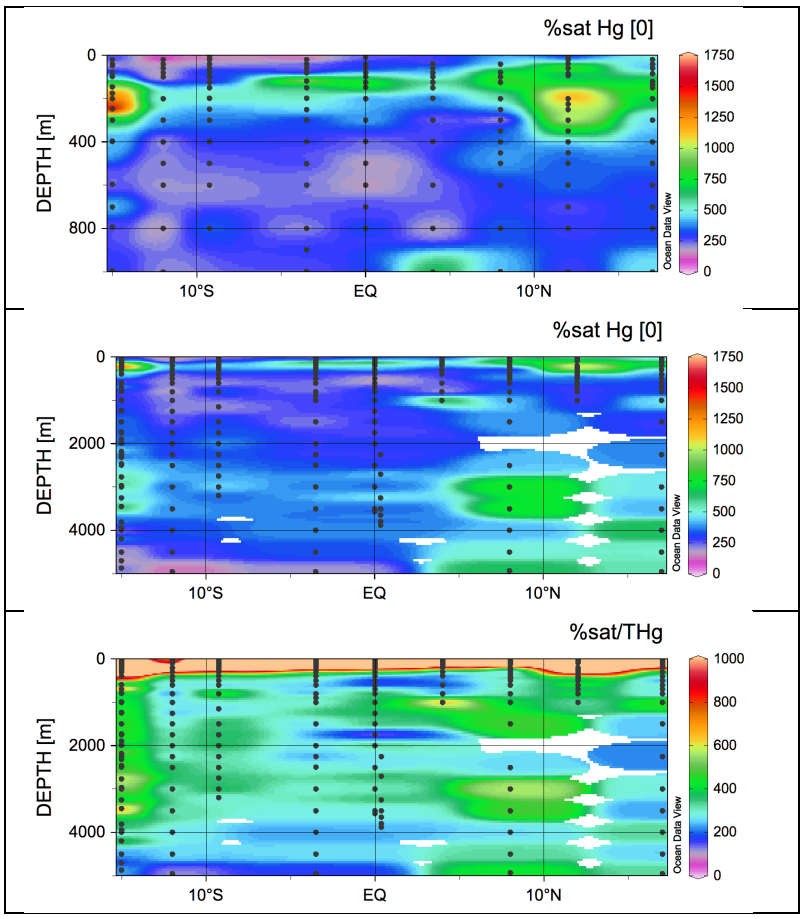

Figure 10: Mercury reduction driven by denitrification at the southern base of the North Pacific Subtropical Gyre. Upper 1000m of transect from Station 1 to Station 10 showing A) measured Hg° concentrations and B) N* calculated from measured [PO_4^{3-}] and [NO_3^-]. Maximum in Hg(0) concentrations between 200-400m at Station 2 correspond with indications of denitrification from N*. In contrast to Hg° maximum at Station 2, maximum at Station 10 does not correspond to denitrification.

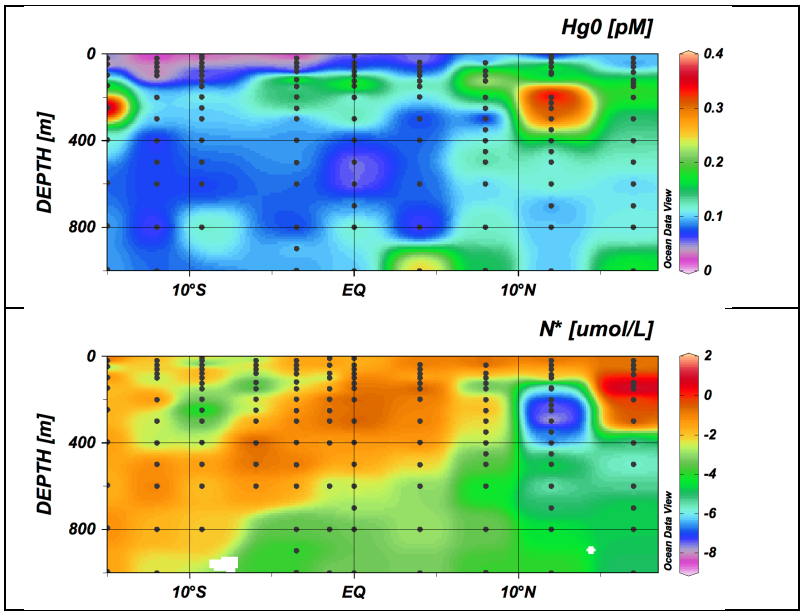

Figure 11: Suspended particulate total mercury and monomethylmercury collected from five stations using in situ pumps. Suspended particulate THg (black circles) and MMHg (white circles) concentrations measured from in situ pump deployments are low throughout surface and intermediate waters. Neither particulate pool contributes significantly to total concentrations of the species in Tropical Pacific waters.

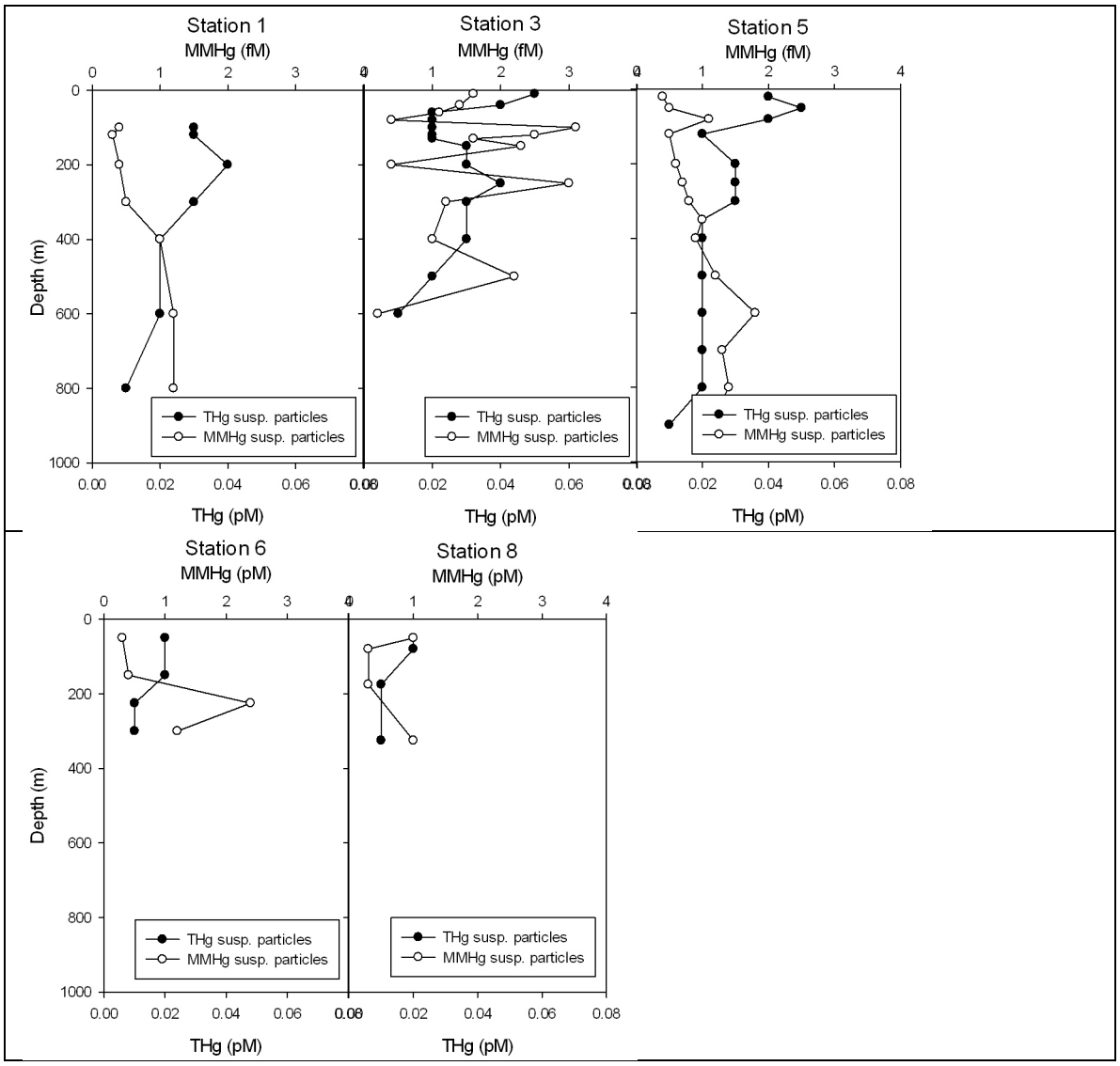

Figure 12: Ratios of monomethylmercury to total mercury in dissolved and suspended particulate pools. Ratios of MMHg to THg in the dissolved pool (white circles) are typically higher than ratios of MMHg to THg in the suspended particulate pool (black circles) in the surface ocean and approach one another below 200 m.

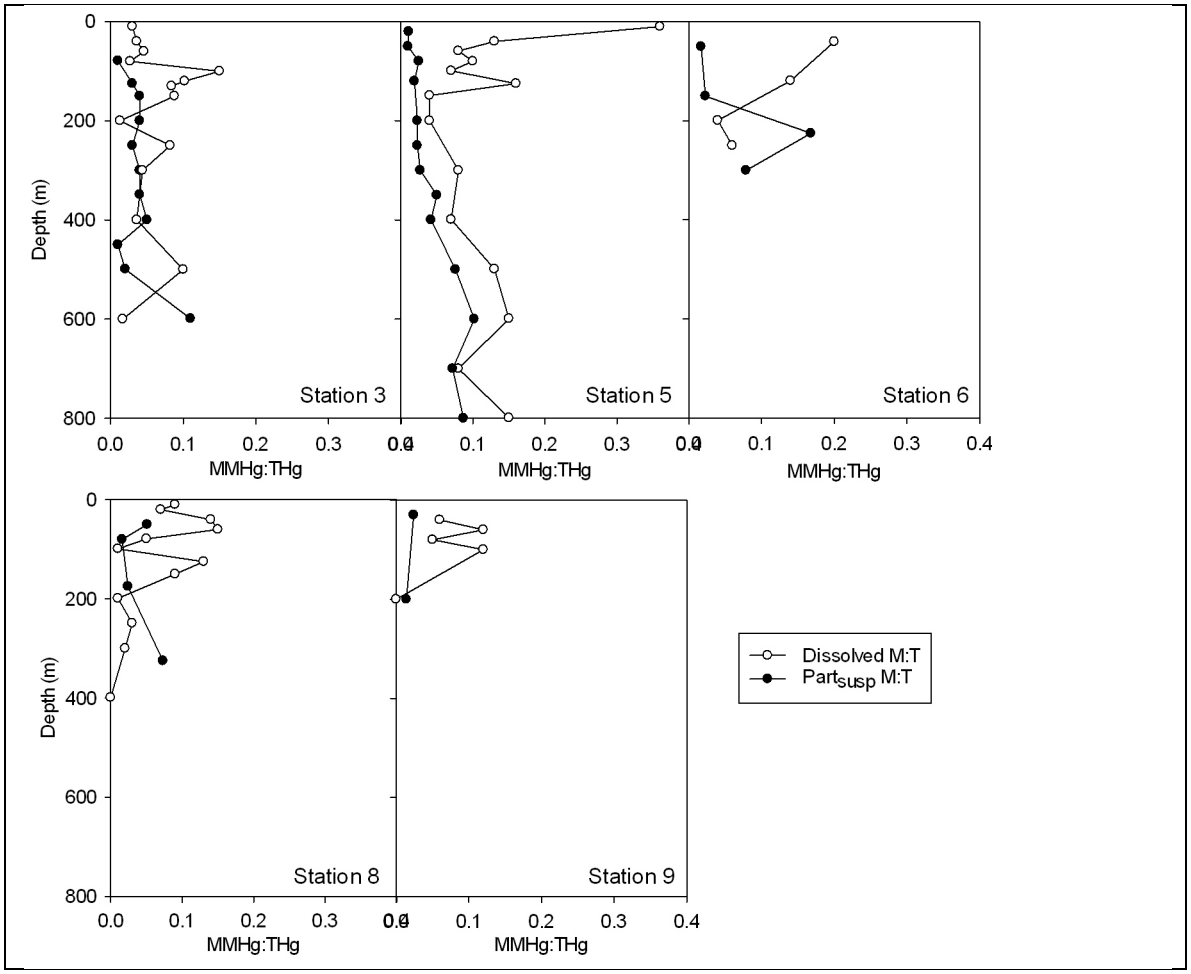

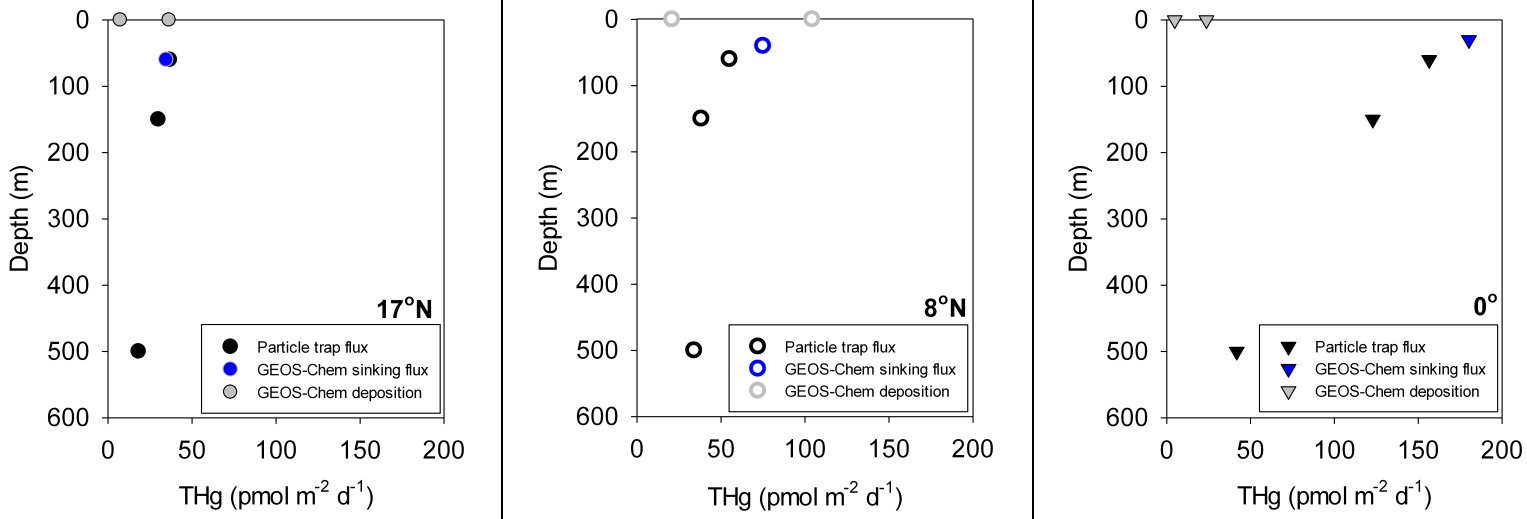

Figure 13: Sinking particulate total mercury fluxes from three stations in the Tropical Pacific Ocean. Particulate total mercury fluxes collected from three-day deployments of particle traps measured at three depths: 60, 150, and 500 m at three stations (black symbols). Fluxes from the mixed layer match well with modeled fluxes from the GEOS-Chem model (blue symbols). Because of rapid evasion of Hg deposited from the atmosphere, Hg retained in the surface ocean falls between 20-100% of the modeled GEOS-Chem atmospheric deposition values (grey values, both 20% and 100% shown).

Figure 14: Total methylated mercury concentrations versus apparent oxygen utilization for all stations along Metzyme cruise track. Sum of methylated mercury (measured separately as DMHg and MMHg) versus AOU (top image). Methylated mercury concentrations increase linearly with AOU at all intermediate depths and clump by station, most noticeably in the North Pacific. THg versus AOU (bottom image) show a similar relationship as MMHg versus AOU. The similar relationships suggest that remineralization does not stimulate methylation from Hg(II) substrate as has been hypothesized from North Pacific data [Sunderland et al, 2009].

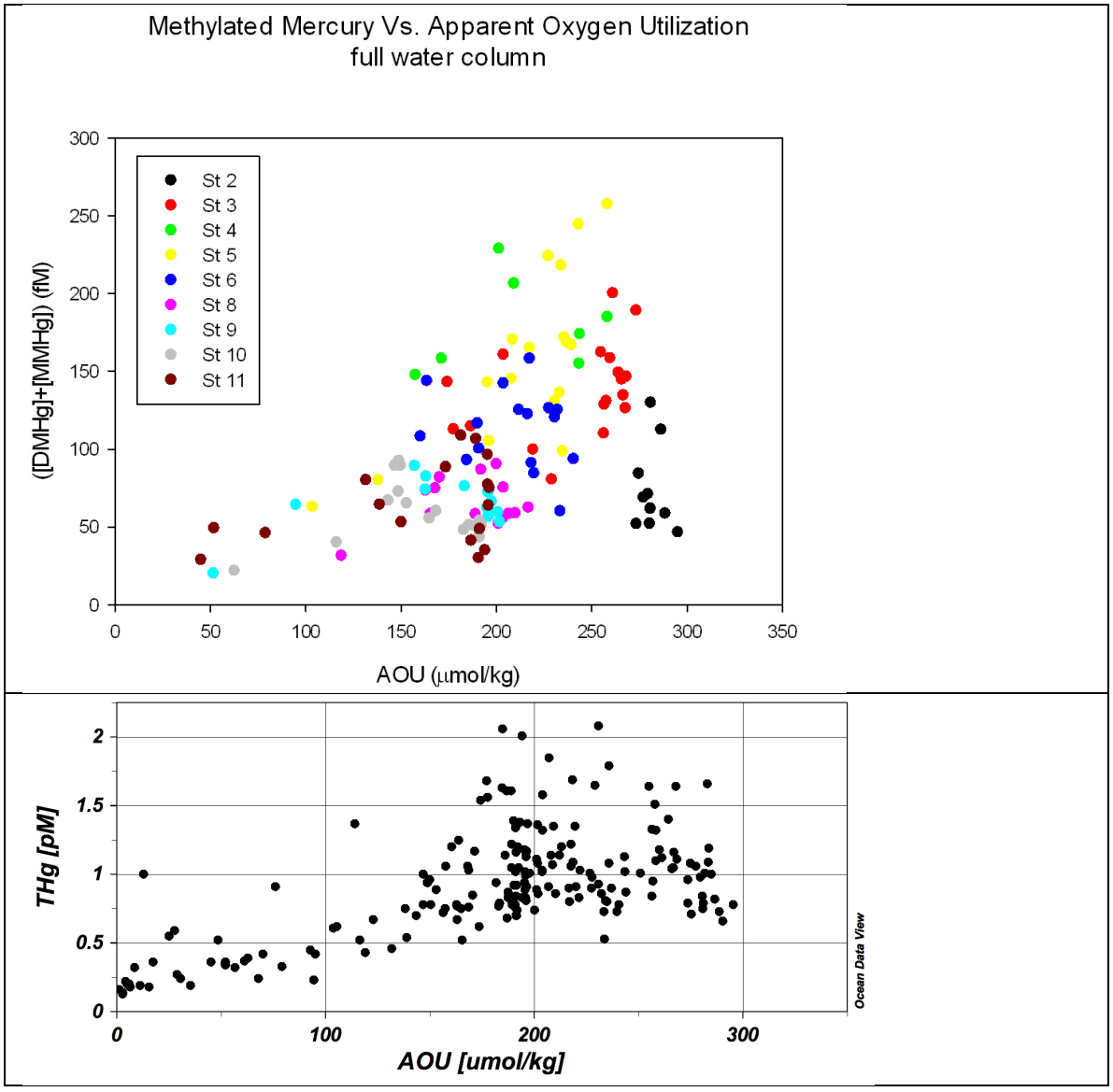

Figure 15: Ratios of monomethylmercury to dimethylmercury versus depth for four stations along the Metzyme cruise track. The ratios of dissolved MMHg:DMHg were generally low throughout the water column. Highest values were found at Station 3 (black circles) and Station 5 (white circles) compared to those observed in the South Pacific (triangles). The maximum and average values are both lower than those observed throughout the water column at the SAFe site North Pacific [Hammerschmidt and Bowman, 2012].

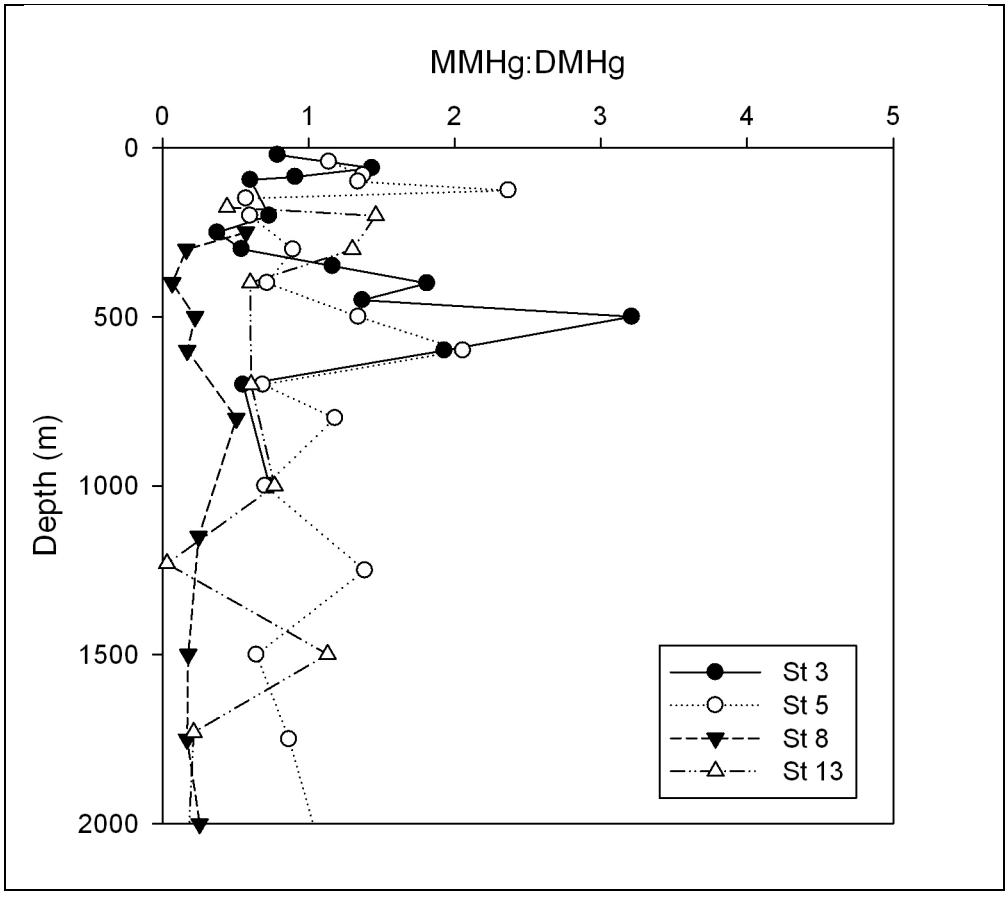

Figure 16: Depth profiles in the upper 1000 m of the Equatorial Pacific water column measured in 1990 by Mason and Fitzgerald and 2011 during the Metzyme cruise. Depth profiles of THg concentrations from stations measured during the 1990 Malcolm Balride cruise [Mason and Fitzgerald, 1993] compared to those stations closest in distance measured during the 2011 Metzyme cruise. Concentrations measured in 2011 appear lower than those measured 2 decades previously. In addition to differences in concentration, the earlier profiles of Mason and Fitzgerald display a more significant increase in THg concentrations both between 100-200 m as well as ~500 m. These features are absent from more recent distributions.

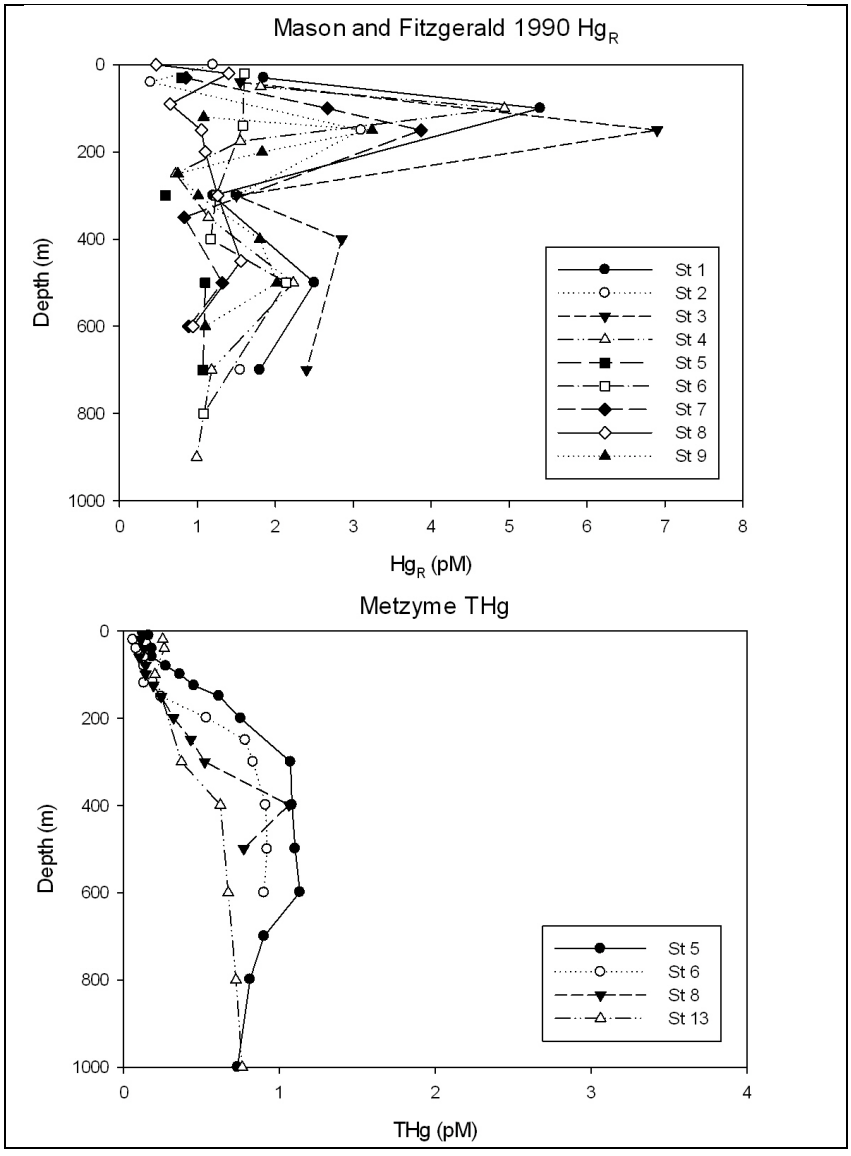

Figure 17: Total dissolved mercury concentrations in the water column measured at three sites in the North Pacific over a nine-year span. The International Oceanographic Commission 2002 (IOC 2002) data from Station Aloha [Laurier et al, 2004], the CLIVAR P16N 2006 data from Station 45 [Sunderland et al, 2009] and Station 1 of Metzyme sampled stations located within ~750 km of one another.

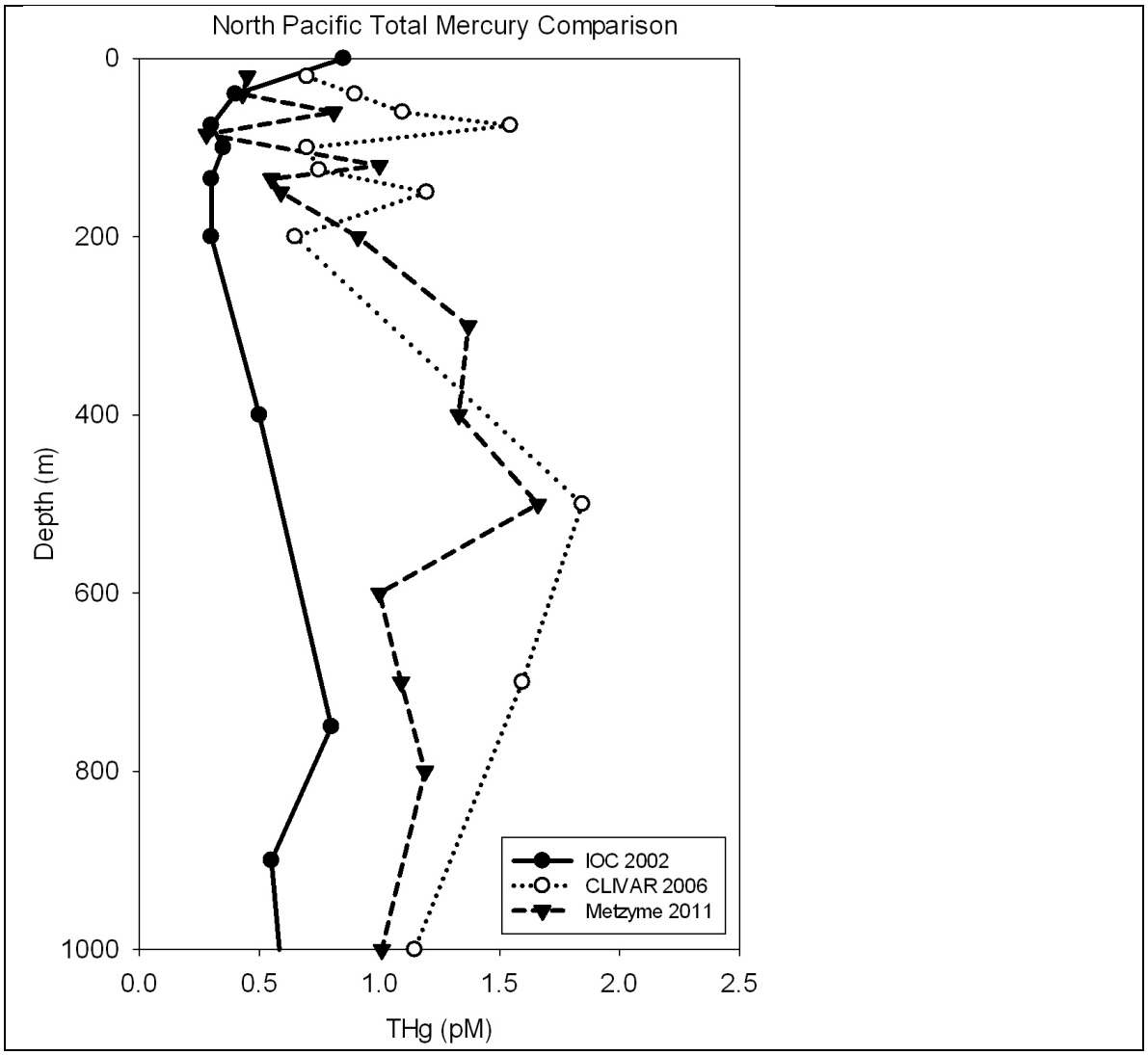

Figure 18: Total dissolved methylated mercury and total mercury concentrations from the CLIVAR P16N section in the North Pacific and the Metzyme cruise in the Tropical Pacific. THg concentrations (top image) and methylated Hg (middle image) in intermediate waters from the CLIVAR P16N section [Sunderland et al, 2004] and continuing southwest with Metzyme stations. THg concentrations reveal the southward extent of North Pacific Intermediate Water is limited to ~15°N. Like THg, methylatedHg shows distinct distributions in the equatorial Pacific compared to those of the North Pacific Intermediate Water mass as indicated by salinity values (bottom right).

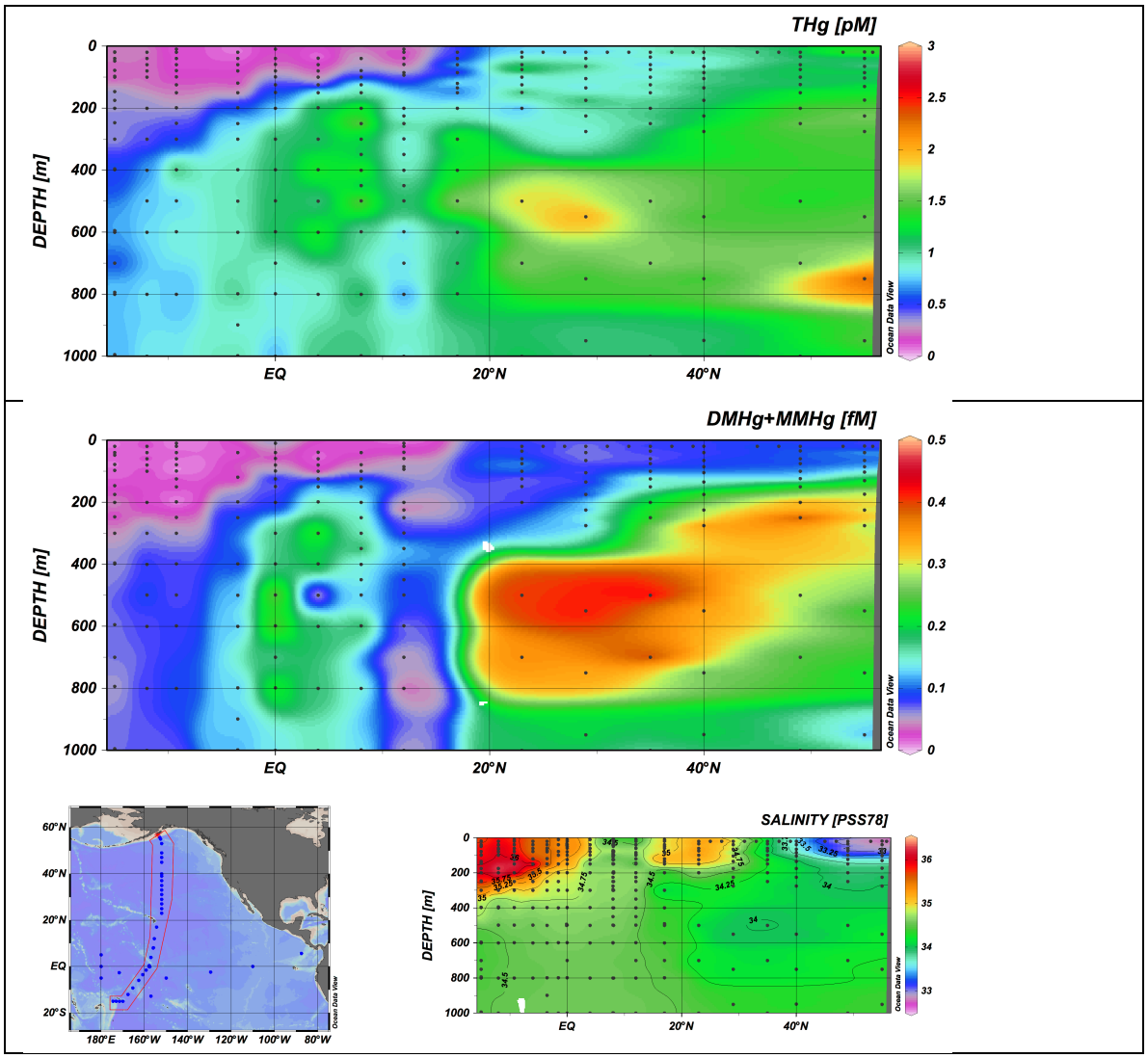

Tables and Table Legends

Table 1: Station coordinates and speciation samples collected at each station of Metzyme cruise.

Station	Lat	Long	Samples
1	17°N	154° 24'W	THg, Hg°, DMHg, THg_{part}, sed traps
2	12°N	155° 27'W	THg, Hg°, DMHg, MMHg (0-1000m)
3	8°N	156 W	THg, Hg°, DMHg, MMHg, THg_{part}, sed traps
4	4°N	157° 05'W	THg, Hg°, DMHg, MMHg (0-1000m)
5	0	158°W	THg, Hg°, DMHg, MMHg, THg_{part}, sed traps (0-3500m)
6	3° 30'S	160° 46'W	THg, Hg°, DMHg, MMHg, THg_{part}
7	5° 58'S	162° 37'W	No Hg samples collected
8	9° 15'S	165° 22'W	THg, Hg°, DMHg, MMHg, THg_{part}
9	12°S	167° 34W	THg, Hg°, DMHg, MMHg, THg_{part}
10	15°S	170 W	THg, Hg°, DMHg, MMHg
11	15°S	171° 30'W	No Hg samples collected
12	15°S	173° 06'W	THg, Hg°, DMHg, MMHg
13	15°S	174° 30'W	THg

Chapter 5
Controsls on Mercury Methylation in the Tropical Pacific Ocean

Abstract:

We measured potential mercury (Hg) methylation rates along a transect in the Pacific Ocean. Using additions of isotopically enriched inorganic (Hg(II)) and monomethylmercury (MMHg) substrates to bottle incubations, we evaluated the potential role of heterotrophic bacteria in mercury methylation from dark incubations. Resulting methylation rates were measured using a linked gas chromatography cold vapor atomic fluorescent spectrometry inductively coupled plasma mass spectrometry (GC-CVAFS-ICPMS) method. Methylated Hg species concentrations are highest at depths of low dissolved oxygen concentrations in all waters along the transect. However, no significant differences in methylation potential were observed between unfiltered water collected from the deep chlorophyll maximum compared to water collected from the oxygen minimum zone within an individual station. Marine waters at a variety of depths have methylation potential despite significant differences in measured MMHg concentrations.

We also measured significant methylation potential in both 0.2 μm filtered and unfiltered water collected from chlorophyll maximum and oxygen minimum depths, suggesting that methylation is not limited to cellular conversion in these waters. Additions of compounds such as cysteine and methylcobalamin, known to influence MMHg production in cultures of methylating anaerobic bacteria, do not indicate analogous mechanisms for marine methylation to that in anoxic sediments. More striking was the observation that addition of bulk organic matter collected from each station did not appear to enhance methylation, suggesting that methylation in Tropical Pacific waters is not unique to zones of net remineralization.

High-resolution sampling of methylation over a 36-hour incubation reveals dynamic methylation and demethylation of added Hg species even at locations with low ambient concentrations of DMHg and MMHg. These results suggest that MMHg available for bioaccumulation is likely controlled by competition between bioaccumulation, particle scavenging, and demethylation.

Introduction

Monomethylmercury (MMHg), the bioaccumulating form of mercury (Hg), was first measured in the open ocean water column over two decades ago [Mason and Fitzgerald, 1990]. Since then, measurements of methylated Hg, measured as either MMHg, the non-bioaccumulating organic species dimethylmercury (DMHg), or the sum of MMHg and DMHg (MeHg), have revealed local maxima of methylated Hg species within regions of low oxygen [Mason and Fitzgerald 1993; Mason et al, 1998; Mason and Sullivan, 1999; Cossa et al, 1997; Cossa et al, 2009; Cossa et al, 2011; Sunderland et al, 2009; Hammerschmidt and Bowman, 2012; Munson, this work—Chapter 4]. As a result, MMHg production has been linked to active organic matter remineralization [e. g. Sunderland et al, 2009]. Limited direct water column measurements of mercury methylation have been performed in the Canadian Arctic Archipelago [Lehnherr et al, 2011] and coastal and open water sites in the Mediterranean [Monperrus et al, 2007a, b] from bottle incubations using additions of isotopically enriched mercury species. However, no mechanistic studies have been performed to identify environmental factors that control the production of MMHg in these regions of the water column.

Anthropogenic loadings of Hg to marine environments are thought to have increased 3-fold since the Industrial Revolution [Lamborg et al, 2002] Various animal records, such as bird feathers [Vo et al, 2011] and egg shells [Xu et al, 2011] suggest that these THg increases result in subsequent increases in MMHg concentrations within marine food webs. Isotopic signatures of Hg in fish collected from the North Pacific indicate water column methylation as the primary source of MMHg [Blum et al, 2013], although the rate of increase in marine fish is debated [Kraepiel et al, 2003]. The transfer between dissolved Hg pools, biota, which result in elevated fish tissues concentrations is complex. Therefore, the controls on MMHg production and thus the available MMHg for bioaccumulation is essential to accurately predict how changes in total global Hg emissions will impact human MMHg exposure.

Anaerobic bacteria are known to methylate mercury in culture and anoxic sediments [Gilmour et al, 2013]. However, MMHg distributions measured in the Pacific Ocean to date have revealed elevated MMHg in open-ocean regions with dissolved O_2 concentrations well above those classified as anoxic [Mason and Fitzgerald, 1993; Sunderland et al, 2009; Hammerschmidt and Bowman, 2012; Munson—this work, Chapter 4]. Analogous to other anaerobic processes, such as sulfate reduction, mercury methylation potentially occurs throughout the marine water column within anoxic microzones on particulate matter [e.g. Shanks and Reeder, 1993].

Alternatively, the requirement of low redox conditions for methylation by sulfate-reducing bacteria may limit their methylation activity in open-ocean regions, such as to areas of denitrification [Malcolm et al, 2010]. Recent measurements of potential methylation rates in high oxygen waters from marine euphotic zones have raised the question of the potential for aerobic mechanisms for Hg methylation that may be unique to marine systems [Monperrus et al, 2007; Lehnherr et al, 2011].

A substantial amount of work with cultured bacteria has revealed the important roles for specific chemical compounds with active marine cycling in anaerobic methylation. Sulfate- and iron-reducing bacteria utilize methylcobalamin (vitamin B_{12}) as the methyl donor for [Ekstrom et al, 2003; Ekstrom and Morel 2008]. The recently identified *hgc* methylation genes in anaerobes have clarified the link between methylcobalamin and Hg methylation as it encodes a cobalamin utilizing methyltransferase [Parks et al, 2013]. Methylcobalamin is produced by cyanobacteria found throughout marine euphotic zones [Bonnet et al, 2010]. However due to its universal requirements among marine phytoplankton, methylcobalamin is actively scavenged, most notably by diatoms [Bertrand et al, 2009]. As a result, concentrations of the vitamin in the open ocean can be limiting [Panzeca et al, 2009].

In addition to its roll in intracellular methylation, methylcobalamin is known to abiotically methylate Hg(II) at pH 4 and has been considered as a potential abiotic mechanism of MMHg production in natural systems from laboratory studies and theoretical calculations [Celo et al, 2006; Jiménez-Moreno, 2013]. However, in marine waters where methylcobalamin is limiting, its dissolved concentrations might be too low to support a high degree of Hg methylation.

Low molecular weight thiols such as the amino acid cysteine and glutathione have been found to alternately stimulate or hinder active Hg(II) uptake by different species of anaerobic bacteria in culture [Schaefer and Morel, 2009; Schaefer et al, 2011]. The potential for stimulation of methylation in natural systems by thiol availability has not been investigated, but may be limited in oxic marine waters. Thiol mediated enhancement or suppression of Hg(II) uptake is specific to reduced species [Schaefer and Morel, 2009; Schaefer et al, 2011] and thiols found in marine waters may be oxidized in its primary role as a copper-binding ligand in low Hg marine waters [Kading, 2013]. Although previous measurements of dissolved thiols in marine waters have found that up to half may persist in their reduced forms [Dupont et al, 2006], distributions of small thiols such as cysteine and glutathione are found at nanomolar concentrations in the surface ocean, with depletion at depth [Kading, 2013; Swarr et al, 2012]. As a result, thiols may not

impact marine methylation. However, the relatively small amount of Hg(II) methylation that is required to account for observed concentrations of MeHg in low oxygen waters, <<1 pM [Munson—this work, Chapter 4], and the ability of cysteine to increase methylation in *E. coli* under oxic conditions [Ndu et al, 2012] make thiols a target for studies of methylation in natural systems.

The potential for methylcobalamin and thiols to influence marine Hg methylation, either biotically or abiotically, has not been studied previously. A correlation between methylated Hg (as [DMHg + MMHg]) and rates of organic matter remineralization has been observed in the North Pacific [Sunderland et al, 2009]. Bulk organic matter remineralization could potentially release MMHg outright or Hg(II) substrate for methylation by microbes. In contrast, remineralization may release a specific compound, such as methylcobalamin or a small thiol, that specifically promotes MMHg production.

We used isotopically enriched Hg species to simultaneously measure potential rates of methylation and demethylation from incubations of water collected along a cruise transect from the tropical North to the tropical South Pacific. In addition to measuring rates of net methylation and demethylation, we also investigated the impact of added organic matter, collected during the cruise as well as individual compounds known to stimulate methylation in culture experiments, including methylcobalamin [Ekstrom and Morel, 2008], and thiols [Schaefer and Morel, 2009, Schaefer et al, 2011]. We took the approach of a limitation experiment in order to determine whether methylation and demethylation in the marine water column are stimulated by bulk organic matter remineralization or the release of a specific compound that controls Hg dynamics. In addition, we compared potential rates of methylation in filtered and unfiltered water to determine the extent of cellular methylation in these environments.

Methods

Isotopically enriched $MM^{198}Hg$ and $MM^{199}Hg$ were prepared from ^{198}HgO and ^{199}HgO (Oak Ridge National Laboratory), respectively, by methylation with methylcobalamin [Hintelmann and Ogrinc, 2003]. A mass of 100 µg of enriched HgO was dissolved in 10 µL HCl (conc, J. T. Baker) and diluted in 500 µL sodium acetate buffer (0.1 M, pH 5). A mass of 500 µg of methylcobalamin (Sigma) was dissolved in 500 µL sodium acetate buffer and added to the Hg solution. The reaction proceeded for 3 hours at room temperature before being stopped with 200 µL KBr (0.3 M KBr in 2 M H_2SO_4). The synthesized enriched MMHg was extracted with toluene

(400 µL, 3x). Extracts were combined and dried over sodium sulfate. A 100 µL aliquot of this primary stock was dissolved in 10 mL isopropanol to produce a secondary stock solution. Because methylcobalmain was a target of our investigation for its potential role in in situ methylation, carryover of methylcobalamin from reaction solution was found to be minimal (<1 pM) from ICPMS analysis with a mixed metal standard.

Water for incubation experiments was collected on board the *R/V Kilo Moana* between 1-24 October 2011 (Figure 1). Water filtration, decanting, and treatment additions were performed under positive pressure from HEPA-filter laminar flow hoods within clean bubbles constructed on board. Concentrations of THg and DMHg were measured at sea using established methods [Lamborg et al, 2012]. MMHg concentrations were measured on shore using ascorbic acid-assisted direct ethylation [Munson—this work, Chapter 2], with the exception of 17°N, where no MMHg samples were preserved. An estimate of MMHg at the Station 1 depths at which incubation experiments were performed was therefore calculated from the CVAFS peak data from incubation samples after correction for the added $MM^{198}Hg$ spike (Table). The calculated values fall within the range of methylHg (sum of DMHg and MMHg) previously measured in North Pacific waters [Sunderland et al, 2009].

Water was collected from two depths at each station: 1) chlorophyll *a* maximum and, 2) the oxygen minimum each identified from the SeaBird package data on prior water sampling casts at each station (Table 1). Water was collected in acid-washed X-Niskin bottles deployed on a dedicated trace metal sampling rosette using Amsteel metal-free wire.

Sufficient water for incubations was decanted under N_2 pressure either unfiltered or filtered through a 0.2 µm capsule filter (47-mm, Supor polycarbonate membrane, Pall Corporation) into 20-L acid-washed polycarbonate mixing carboys (Nalgene). The carboys were kept covered in dark plastic bags as much as possible during incubation preparation to minimize exposure to light.

Pre-equilibrated spikes of isotopically enriched $MM^{198}Hg$ and $^{202}Hg(II)$ were prepared by adding concentrated $^{202}Hg(II)$ and $MM^{198}Hg$ to 0.2-µm filtered seawater and equilibrating at 16°C in the dark for 24 hours prior to use. Spikes were added using gas-tight syringes dedicated for use in isotope enrichment experiments (Hamilton).

Incubations were performed in triplicate in 250-mL amber glass bottles (I-Chem) filled to the shoulder from mixing carboys. All bottles had approximately 25 mL of headspace. As a result, in situ redox conditions were not maintained during incubation. After water addition, pre-

equilibrated spikes of ^{202}Hg(II) (396 fmoles) and MM^{198}Hg (126 fmoles) were added. Treatments of C (as succinate), Cys, GSH, Co, B_{12}, ½ of 2-cm punches from McLane in situ pumps [Munson—this work, chapter 4], and additive treatments C+Co and Cys+Co were added to triplicate bottles (Table 2). Prior to addition C, Cys, and GSH treatments were passed through a Chelex 100 resin (Bio Rad) column to remove Co and other divalent cations to avoid contamination by Co or other divalent metals.

Bottles for t0 measurements were fixed after treatment addition with 1 mL (~0.5%, final) H_2SO_4 (conc., Fisher TM grade) and were stored at -4°C until analysis except for bottles amended with methylcobalamin, which were frozen at -40°C to avoid abiotic methylation under acidic conditions during storage. Station 1, 3, 5 bottles were incubated in the dark for 24 hr at temperatures maintained in refrigerators set at their highest temperature setting (Table 1). Station 9 bottles were incubated in the dark up to 36 hr in a time course study. After incubation, bottles for all time points were fixed with H_2SO_4 and stored at -4°C or -40°C for methylcobalamin as noted above. Because DMHg decomposes to MMHg in acidic conditions [Black et al, 2009], all measured MMHg concentrations represent the sum of DMHg and MMHg present at in each bottle at the time of acidification.

Analysis of MMHg concentrations and isotopic composition was performed on a Thermo Element 2 ICPMS in the Plasma Laboratory at the Woods Hole Oceanographic Institution. The inlet of the ICPMS was linked via a polyethylene y-junction to a Tekran 2700 Automated Methyl Mercury Detector.

Samples were prepared as for MMHg determination (above) using ascorbic-assisted direct ethylating of MMHg and simultaneous measurement of MMHg concentrations as well as isotopic composition by ICPMS.

Hg isotopes were measured individually and were integrated using MATLAB scripts to quantify relative isotopic ratios in the MMHg (as methylethylHg) and Hg(II) (as diethylHg) peaks. Resulting methylation of ^{202}Hg(II) and demethylation of MM^{198}Hg were quantified using a matrix linear approach [Hintelmann and Ogrinc, 2003, see Appendix I for explicit calculations]. We added MM^{199}Hg as an internal standard to samples and equilibrated for 24-hours prior to MMHg determination for isotope ratio-ICPMS [Hintelmann and Evans, 1997].

The two previously reported marine methylation rate measurements have used different methods to calculate k_m values. Lehnherr et al, 2011 considered decreases in the available ^{198}Hg(II) substrate in their rate measurements. From CVAFS measurements of decreases in

^{198}Hg(II) concentrations overtime from separate incubations of seawater, Lehnherr et al, 2011 fitted an exponential curve to the decrease in ^{198}Hg(II) that they incorporated into their calculations of k_m [Lehnherr et al, 2011]. This was necessary because MMHg and Hg(II) could not be simultaneously determined with their analytical set up in individual bottles. In contrast, earlier measurements from Monperrus et al, 2007, assumed no decrease in Hg(II) substrate availability. Hg(II) is typically measured from tin chloride reduction followed by CVAFS analysis. Although not analytically identical, we observed quantitative recovery of Hg(II) from the diethylHg peak of the Tekran 2700 instrument used for CVAFS analysis (Figure 2A, also Figure 1 Munson—this work, Chapter 3). As a result, our rate measurements are presented as a modification of the Lehnherr et al, 2011 method. Instead of fitting a generalized curve of ^{202}Hg(II) substrate availability, we calculated methylation of ^{202}Hg(II) relative to available ^{202}Hg(II) measured in individual bottles. Results are presented as percentages of methylated ^{202}Hg(II) substrate. Potential methylation rate constants, k_m, were calculated as the percentage of methylated ^{202}Hg(II) substrate over the incubation time.

Potential demethylation rates were calculated assuming first order kinetics from the slope of the linear best fit line of Ln(MM^{198}Hg) vs. time.

Results

Mercury Methylation: Unamended Samples

Potential rates were measured across a variety of hydrographic parameters [Munson—this work, Chapter 4] as well as ambient dissolved Hg concentrations. In general, concentrations of methylated Hg, THg, dissolved O_2, and apparent oxygen utilization (AOU) [Sarmiento and Gruber, 2006; Garcia and Gordon, 1992] decreased north to south (Figure 3). A region of low oxygen intermediate waters centered at 12°N set apart high methylated Hg intermediate waters in the North Pacific [Sunderland et al, 2009] seen at 17°N (Figure 4) from a band of lower methylated Hg species concentrations between 8°N and 5°S. Methylated Hg concentrations are higher in waters from oxygen minimum depths (82-310 fM methylated Hg) relative to chlorophyll maximum depths (26-45 fM methylated Hg; Figure 4).

Production of Me^{202}Hg(II) during 24-hour incubations did not correspond to ambient methylated Hg concentrations (Figure 10). Within the chlorophyll maximum, values for k_m were highest at 8°N (CMX: 5.71-10.19 %/d) and lowest at 17°N in the North Pacific (CMX: 0.39-0.43 %/d; Table 3) despite nearly identical ambient concentrations of methylated Hg (Table 1). Values

for k_m in oxygen minimums depths generally increased as ambient methylated Hg concentrations decreased, with the highest k_m values measured at 8°N in the Tropical Pacific (OMZ: 3.77-7.40 %/d), intermediate k_m values at the Equator (OMZ: 1.00-1.74 %/d) and South Pacific (OMZ: 1.12-2.28 %/d), and the lowest k_m values measured at 17°N in the North Pacific (OMZ: 0.64-0.95 %/d) despite the fact that methylated Hg concentrations at 17°N were four times higher than those measured at 12°S (Table 1).

Difference in k_m values between 0.2 μm filtered and unfiltered waters were largely insignificant at either depth measured (Table 3). Nor were there clear trends in k_m values measured in waters from chlorophyll maximum depths compared to those measured from low oxygen depths.

Consistent with our methylation measurements from the Sargasso Sea [Munson—this work, Chapter 3], we observed significant initial production of $Me^{202}Hg$ relative to added $^{202}Hg(II)$ spike within the ~2 hours of time between $^{202}Hg(II)$ spike addition and t0 sample preservation with acid (Figures 5). Initial methylation, like that of potential methylation rates, were highest at 8°N (CMX: 8.27-12.17 %/d; OMZ: 2.45-6.84 %/d), where it accounts for all methylation observed during the 24-hour incubations in the chlorophyll maximum waters (Figure 5). Initial methylation was lowest at 17°N (CMX: 0.28-0.47 %/d; OMZ: 0.54-0.66 %/d), where methylation continued throughout the incubation period (Figure 5) as indicated by significant increases in methylation between t0 and t24-hr bottles.

Higher temporal resolution of sampling at the South Pacific station, 12°S, reveals that methylation of added $^{202}Hg(II)$ is rapid, with maximum methylation reached within 6 hours, in unfiltered waters and subsequent demethylation of $Me^{202}Hg$ occurs within ~12 hours of total incubation time (Figure 6, white triangles). In contrast, $Me^{202}Hg$ produced in filtered waters is not rapidly demethylated and persists over the course of the incubation (Figure 6, black triangles). In contrast to Sargasso Sea waters, in which unfiltered waters appeared to support methylation throughout 24-hour incubations [Munson—this work, Chapter 3], the presence of particulate matter, either biotic or abiotic in origin, appears to enhance demethylation.

Mercury Methylation: Amended Samples

In general, the addition of compounds and bulk organic matter did not enhance the continual methylation of Hg(II) in 24-hour incubations. Since methylated Hg concentrations are typically highest in oxygen minimum zones of the water column, we hypothesized that the release

of specific compounds, such as methylcobalamin and cysteine, could increase measured methylation rates at the chlorophyll maximum as these are areas of maximum plankton growth which may limit the availability of these compounds in Hg cycling. Limitation by any one of these compounds would have been indicated by increased $Me^{202}Hg$ production in amended waters collected from the chlorophyll maximum compared to those from the oxygen minimum. Amendment addition of all treatments, with the exception of methylcobalamin, appeared to increase initial methylation in both filtered and unfiltered waters (Figure 8, left panels) in waters from the chlorophyll maximum at 17°N and 12°S. The magnitude of methylation upon treatment addition was enhanced in unfiltered waters compared to filtered waters (Figure 8, lower panels). In both filtered and unfiltered waters the combined cobalt and succinate treatment (CoC) produced the greatest stimulation of methylation relative to unamended samples as indicated by the values of the stimulation factor normalized to unamended incubations (0.2 μm: 2.48 ± 0.41 unfiltered: 3.64 ± 0.32) (Figure 8).

In oxygen minimum waters, treatment addition stimulated methylation in filtered waters at the Equator (Figure 9, top panels). This stimulation was maintained over the 24-hour incubation period (Figure 9, top right). The addition of treatments to unfiltered waters from oxygen minimum depths did not produce clear responses and high variability was seen between replicate samples (Figure 9, bottom panels).

Waters amended with methylcobalamin showed no abiotic methylation of $^{202}Hg(II)$. In contrast, addition of methylcobalamin appeared to promote reduction of $^{202}Hg(II)$ as indicated by the increase in ^{202}Hg in the Hg(0) peaks in the chromatograms (Figure 2). However, recovery of Hg(0) concentrations were not quantified in our analysis, so the extent to which reduction takes place and whether $^{202}Hg(II)$ is reduced prior to or following methylation could not be precisely determined.

Despite the ability of many individual compound additions to stimulate methylation in waters from chlorophyll maximum depths (Figure 8), the addition of bulk organic matter from McLane pump filters did not appear to stimulate methylation for most stations. The only exception was modest stimulation in filtered waters from the chlorophyll maximum at 8°S (stimulation factor normalized to unamended incubations, punch: 1.65 ± 0.20). The pump filter punch additions are a complex, and uncharacterized, mixture of inorganic matter and organic matter, including cells that are smaller than the ~51 μm. As a result, addition of pump punches to 0.2 μm filtered seawater inoculates these samples with uncharacterized bacterial communities as

well as adding both particles and organic matter. The punch treated 0.2 μm filtered samples therefore represent a combination of cellular and non cellular methylation potential.

Mercury Demethylation

Measurements of $MM^{198}Hg$ remaining at time points indicated initial demethylation of the added $MM^{198}Hg$ spike prior to t0, which prevented calculations of k_d. The only exception to this was in unfiltered water from the oxygen minimum depth of 12°S (Figure 7). In these samples, $MM^{198}Hg$ persisted through 12 hours of incubation resulting in a calculated k_d of 5.06 (d^{-1}) from the slope of the line of $\ln(MM^{198}Hg)$ vs. incubation time.

Discussion

Correlations between methylated Hg concentrations and regions of net organic matter remineralization have implicated in situ methylation as a significant source of methylated Hg to the marine water column [Sunderland et al, 2009; Cossa et al, 2011; etc.]. Parallels between oxygen minimum zones within the marine water column and the production of MMHg by anaerobic bacteria have led to suggestions that marine bacteria methylate Hg in these environments [Mason and Fitzgerald, 1993]. However, previous measurements of methylation in low oxygen waters have failed to identify marine anaerobes that are capable of methylating Hg [Malcolm et al, 2010]. In the two previous measurements of potential methylation rates in marine waters only those in the Mediterranean distinguished between abiotic and biotic methylation [Monperrus et al, 2007]. However, the use of a 45-μm size cut off between filtered and unfiltered water and dark controls compared to diurnal incubations in that study did not account for the activity of heterotrophic bacteria, which are often small enough to pass through 45-μm filters [Lalli and Parsons, 1997]. Potential methylation rates have also been measured in unfiltered water in the Canadian Arctic Archipelago and methylation observed during incubations were assumed to be due to bacterial activity [Lehnherr et al, 2011]. As a result, the current study is the first to quantify methylation potential by particulate matter including heterotrophic bacteria and to examine potential limitations of Hg methylation by compounds released during organic matter remineralization.

Across substantial gradients in the Pacific Ocean, we observed significant methylation potential in waters from both the chlorophyll maximum and oxygen minimum depths. In addition, methylation potential was not limited to unfiltered water. Despite pre-equilibration of enriched

Hg species spikes in filtered seawater prior to addition to bottle incubation, initial methylation was measured in all waters and contributed the majority of methylation in oligotrophic waters at 12°S. Higher temporal resolution of incubations from 12°S show dynamic methylation and demethylation processes take place within the time course of incubations, similar to observations of methylation in oligotrophic waters of the Sargasso Sea [Munson—this work, Chapter 3]. However, in the South Pacific, methylation over the entire 36-hour incubation period appears to be controlled by particle-induced demethylation of newly produced $Me^{202}Hg$ after rapid production. The $Me^{202}Hg$ produced in unfiltered waters from the oxygen minimum depth at 12°S is quickly demethylation (Figure 6, white triangles). Methylation in filtered waters is similar in magnitude to that in unfiltered waters but persists over the course of the incubation (Figure 6, black triangles).

Consistent with previous measurements from Arctic and Mediterranean waters [Lehnherr et al, 2011; Monperrus et al, 2007], values of k_m measured in the water column along a transect of the Pacific are decoupled from ambient concentrations of methylated Hg (Figure 10). Previous work has suggested that in situ methylation within low oxygen depths of the North Pacific result in elevated methylated Hg concentrations [Sunderland et al, 2009]. The northernmost of our incubations, at 17°N, took place within 750 km of waters sampled by Sunderland et al, 2009. At 17°N, we observed no significant difference in potential methylation rates between the chlorophyll maximum and oxygen minimum depths despite a difference of ~300 fM between ambient methylated Hg concentrations between the two depths (Figure 4). Furthermore, the addition of bulk organic matter from McLane pump filters to bottle incubation did not enhance potential methylation in waters collected from this site. These observations suggest that delivery of Hg(II) by organic matter does not limit methylated Hg production in North Pacific waters.

Full Hg speciation measurements at Station 1 [Munson—this work, Chapter 3] reveal substantial concentrations of Hg(II) (~1 pM, calculated as: [THg] – [Hg(0)] – [DMHg] – [MMHg]) are found in low oxygen waters at all stations where potential methylation rates were measured (Figure 11). The detection of Hg(II) does not provide information about its availability to processes or metabolisms involved in methylation. However, the relatively high concentrations of Hg(II) implies that methylation along the transect is not solely limited by Hg(II) substrate availability.

Laboratory studies have speculated that abiotic methylation of Hg(II) by methylcobalamin may be a possible methylation pathway in natural systems [Celo et al, 2006;

Jimenez-Moreno, 2013]. The addition of methylcobalamin to seawater incubations resulted net reduction of Hg(II) to Hg(0) rather than methylation (Figure 2). As a result, we do not believe abiotic methylation by methylcobalamin is a significant source of methylated Hg to Equatorial Pacific waters.

Despite the lack of methylation by methylcobalamin, non cellular methylation appears to be a significant source of MMHg production and dominated total methylation measured over 24-hour incubations (Figure 5). The use of 0.2 μm filtered and unfiltered seawater to quantify methylation by heterotrophic bacteria is an operational distinction. Although hard to quantify, cells have been found in marine waters after filtration through 0.2 μm filters in the Mediterranean and Sargasso Sea [Haller et al, 1999; Li and Dickie, 1985] under vacuum filtration. These so-called ultramicrobacteria (<0.1 μm^3 volume) [reviewed by Duda et al., 2012] may include cells in starvation or inactive forms, cells with flexible walls that allow them to pass through filter pores, and cells that are < 0.2 μm regardless of their stage of life or nutrient status [Heller et al, 1999]. The smallest identified free-living marine cells, the SAR11 clade, have diameters of 0.12-0.20 μm [Rappé et al, 2002]. In addition, viruses, and cell materials may pass through filters. As a result, we have avoided referring to filtered water as abiotic because they likely contain materials of biological origin. However, 0.2 μm filtration would potentially collect a subset any potentially intact cells such as SAR11 due to clogging of filters. In addition, if the cells that pass through filters are sessile or, like SAR11, have slow growth rates (0.40-0.58 d^{-1}) [Rappé et al, 2002], filtered waters would likely have lower cell density and less diversity in the active metabolisms present compared to unfiltered waters. As a result, we have not attributed the high methylation observed in filtered waters to cellular mechanisms because such an assumption would require a number of processes, such as reactivation of sessile cells, rapid rates of cell growth, and/or preferential selection of Hg(II) methylating cells during filtration that cannot be determined from our experimental design. Under the assumption that filtration removed a majority of the heterotrophic bacteria relative to unfiltered waters, methylation in 0.2 μm filtered Tropical Pacific waters that was equal or greater than that of unfiltered waters (Figure 5) suggests that heterotrophic bacterial methylation is not the primary source of methylated Hg to these waters. Instead, the presence of particles appeared to enhance demethylation of $Me^{202}Hg$ that can be rapidly produced in all marine waters.

Previous reports of methylation rates have differed in their considerations of available Hg(II) substrate. Monperrus et al, 2007 assumed a constant supply of Hg(II) substrate for

methylation. In contrast, the rates presented by Lehnherr et al, 2011 were calculated from an increase in isotopically enriched MMHg relative to available Hg(II) substrate. However, in their experiments the available Hg(II) substrate was measured in separate bottle experiments [Lehnherr et al, 2011]. Although we were unable to calculate demethylation rates in the majority of samples, methylation potential was seen in 0.2 μm filtered water, and often in excess of methylation potential in unfiltered samples, suggesting that a generalized loss of Hg(II) in not an accurate representation of Hg(II) availability for calculations for similar dual isotope tracer experiments.

Acknowledgements

This work was funded by the National Science Foundation in a Chemical Oceanography Program Grant (OCE-1031271) awarded to C. H. Lamborg and M. A. Saito and a Graduate Student Fellowship to K. M. Munson. The authors thank Vic Polidoro, Trevor Young, Captain Drewry, and the crew of the *R/V Kilo Moana*.

References

Bertrand, E. M, M. A. Saito, J. M. Rose, C. R. Riesselman, M. C. Lohan, A. E. Noble, P. A. Lee, and G. R. DiTullio (2007) Vitamin B12 and iron co-limitation of phytoplankton growth in the Ross Sea. Limnol. Oceanogr., 52, 1079-1093.

Black, F. J., C. H. Conaway, and A. R. Flegal (2009) Stability of dimeethylmercury in seawater and its conversion to monomethyl mercury. Environ. Sci. Technol., 43, 4056-4062.

Blum, J. D., B. N. Popp, J. C, Drazen, C. A. Choy, and M. W. Johnson (2013) Methylmercury production below the mixed layer in the North Pacific Ocean, Nature Geosci. 6, 879-884.

Bonnet, S., E. A. Webb, C. Panzeca, D. M. Karl, D. G. Capone, and S. A. Sañudo-Wilhelmy (2010) Vitamin B12 excretion by cultures of the marine cyanobacteria Crocosphaera and Synechococcus, Limnol. Oceanogr., 55, 1959-1964.

Celo, V., D. R. S. Lean, and S. L. Scott (2006) Abiotic methylation of mercury in the aquatic environment, Sci Tot Environ., 368, 126-137.

Cossa, D., J.-M. Martin, K. Takayanagi, J. Sanjuan (1997) The distribution and cycling of mercury species in the western Mediterranean. Deep-Sea Res. II 44, 721-740.

Cossa, D., B. Averty, and N. Pirrone (2009) Origin of methylmercury in open Mediterranean waters, Limnol. Oceanogr. 54, 837-844.

Cossa, D., L.-E. Heimbürger, D. Lannuzel, S. R. Rintoul, E. C. V. Butler, A. R. Bowie, B. Averty, R. J. Watson, and T. Remenyi (2011) Mercury in the Southern Ocean, Geochim Cosmochim Acta, 75, 4037-4052.

Droop, M. R. (2007) Vitamins, phytoplankton and bacteria: symbiosis and scavenging? J. Plankton Res., 29, 107-113.

Duda, V. I., N. E. Suzina, V. N. Polvtseva, and A. M. Boronin (2012) Ultramicrobacteria: formation of the concept and contribution of ultramicrobacteria to biology, Microbiol. 81, 379-390.

Dupont, C. L., J. W. Moffett, R. R. Bidigare, and B. A. Ahner (2007) Distributions of particulate and dissolved thiols in the sub-polar North Pacific. Deep-Sea Res. I 53, 1961-1974.

Ekstrom, E. B., F. M. M. Morel, and J. M. Benoit (2003) Mercury methylation independent of the acetyl-coenzyme A pathway in sulfate-reducing bacteria, Appl. Environ. Microbiol., 69, 5414-5422.

Ekstrom, E. B, and F. M. M. Morel (2008) Cobalt limitation of growth and mercury methylation in sulfate-reducing bacteria. Environ. Sci. Technol., 42, 93-99.

Filipelli, M., and F. Baldi (1993) Alkylation of ionic mercury to methylmercury and dimethylmercury by methylcobalamin: simultaneous determination by purge-and-trap GC in line wth FTIR, Appl. Organometallic Chem., 7, 487-493.

Garcia, H. E., and L. I. Gordon (1992) Oxygen solubility in seawater: better fitting equations, Limnol. Oceanogr., 37(6), 1307-1312.

Gilmour, C. C., M. Podar, A. L. Bullock, A. M. Graham, S. D. Brown, A. C. Somenahally, A. Johs, R. A. Hurt Jr., K. L. Bailey, and D. A. Elias (2013) Mercury methylation by novel microorganisms from new environments, Environ. Sci. Technol., 47, 11810-11820.

Gosnell, K., R. P. Mason, and P. H. Balcom (2013) Inorganic mercury and methylmercury concentrations in south-central Pacific phytoplankton and zooplankton, International Conference on Mercury as a Global Pollutant, Edinburgh, UK.

Graham, A. M., A. L. Bullock, A. C. Maizel, D. A. Elias, and C. C. Gilmour (2012) Detailed assessment of the kinetics of Hg-cell association, Hg methylation, and methylmercury degradation in several Desulfovibrio species, Appl. Environ. Microbiol., 78, 7337-7346.

Haller, C. M., S. Rolleke, D. Vybiral, A. Witte, B. Velimirov (1999) Investigation of 0.2 μm filterable bacteria from the Western Mediterranean Sea using a molecular approach: dominance of potential starvation forms. FEMS Microbiol. Ecol., 31, 153-161.

Hammerschmidt, C. R., and K. L. Bowman (2012) Vertical methylmercury distribution in the subtropical North Pacific Ocean, Mar. Chem., 132-133, 77-82.

Hintelmann, H., and R. D. Evans (1997) Application of stable isotopes in environmental tracer studies – measurement of monomethylmercury (CH_3Hg^+) by isotope dilution ICP-MS and detection of species transformation, Fresenius J. Anal. Chem., 358, 378-385.

Hintelmann, H., and N. Ogrinc (2003) Determination of stable mercury isotopes by ICP/MS and their application in environmental studies, in Biogeochemistry of environmentally important trace elements, Eds: Cai, Y., and C. O. Braids, ACS Symp Ser Vol. 835, Washington, DC, p. 321-338.

Jiménez-Moreno, J., V. Perot, V. N. Epov, M. Monperrus, and D. Amouroux (2013) Chemical kinetic isotope fractionation of mercury during abiotic methylation of Hg(II) by methylcobalamin in aqueous chloride media, Chem. Geol., 336, 26-36.

Kading, T. (2013) Distribution of thiols in the northwest Atlantic Ocean. Master's thesis. MIT/WHOI Joint Program in Chemical Oceanography.

Kraepiel, A. M. L., K. Keller, H. B. Chin, E. G. Malcolm, F. M. M. Morel (2003) Sources and variations of mercury in tuna. Environ. Sci. Technol., 37, 5551-5558.

Lalli, C., and T. Parsons (1997) Biological Oceanography: An introduction. 2nd ed. Butterworth-Heinemann.

Lamborg, C., W. Fitzgerald, J. O'Donnell, and T. Torgensen (2002) A non-steady-state compartmental model of global scale mercury biogeochemistry with inter-hemispheric atmospheric gradients. Geochim. Cosmochim. Acta 66, 1105-1118.

Lamborg, C. H., C. R. Hammerschmidt, G. A. Gill, R. P. Mason, and S. Gichuki (2012) An intercomparison of procedures for the determination of total mercury in seawater and recommendations regarding mercury speciation during GEOTRACES cruises. Limnol. Oceanogr. Methods, 10, 90-100.

Lehnherr, I., V. L. St Louis, H. Hintelmann, and J. L. Kirk (2011) Metyhlation of inorganic mercury in polar marine waters, Nature Geosci., 4, 298-302.

Li, W. K. W., and P. M. Dickie (1985) Growth of bacteria in seawter filtered throu 0.2 μm Nucleopore membraines: implications for dilution experiments. Mar. Ecol. Prog. Ser. 26, 245-252.

Malcolm, E. G., J. K. Schaefer, E. B. Ekstrom, C. B. Tuit, A. Jayakumar, H. Park, B. B. Ward, and F. M. M. Morel (2010) Mercury methylation in oxygen deficient zones of the oceans: no evidence for the predominance of anaerobes, Mar. Chem., 122, 11-19.

Mason, R. P., and W. F. Fitzgerald (1990) Alkylmercury species in the equatorial Pacific. Nature 347, 457-459.

Mason, R. P., and W. F. Fitzgerald (1993) The distribution and cycling of mercury in the equatorial Pacific Ocean. Deep Sea Res. Part I 40, 1897-1924.

Mason, R. P., K. A. Sullivan (1999) The distribution and speciation of mercury in the south and equatorial Atlantic. Deep Sea Res II, 46, 937-956.

Mason, R. P., K. R. Rolfhus, W. F. Fitzgerald (1998) Mercury in the North Atlantic. Mar. Chem. 61, 37-53.

Monperrus, M., E. Tessier, D. Amouroux, A. Leynaert, P. Huonnic, and O. F. X. Donard (2007) Mercury methylation, demethylation and reduction rates in coastal and marine surface waters of the Mediterranean Sea, Mar. Chem., 107, 49-63.

Monperrus, M., E. Tessier, D. Point, K. Vidimova, D. Amouroux, R. Guyoneaud, A. Leynaert, J. Grall, L. Chauvaud, G. Thouzeau, and O. F. X. Donard (2007) The biogeochemistry of mercury at the sediment-water interface in the Thau Lagoon. 2. Evaluation of mercury methylation potential in both surface sediment and the water column. Est. Coast. Shelf Sci., 72, 485-496.

Ndu, U., R. P. Mason, H. Zhang, S. Lin, and P. T. Visscher (2012) Effect of inorganic and organic ligands on the bioavailability of methylmercury as determined by using a mer-lux bioreporter. Appl. Environ. Microbiol., 78, 7276-7282.

Panzeca, C., A. J. Beck, A. Tovar-Sanchez, J. Segovia-Zavala, G. T. Taylor, C. J. Gobler, and S. A. Sanudo-Wilhelmy (2009) Distributions of dissolved vitamin B12 and Co in coastal nad open-ocean environments, Estuar. Coast. Shelf Sci., 85, 223-230.

Parks, J. M., A. Johs, M. Podar, R. Bridou, R. A. Hurt, S. D. Smith, S. J. Tomanicek, Y. Qian, S. D. Brown, C. C. Brandt, A. V. Palumbo, J. C. Smith, J. D. Wall, D. A. Elias, and L. Liang (2013) The genetic basis for bacterial mercury methylation, Science, 339, 1332-1335.

Rappé, M. S., S. A. Connon, K. L. Vergin, and S. J. Giovannoni (2002) Cultivation of the ubiquitous SAR11 marine bacterioplankton clade, Nature, 418, 630-633.

Sarmiento, J. L., and N. Gruber (2006) Ocean Biogeochemical Dynamics, 526pp., Princeton University Press, Princeton, New Jersery.

Schaefer, J. K., and F. M. M. Morel (2009) High methylation rates of mercury bound to cysteine by Geobacter sulfurreducens, Nature Geosci., 2, 123-126.

Schaefer, J. K., S. S. Rocks, W. Zheng, L. Liang, B. Gu, and F. M. M. Morel (2011) Active transport, substrate specificity, and methylation of Hg(II) in anaerobic bacteria. Proc. Natl. Acad. Sci., 108, 8714-8719.

Shanks, A. L., and M. L. Reeder (1993) Reducing microzones and sulfide production in marine snow. Mar. Ecol. Prog. Ser. 96, 43-47.

Stramma, L., Johnson, G. C., Sprintall, J., and V. Mohrholz (2008) Expanding oxygen-minimum zones in the tropical oceans, Science, 320, 655-658.

Sunderland, E. M., D. P. Krabbenhoft, J. W. Moreau, S. A. Strode, and W. M. Landing (2009) Mercury sources, distribution, and bioavailability in the North Pacific Ocean: insights from data and models. Gobal Biogeochem. Cy., 23, GB2010.

Swarr, G., T. Kading, C. Lamborg, and C. Hammerschmidt (2013) Profiles of cysteine and glutathione from the U.S. North Atlantic GEOTRACES zonal transect. Presentation at the Aquatic Science Meeting of the Association of Limnology and Oceanography, New Orleans, LA.

Vo, A.-T. E., M. S. Bank, J. P. Shine, and S. V. Edwards (2011) Temporal increase in organic mercury in an endangered pelagic seabird assessed by century-old museum specimens. Proc. Natl. Acad. Sci. 108, 7466-7471.

Xu, L.-Q., X.-D. Liu, L.-G. Sun, Q.-Q. Chen, H. Yan, Y. Liu, Y.-H. Luo, and J. Huang (2011) A 700-year record of mercury in avian eggshells of Guangjin Island, South China Sea. Environ. Pollut., 159, 889-896.

Figures and Figure Legends

Figure 1: Map of stations where mercury methylation incubations were performed in the Pacific Ocean along the Metzyme cruise track. Measurements of potential methylation were performed at 17°N, 8°N, 0°, and 12°S (circled) in the Tropical and Equatorial Pacific Ocean. The cruise track spanned a large gradient in hydrographic parameters and ambient methylated Hg species concentrations.

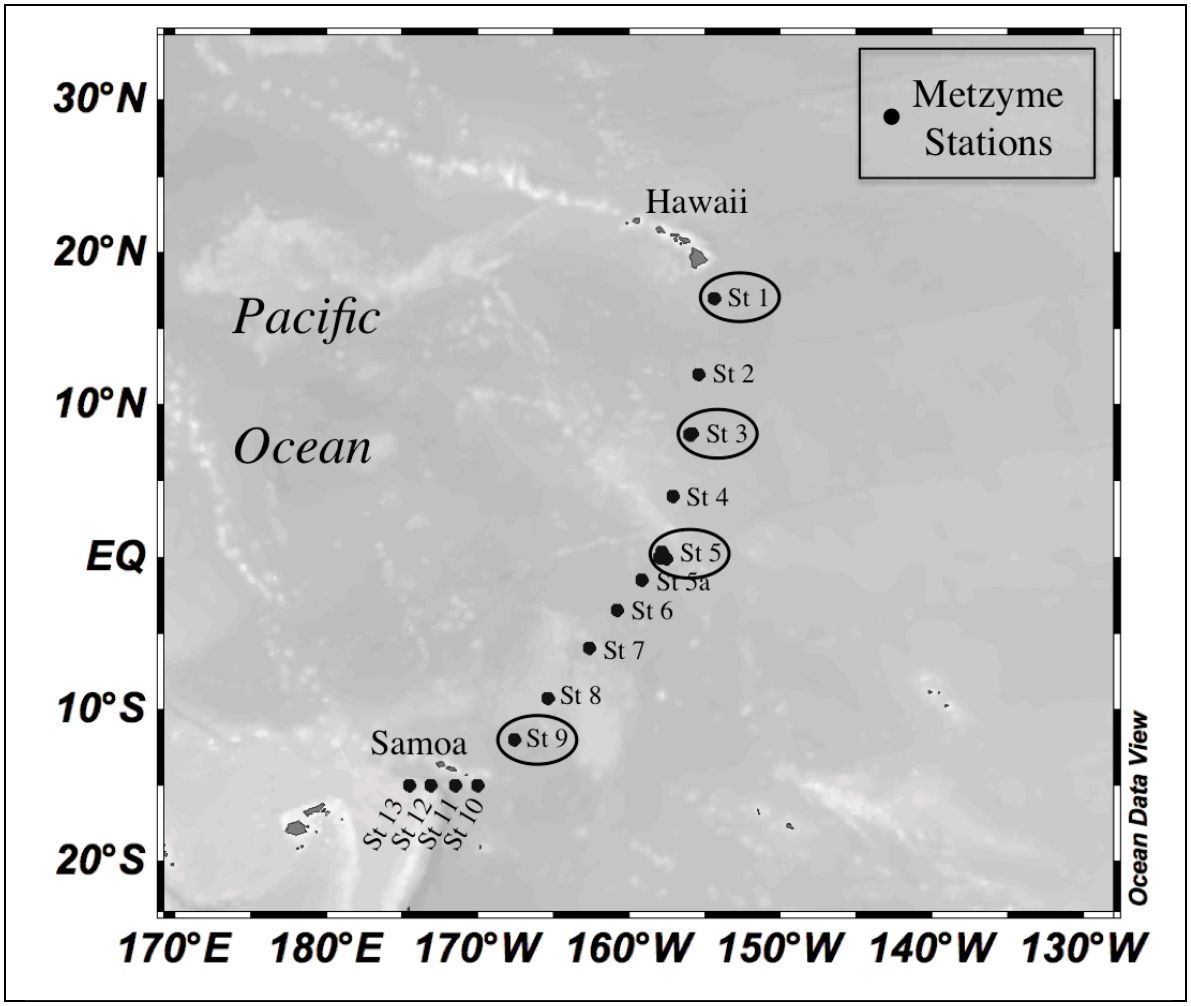

Figure 2: Reduction of mercury in incubations of marine waters amended with methylcobalamin. Chromatograms of ICPMS intensity for Hg isotopes monitored to trace methylation and demethylation, ^{198}Hg (black), ^{200}Hg (grey), ^{202}Hg (dotted) from two replicate bottles of t0 unfiltered water from the North Pacific (17°N). In one replicate (A), Hg° (1), MMHg (2,), and Hg(II) (3) peaks are quantifiable. In the second replicate (B) a substantial amount of ^{202}Hg(II) is lost to reduction and is apparent in the increase of the Hg(0) peak. None of the isotope traces in the resulting MMHg peak (2) are measurable relative to the baseline.

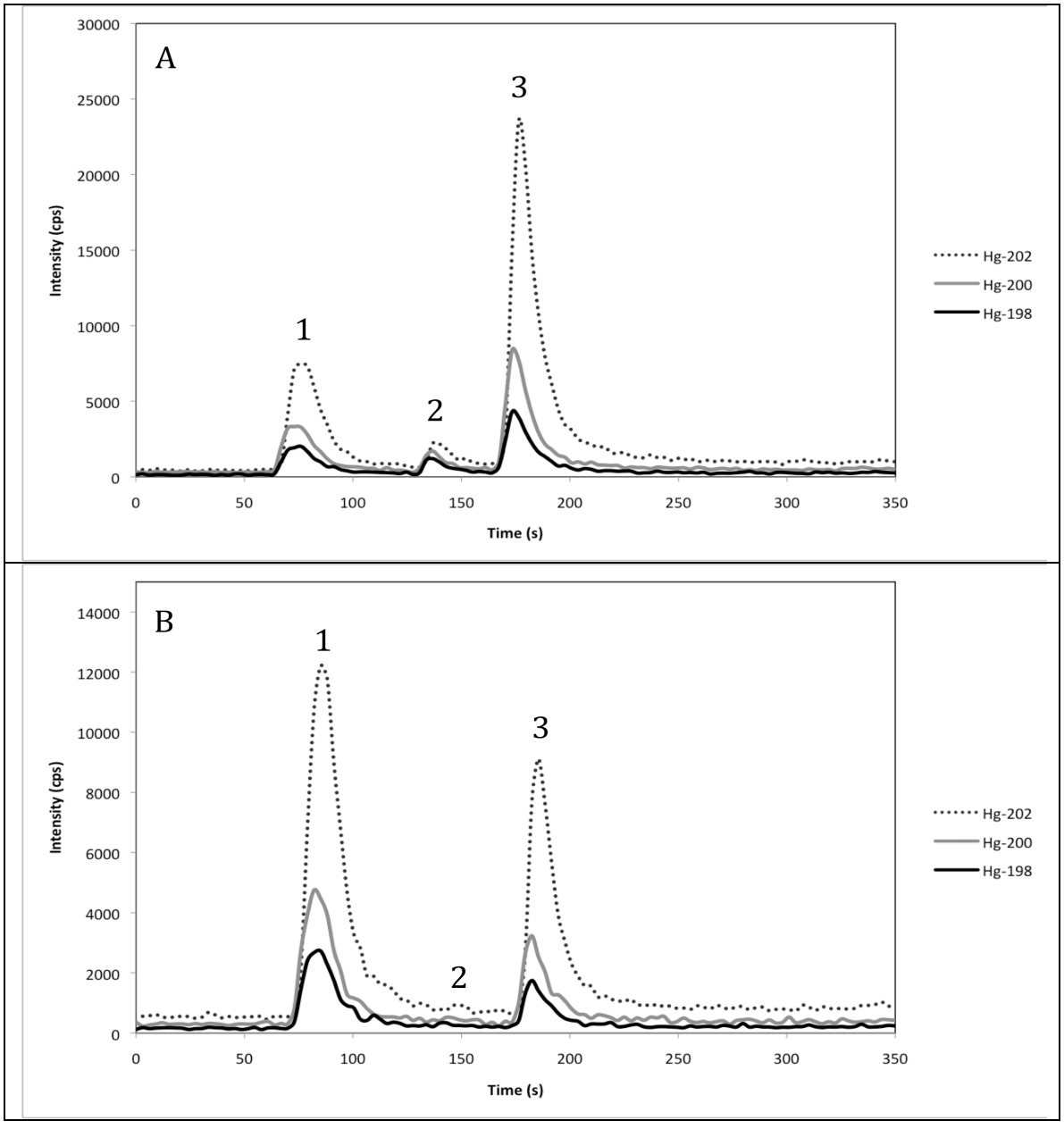

Figure 3: Concentrations of dissolved oxygen and and calculated values of apparent oxygen utilization at incubation stations. Dissolved oxygen concentrations (top panel) in intermediate waters are lowest in the North Pacific, increase in the Equatorial Pacific, and are highest in the South Pacific. Values of AOU (bottom panel) match closely with oxygen throughout cruise transect. At 12°S (Station 9), an unusual dissolved O_2 depth profile showed two low dissolved O_2 depths (175 m and 400 m), both of which were used for incubation experiments.

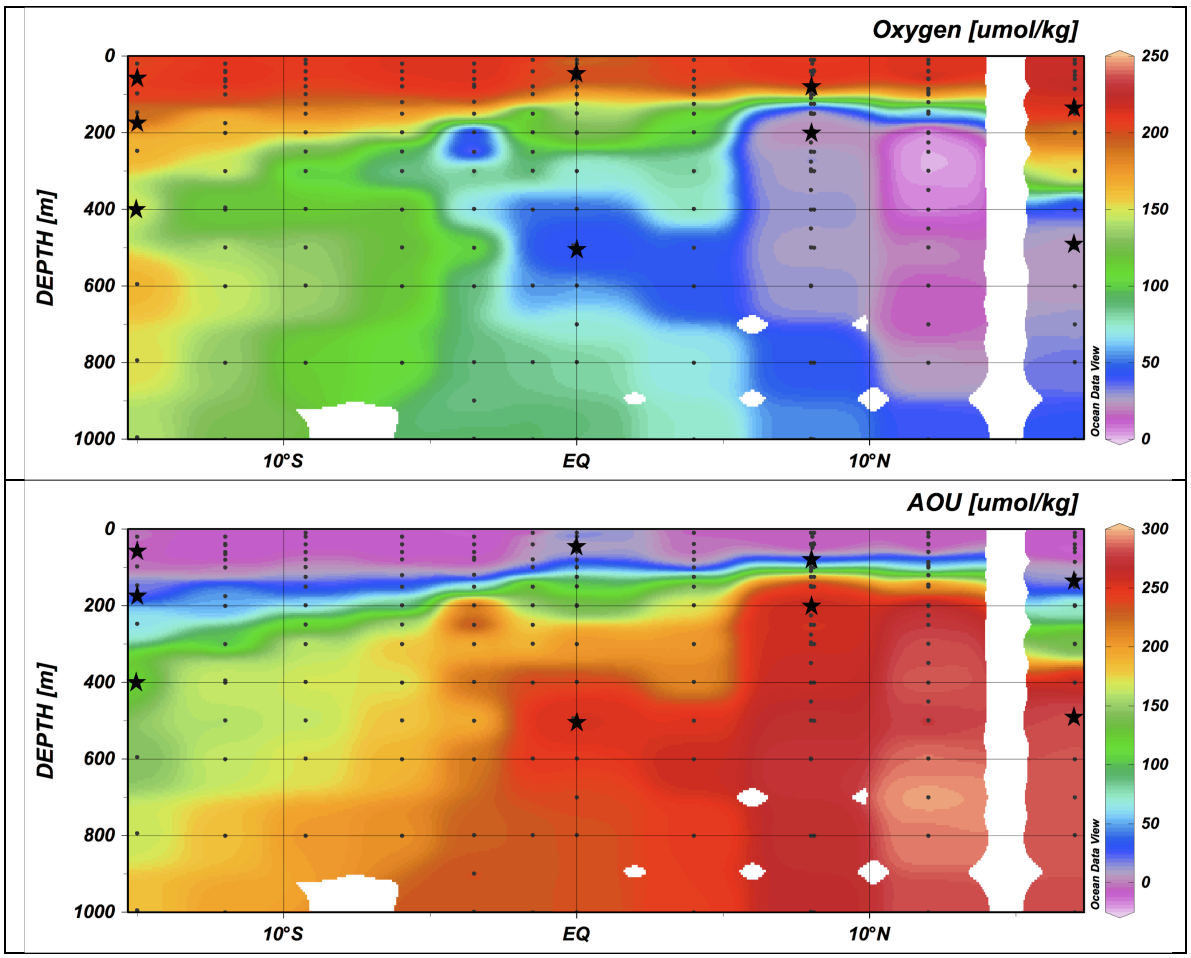

Figure 4: Concentrations of dissolved total and methylated mercury at incubation stations. Methylated Hg (measured as [DMHg] and [MMHg]) concentrations are shown along cruise transect with incubation locations and depths indicated by stars. Incubations were performed at depths of the chlorophyll-a maximum and minimum dissolved O_2 concentration from CTD data at each station. At 17°N (Station 1), MMHg concentrations were estimated from concentrations in incubations bottles.

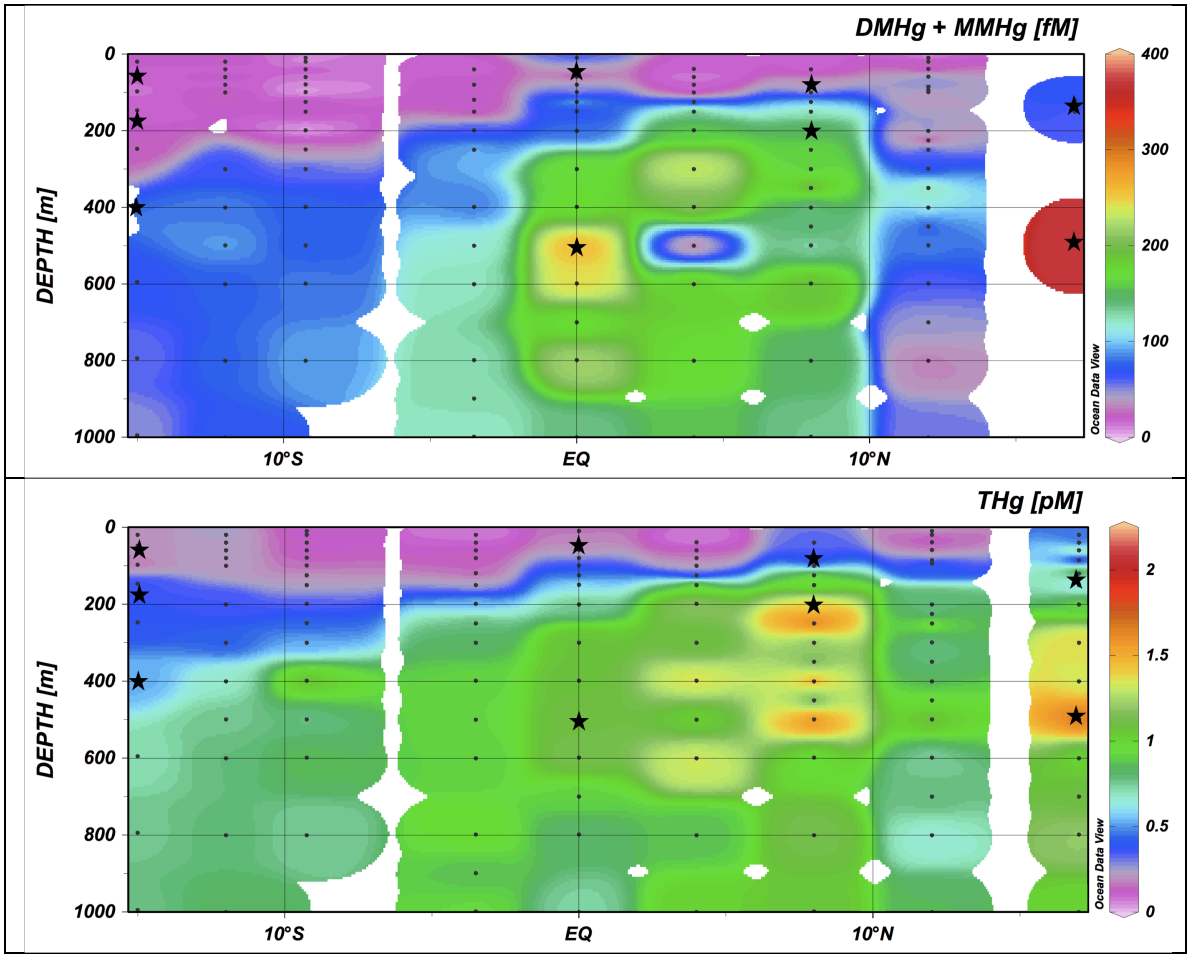

Figure 5: Initial and total methylation of Hg(II) in Tropical Pacific waters. Methylation, calculated as the percentage of $Me^{202}Hg$ produced from available $^{202}Hg(II)$ substrate from isotope spike additions, is shown for four stations along the Metzyme cruise track from the North to South Pacific. Methylation was measured in 0.2 µm filtered (0.2 µm) and unfiltered (un) from the chlorophyll maximum (CMX) and oxygen minimum (OMZ) at each station. At all stations, initial methylation (black bars) was measureable in t0 bottles relative and could account for the total methylation observed over 24-hour incubations (grey bars).

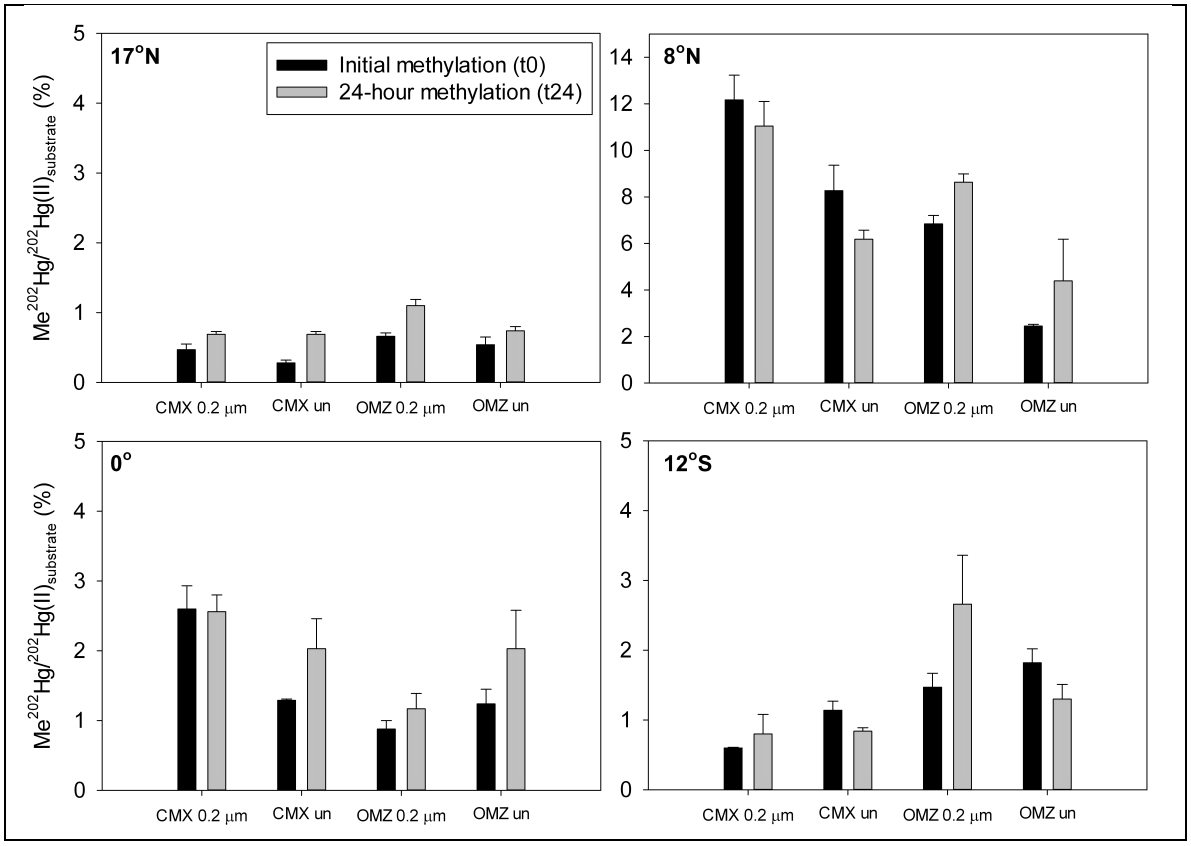

Figure 6: Methylated mercury production over a 36-hour time course in South Pacific waters. Methylation, calculated as the percentage of $Me^{202}Hg$ produced from available $^{202}Hg(II)$ substrate from isotope spike additions, is shown for 6 time points over a 36-hour incubation time course at 12°S. Methylation was measured in 0.2 μm filtered (0.2 μm, black symbols) and unfiltered (un, white symbols) seawater from the chlorophyll maximum (CMX, circles) and oxygen minimum (OMZ, triangles) depths at this station. Higher resolution sampling reveals dynamic cycling between methylation and demethylation compared to net changes over 24-hour incubation periods (Figure 5). Demethylation of newly formed methylated Hg occurs after 6 hours in unfiltered water from the oxygen minimum depth (white triangles) and is enhanced by the presence of particulate matter compared to 0.2 μm filtered water (black triangles) in which produced $Me^{202}Hg$ persists throughout the full incubation period.

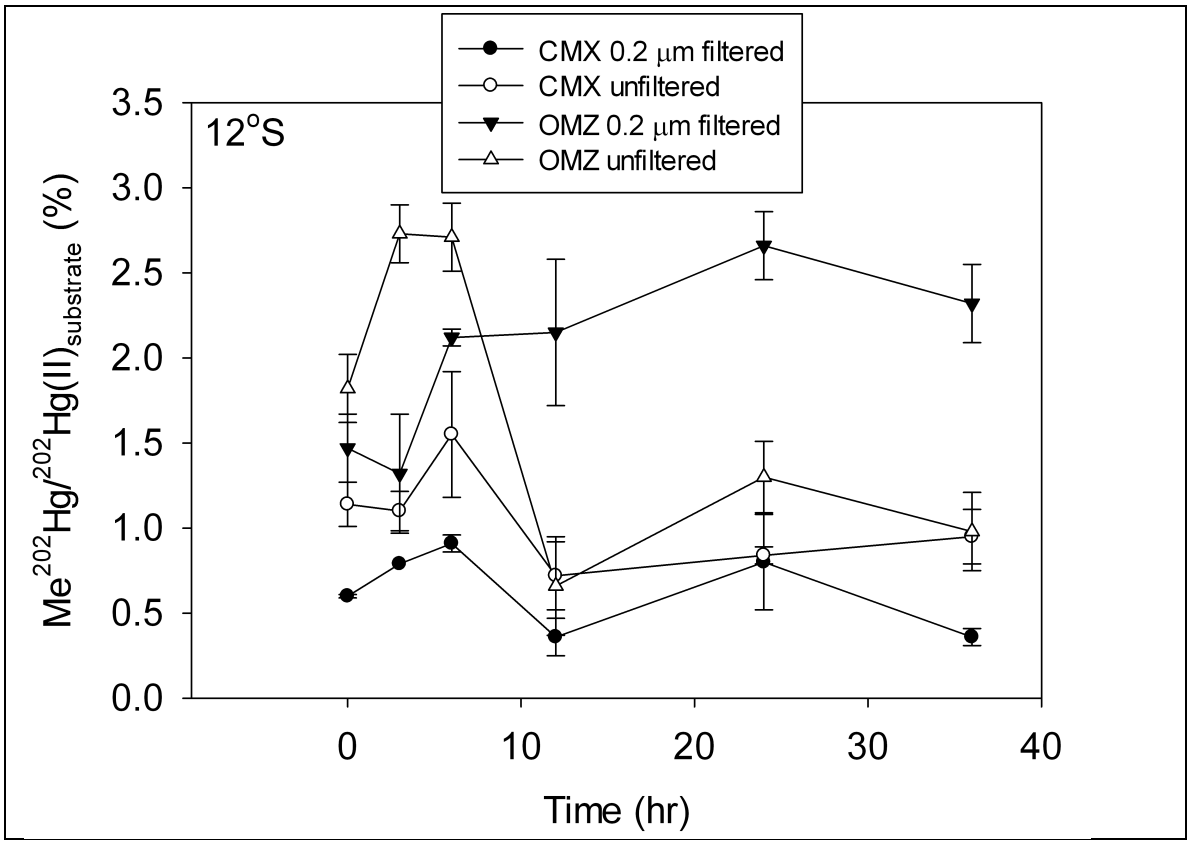

Figure 7: Demethylation of monomethylmercury over a 36-hour time course incubation in South Pacific waters. Demethylation is measured as the loss of added $MM^{198}Hg$ over from 0.2 μm filtered (0.2 μm, black symbols) and unfilterd (un, white symbols) waters from the chlorophyll maximum (CMX) and oxygen minimum (OMZ) depths at 12°S. Rapid demethylation of ~300 fM added $MM^{198}Hg$ spikes pre-equilibrated with natural ligands in filtered seawater was implied by the loss of added spike prior to fixation of t0 sample bottles for chlorophyll maximum waters (circles) and filtered oxygen minimum waters (black triangles). Quantitative demethylation was limited to unfilterd waters from the oxygen minimum depth (white triangles) at 12°S.

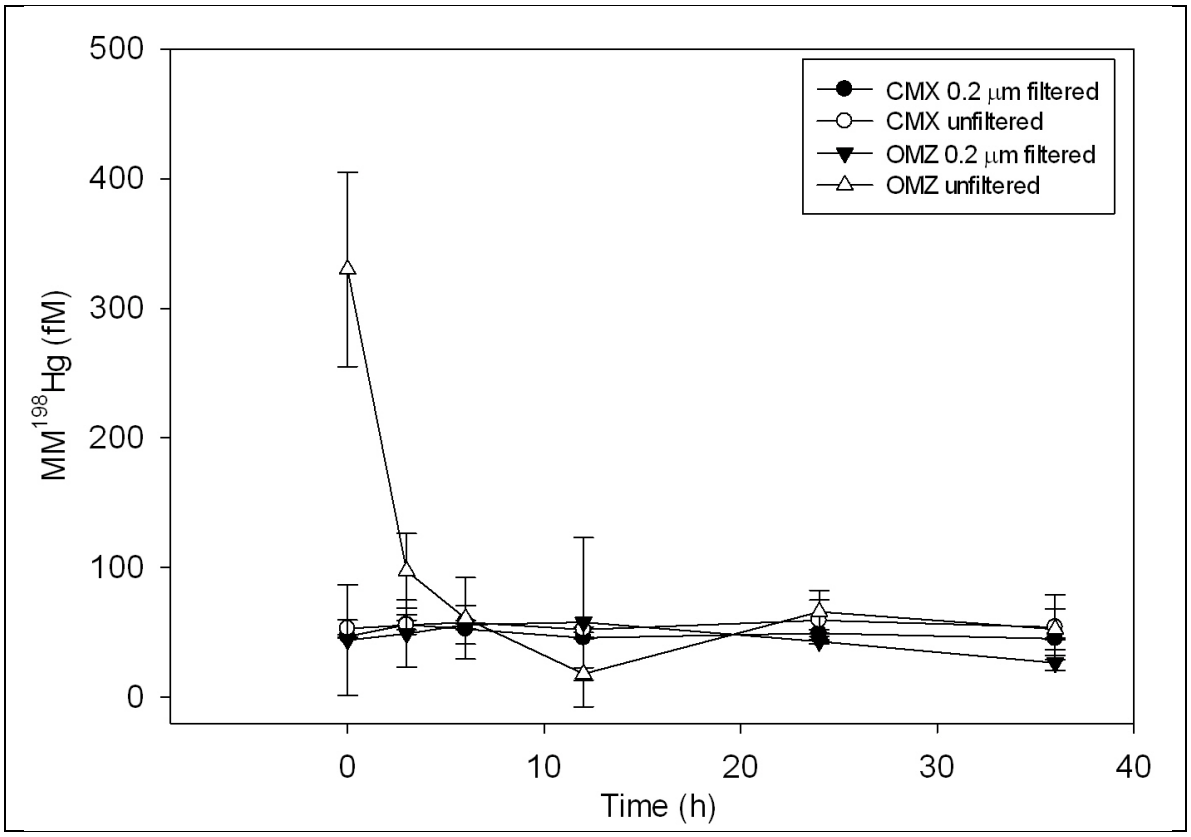

Figure 8 (following page): Methylation of mercury in treatment-amended incubations of water from chlorophyll maximum waters in the Tropical Pacific. Methylation, calculated as the percentage of $Me^{202}Hg$ produced from available $^{202}Hg(II)$ substrate from isotope spike additions, for waters amended with additions of compounds thought to be involved with Hg(II) uptake and methylation normalized to unamended (un) samples. Treatments are abbreviated as follows: succinate (C), cobalt (Co), succinate and cobalt (CoC), McLane pump sections (punch), cobalt and cysteine (CoCys), cysteine (Cys), glutathione (GSH), methylcobalamin (B12), and cysteine and succinate (CysC). Grey bars in upper panel indicate incubation treatments that were not performed for filtered water. Only unfiltered waters (lower panel) from 12°S (yellow) were amended with treatments. The error bars represent one standard deviation from triplicate incubation bottles.

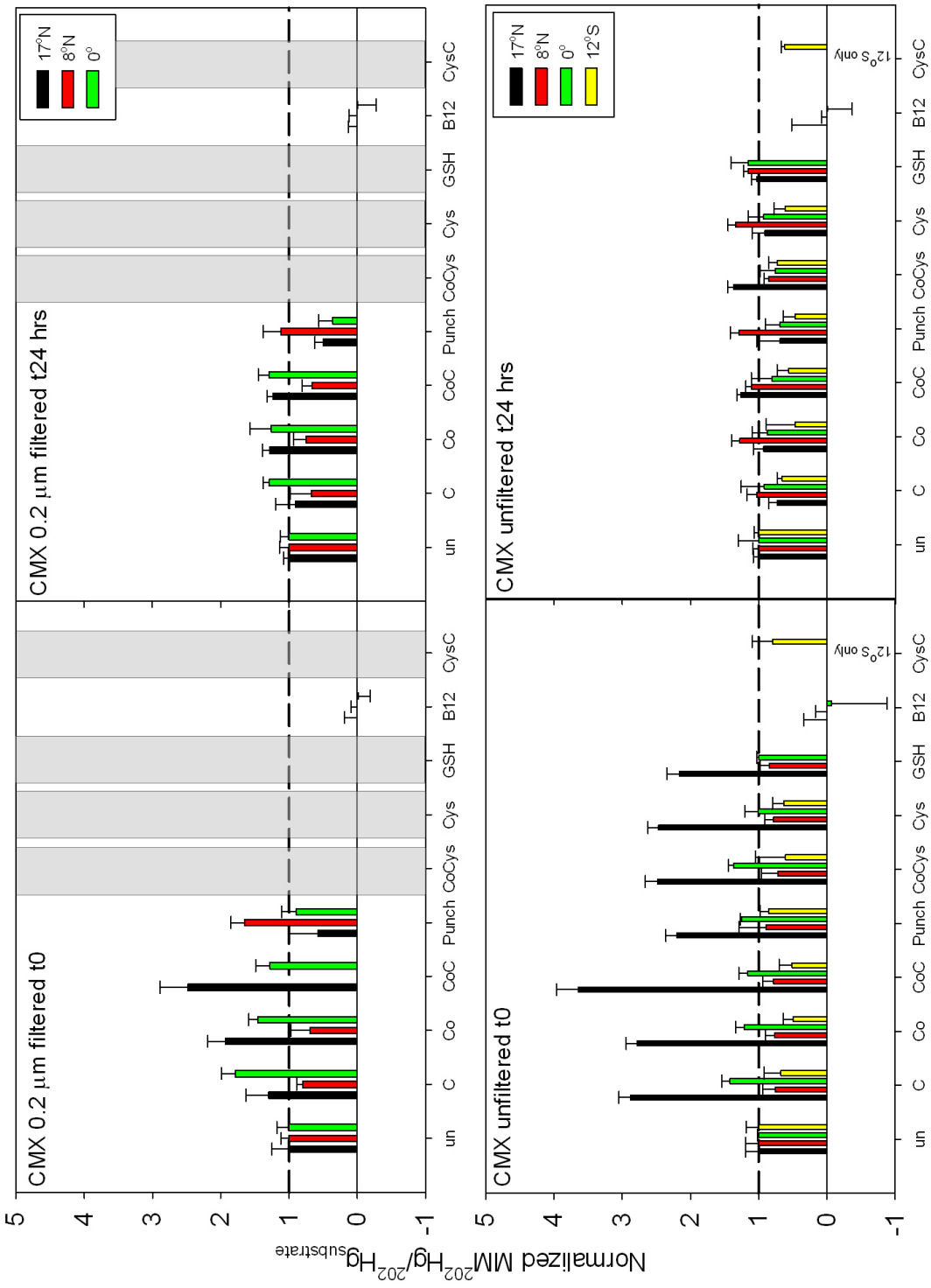
CMX 0.2 µm filtered t0
CMX 0.2 µm filtered t24 hrs
CMX unfiltered t0
CMX unfiltered t24 hrs
17°N
8°N
0°
12°S
12°S only
un
C
Co
CoC
Punch
CoCys
Cys
GSH
B12
CysC
Normalized MM202Hg/202Hgsubstrate

Figure 9 (following page): Methylation of mercury in treatment-amended incubations of water from oxygen minimum waters in the Tropical Pacific. Methylation, calculated as the percentage of $Me^{202}Hg$ produced from available $^{202}Hg(II)$ substrate from isotope spike additions, for waters amended with additions of compounds thought to be involved with Hg(II) uptake and methylation normalized to unamended (un) samples. Treatments are abbreviated as follows: succinate (C), cobalt (Co), succinate and cobalt (CoC), McLane pump sections (punch), cobalt and cysteine (CoCys), cysteine (Cys), glutathione (GSH), methylcobalamin (B12), and cysteine and succinate (CysC). Grey bars in upper panel indicate incubation treatments that were not performed for filtered water. Only unfiltered waters (lower panel) from 12°S (yellow) were amended with treatments. The error bars represent one standard deviation from triplicate incubation bottles.

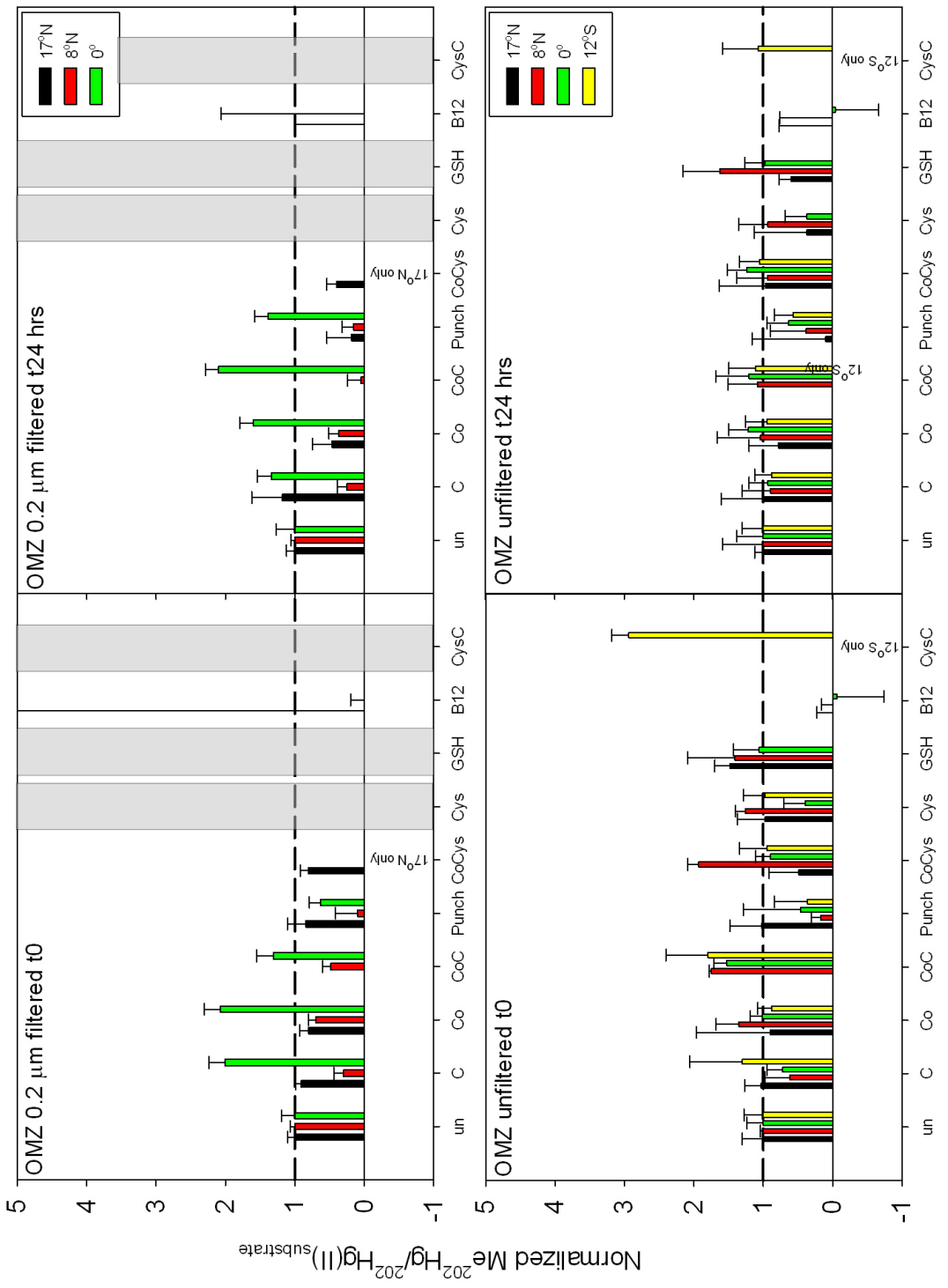
OMZ 0.2 µm filtered t0
OMZ 0.2 µm filtered t24 hrs
OMZ unfiltered t0
OMZ unfiltered t24 hrs
17°N
8°N
0°
12°S
17°N only
12°S only
un
C
Co
CoC
Punch
CoCys
Cys
GSH
B12
CysC
Normalized Me202Hg/202Hg(II)substrate

Figure 10: Relationships between methylation and measured MeHg and THg concentrations in Tropical Pacific waters. Initial methylation (black symbols) and 24-hour incubation methylation (grey symbols) from unfiltered waters from the chlorophyll maximum (CMX, left panels) and oxygen minimum (OMZ, right panels) depths in Tropical Pacific waters versus measured concentrations of total mercury (THg, top panels) and methylated mercury ([DMHg] + [MMHg]). No clear relationship was observed between methylation and mercury species concentrations.

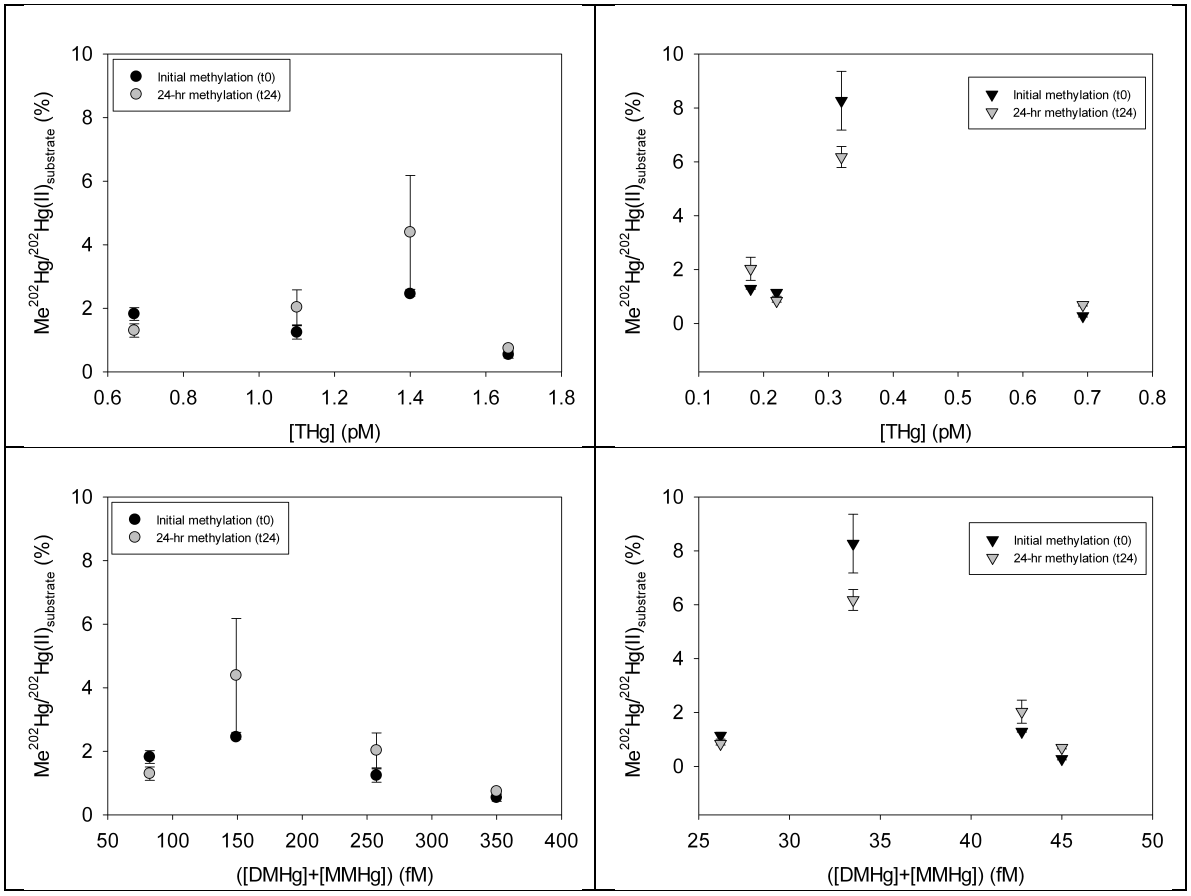

Figure 11: Calculated dissolved Hg(II) in the Tropical Pacific. Dissolved Hg(II) (pM) was calculated as the difference between THg and the sum of Hg(0), DMHg, and MMHg measured as distinct chemical species along Metzyme cruise track. In regions of high methylatedHg (500m at St 5, 500m at St 1), The close relationship observed in the North Pacific between methylated Hg concentrations and organic carbon remineralization rates implies methylation is limited by Hg(II) substrate delivery to depths of organic matter remineralization [Sunderland et al, 2009]. The persistence of dissolved Hg(II) in concentrations between 1-1.25 pM, suggests that methylation may not be limited by dissolved Hg(II) concentrations at these depths and is limited by additional factors such as Hg(II) availability or methyl donors.

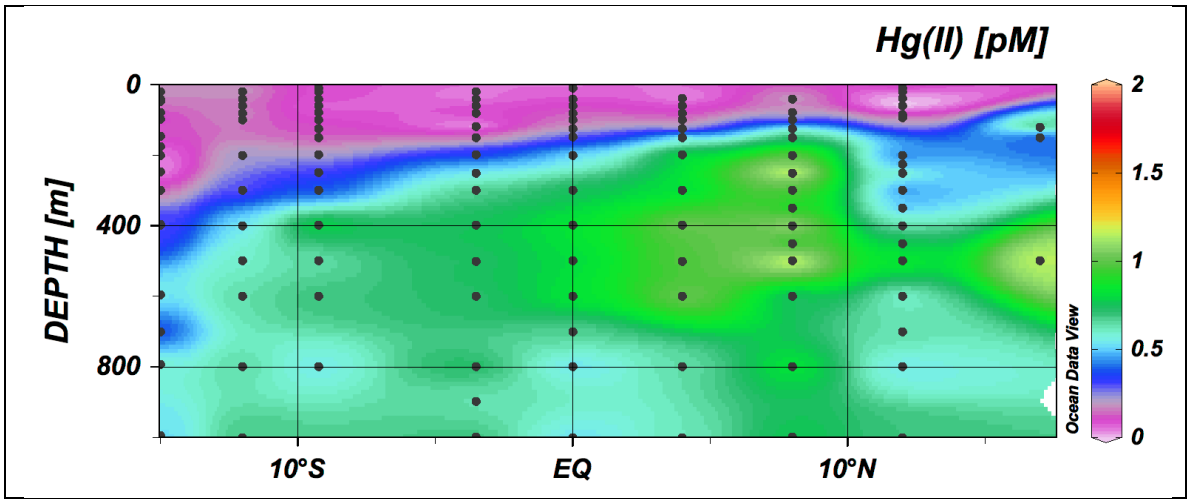

Tables and Table Legends

Table 1: Water column characteristics for Pacific Ocean waters from which potential mercury methylation rates were measured.

Sta	Depth (m)	Temp (°C)	$Temp_{inc}$ (°C)[1]	O_{2diss} (µmol/kg)	AOU* (µmol/kg)	THg (pM)	DMHg (fM)	MMHg (fM)
17°N	1:3 mix 120:150 [2]	22	19-26	214:205	-	1:0.59	40:30	10[3]
17°N	500	7	13	20	282.9	1.66	40	310[3]
8°N	75-80	21	23	218	-	0.32	30	3.5
8°N	200	11	13	15	264.1	1.4	100	49.1
0°	50	26	23	202	-	0.18	20	22.8
0°	500	8	14	43	252	1.1	110	147.3
12°S	60	28	13-16	207	-	0.22	0	26.2
12°S	175	25	13-16	162	47.0	0.35	20	0
12°S	400	11	13-16	116	163	0.67	40	42.4

[1]Ranges represent monitored variations in temperature observed over incubation period. Values without ranges were constant for duration of incubation.

[2]Water was mixed for CMX at Station 1 due to water budget limitations.

[3]MMHg concentrations calculated from ambient 200Hg in t0 incubation bottles after subtraction of contribution from added MMHg spike.

[4]Because station 9 displayed an unusual O_2 depth profile, an additional low O_2 depth was selected for non-amended incubations.

*Note that values of AOU cannot be accurately determined in the upper water column due to the influence of gas exchange and mixing. Values for AOU in waters above 100 m are therefore not shown.

Table 2: Amendments tested for enhancement of mercury methylation. McLane punches were collected from matching stations as those used for incubation water collection and contain particles > 51 μm including organic matter, cells, and inorganic material.

Treatment	Final concentration
McLane punches	½ of 2-cm punch
Inorganic Co	500 pM
C (as succinate)	1 mM
Cysteine	10 nM
Glutathione	10 nM
Methylcobalamin	100 pM
CoC	500 pM, 1 mM
CoCys	500 pM, 10 nM
CysC	10 nM, 1 mM

Table 3: Potential methylation rates from Tropical Pacific waters. Total potential methylation rates (M) calculated from t-1 to t24hr corrected for ^{202}Hg(II) from diethylHg peak. Potential methylation rate constants (k_m) for production of methylated Hg ([DMHg] + [MMHg]) relative to isotopically enriched Hg(II) substrate in 0.2 μm filtered and unfiltered seawater from the Pacific Ocean. The errors given represent one standard deviation of triplicate bottle incubations.

Station	Depth	M-0.2 μm filt ($x10^{-2}$ d^{-1})	M-unfilt ($x10^{-2}$ d^{-1})
17°N	CMX	0.39 ± 0.11	0.43 ± 0.02
	OMZ	0.95 ± 0.08	0.64 ± 0.05
8°N	CMX	10.19 ± 0.98	5.71 ± 0.36
	OMZ	7.40 ± 0.31	3.77 ± 1.54
0°	CMX	2.19 ± 0.20	1.74 ± 0.37
	OMZ	1.00 ± 0.19	1.74 ± 0.47
12°S	CMX	0.69 ± 0.28	0.72 ± 0.02
	OMZ[2]	0.20 ± 0.04	0.49 ± 0.08
	OMZ	2.28 ± 0.70	1.12 ± 0.21

[2]Because station 12°S displayed an unusual O_2 depth profile, an additional low O_2 depth was selected for non-amended incubations.

Chapter 6
Conclusions

Despite longstanding debate over the importance of monomethylmercury (MMHg) production in the marine water column relative to transport from coastal sediments, few direct measurements have been performed to quantify these processes in open ocean locations. Measurements of potential methylation and demethylation rates provide quantitative constraints on the magnitude of in situ MMHg production. However, we present only the third report of these measurements in marine systems. In addition, we are the first to incorporate experiments that probe potential mechanisms for environmental conditions that lead to MMHg production in open ocean waters.

Our experimental design incorporated pre-equilibration of concentrated spikes of isotopically enriched Hg and MMHg. Previous measurements have relied on additions of MMHg and, especially, Hg well in excess of ambient concentrations [Lehnherr et al, 2011] that are added bound to chloride ligands [Lehnherr et al, 2011; Monperrus et al, 2007]. Because isotope tracer experiments require additions of exogenous Hg, we aimed to add low concentrations of spikes that more closely mimic the Hg species that a parcel of ocean water would encounter in situ. Even low concentrations of pre-equilibrated spike underwent methylation and demethylation within minutes of introduction, suggesting that methylation in marine waters is widespread and dynamic, regardless of the ambient concentrations of methylated Hg species.

We measured potential methylation rates from Hg(II) in waters across large gradients of oxygen utilization, primary productivity, and ambient Hg(II) and MMHg concentrations. Notably, in oligotrophic waters in both the South Pacific and the Sargasso Sea, we observed significant methylation potential in filtered waters. In addition, the only methylation attributed to cellular processes was observed in oxygen minimum waters of the Sargasso Sea. These findings are inconsistent with known mechanisms of MMHg production in anoxic sediments, which occurs primarily by cellular processes in anaerobic bacteria [Gilmour et al, 2013]. We also did not see significant abiotic methylation after addition of methylcobalamin, despite its ability to methylate Hg in buffered pH 5 solutions [Jiminez-Martinez, 2013]. Combined, these results suggest that Hg methylation in marine waters is controlled by factors specific to these environments.
Time course experiments in both oligotrophic regions suggest that rapidly produced MMHg is short lived, especially in the presence of particulate matter. This is contrary to observed bioaccumulation factors in marine particulate matter, $> 10^4$ [Hammerschmidt et al, 2013], relative

to dissolved Hg concentrations. How particles can both promote demethylation and serve as the first step of Hg bioaccumulation, the step that results in the highest bioaccumulation factor, is an important question that should be addressed in future open ocean studies of Hg speciation.

Both our Hg speciation data in the Tropical Pacific as well as our methylation rate measurements suggest that a simple model of marine Hg methylation is not comprehensive enough to account for differences among ocean basins. Although methylation is likely ultimately limited by Hg(II) substrate, the strong relationship between methylated Hg concentrations and organic carbon remineralization rates observed in the North Pacific [Sunderland et al, 2009] does not extend into the Equatorial Pacific (Figure 1). Instead, factors that influence the availability of Hg(II) to methylation appear to limit DMHg and MMHg production even in low oxygen waters. We have identified denitrification as a likely control on THg availability for methylation (Figure 2). Although some sulfate-reducing bacteria appear to methylate Hg(0) directly in culture studies [Hu et al, 2013], this does not appear to occur in the low oxygen regions of the marine water column as a region of strong denitrification observed in the Tropical Pacific suggested that reduction inhibited MMHg and DMHg production [Munson—this work, Chapter 4]. In addition, the reduction induced by methylcobalamin additions to filtered and unfiltered seawater prohibited methylation [Munson—this work, Chapter 5], making Hg(0) an unlikely substrate for marine Hg methylation.

In our amended methylation rate measurement experiments, we aimed to test whether individual compounds limit Hg methylation, especially in high productivity waters where cells compete for limited dissolved nutrients. Compound addition appeared to induce methylation in both filtered and unfiltered water, which might implicate methyl transfer to Hg(II) facilitated by ligand binding, or another unidentified process. Whatever the mechanism of this rapid methylation, it appears to be distinct from cellular methylation, as indicated by the steady production of MeHg over 24-hour incubations in unfiltered low oxygen waters from the Sargasso Sea [Munson—this work, Chapter 3].

The relative importance of rapid methylation, which occurs in the absence of cells in our filtered water incubations, and cellular methylation, that was measured only in the Sargasso Sea, for bioaccumulation is beyond the scope of our current study. However, future work should address to what extent these seemingly distinct processes impact MMHg uptake and transfer in marine biota.

Despite the low concentrations of Hg species measured in Tropical Pacific waters, we observed active methylation in these waters. If the resulting MMHg is incorporated into biomass, increases in Hg emissions since the Industrial Revolution will ultimately be transferred from marine waters to marine food webs and pose increasing threats to human health.

References

Gilmour, C. C., M. Podar, A. L. Bullock, A. M. Graham, S. D. Brown, A. C. Somenahally, A. Johs, R. A. Hurt Jr., K. L. Bailey, and D. A. Elias (2013) Mercury methylation by novel microorganisms from new environments, Environ. Sci. Technol., 47, 11810-11820.

Hammerschmidt, C. R., M. B. Finiguerra, R. L. Weller, and W. F. Fitzgerald (2013) Methylmercury accumulation in plankton on the continental margin of the Northwest Atlantic Ocean, Environ. Sci. Technol., 47, 3671-3677.

Hu, H., H. Lin, W. Zheng, S. J. Tomanicek, A. Johs, X. Feng, D. A. Elias, L. Liang, and B. Gu (2013) Oxidation and methylation of dissolved elemental mercury by anaerobic bacteria. Nat. Geosci., 6, 751-754.

Jiménez-Moreno, J., V. Perot, V. N. Epov, M. Monperrus, and D. Amouroux (2013) Chemical kinetic isotope fractionation of mercury during abiotic methylation of Hg(II) by methylcobalamin in aqueous chloride media, Chem. Geol., 336, 26-36.

Lehnherr, I., V. L. St. Louis, H. Hintelmann, and J. Kirk (2011) Methylation of inorganic mercury in polar waters. Nat. Geosci., 4, 298-302.

Monperrus, M., E. Tessier, D. Amouroux, A. Leynaert, P. Huonnic, and O. F. X. Donard (2007) Mercury methylation, demethylation and reduction rates in coastal and marine surface waters of the Mediterranean Sea. Mar. Chem. 107, 49-63.

Sunderland, E. M., D. P. Krabbenhoft, J. W. Moreau, S. A. Strode, and W. M. Landing (2009) Mercury sources, distribution, and bioavailability in the North Pacific Ocean: Insights from data and models. Global Biogeochem. Cy. 23:GB2010.

Figure 1: Methylated mercury concentrations in marine intermediate waters (100-1000 m) versus organic carbon remineralization rates. The correlation between metylated Hg and OCRR, first observed in North Pacific Intermediate Waters by Sunderland et al, 2009 (blue) does not appear to exist in all ocean basins. Concentrations of methylated Hg measured at two off-shore stations of in the North Atlantic (red, Bowman et al, 2013) appear to increase with ORCC, coastal stations have low methylated Hg concentrations across the full OCRR range. Methylated Hg concentrations and OCRR are low in Indian waters (purple, Sunderland et al, 2011). Intermediate concentrations of methylated Hg measured in waters from the Tropical Pacific (white, Metzyme, Munson—this work, chapter 3) are found at intermediate OCRR values.

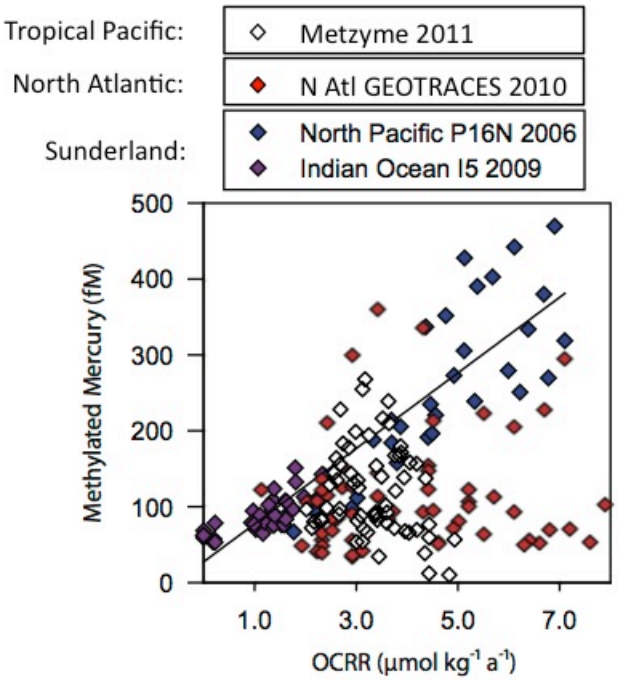

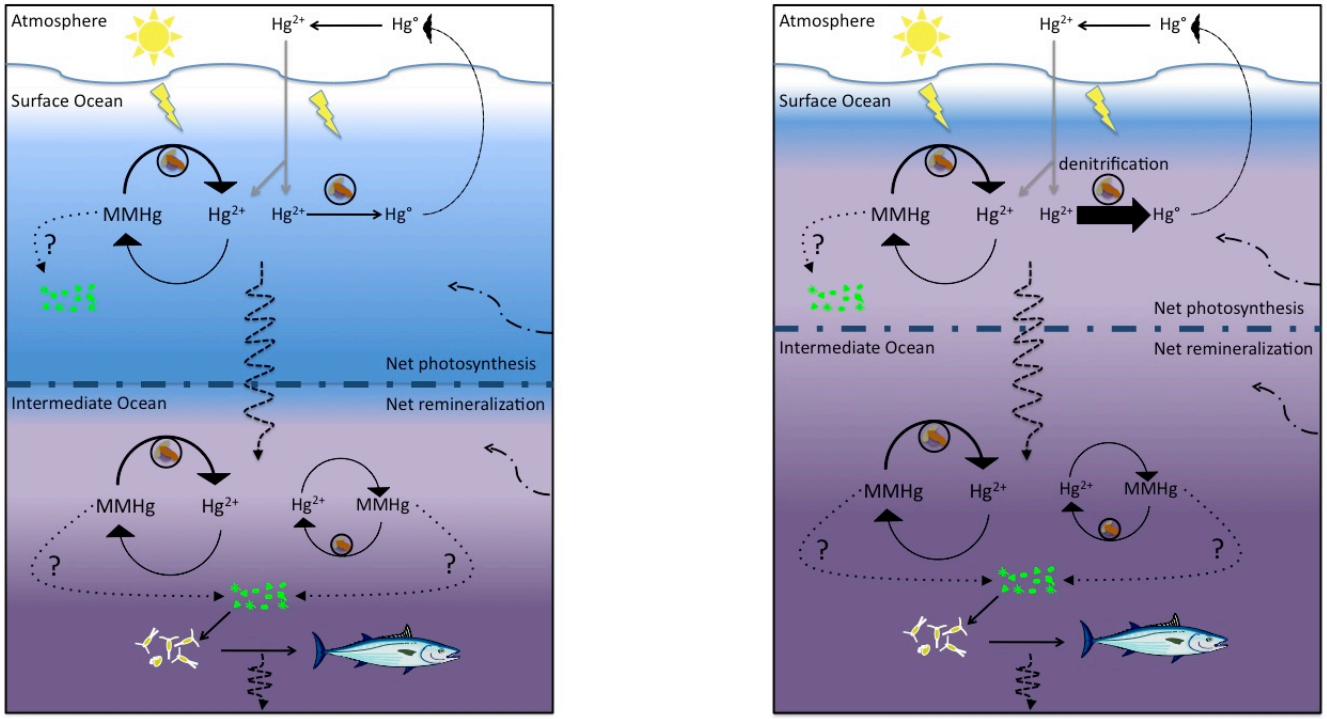

Figure 2: Schematic representation of marine mercury transformations in surface and intermediate waters: Hg(II) deposited to the oxygenated surface ocean from the atmosphere (left) is subject to photoreducton, microbial reduction, and rapid methylation/demethylation. Additional Hg(II) is delivered by entrainment and upwelling (dashed-dotted lines). The presence of particles enhances demethylation of MMHg. Sinking fluxes of Hg(II) (dashed lines) deliver Hg(II) to intermediate waters, but do not appear to increase the capacity for methylation, as indicated by the relative size of the loop. However, in some marine low oxygen waters, microbial methylation enhances total methylation. The relative importance of rapid methylation/demethylation versus microbial methylation to bioaccumulating Hg in marine biota is unknown. When oxygen is sufficiently low to allow for denitrification (right), Hg(II), either directly or after DMHg or MMHg demethylation, is reduced to Hg°, thereby removing methylation capacity in the surface ocean.

Appendix I
Methylation and Demethylation Rate Measurements

Adapted from: Hintelmann and Evans, 1997 and Hintelmann and Ogrinc, 2003.

The 7 stable isotopes of Hg allow for simultaneous detection of multiple tracers of Hg species transformations. In the experiments described in Chapters 4 and 5, we used isotopically enriched Hg species to trace methylation and demethylation in water samples. By adding Hg(II) and MMHg, each enriched in different isotopes, we were able to simultaneously track methylation and demethylation within the same bottle over the incubation period.

Using $^{202}Hg(II)$, we measured the following methylation reaction:

$$^{202}Hg^{2+} + CH_3^{2-} \rightarrow CH_3\,^{202}Hg^{+}$$

Using $CH_3{}^{198}Hg^{+}$, we measured the following demethylation reaction:

$$CH_3\,^{198}Hg^{+} \rightarrow {}^{198}Hg^{2+} + CH_3^{2-}$$

These two reactions were monitored by quantifying the isotopic composition of the CH_3Hg^{+} peak using a linked CVAFS-ICPMS protocol modeled after descriptions by Hintelmann and Evans (1997) and the USGS Wisconsin District Mercury Laboratory, Madison, Wisconsin [as used by DeWild et al, 2002].

Analytical Setup:

The hardware of the linked system is easily set up. The outlet of the 2700 Tekran Automated Methylmercury Analyzer can be attached to a y-junction or the side arm of a t-junction to join the ICPMS sample gas flow, typically ~1 L/min. The two Thermo Element 2 instruments in the WHOI Plasma Facility were used in these experiments. The Tekran 2700 was transported and set up on a trolley. The Tekran instrument was controlled by the Lamborg Lab MMHg computer and run off of a separate Ar gas cylinder. Troubleshooting the linked set-up typically requires careful attention to the backpressure from the ICPMS system, which may result due to the flow differential between the CVAFS and ICPMS systems.

When connected to the CO_3^{2-} Thermo Element 2, the ICPMS data collection could be triggered by an electrical signal from the Tekran 2700 prior to heating of the Tenax trap. A command was added to the ETF of the Tekran 2700. In the Sequence Editor of the ICPMS software, the external signal was added to the sample template and the sequence was set to continue automatically.

In order to tune the instrument, a glass U was inserted between the tubing from the Tekran 2700 cell outlet and the y-junction into the ICPMS sample gas flow. The glass U contained a drop of Hg contained in a small capped plastic cylinder. The volatile Hg(0) carried through the U by the Tekran 2700 provided sufficient signal for instrument tuning. Because of the high Hg signal of the standard relative to sample concentrations, the ICPMS signal was allowed to re-establish a baseline for >30 minutes prior to analyzing standards or samples.

Although not used for these experiments, the tubing (type?) between the CVAFS and the ICPMS can be heated by means of a heated strip to avoid loss of Hg signal to the walls of the tubing.

Sample and standard CH_3Hg^+ derivitization was performed in the Watson Building clean room and bottles were transported to the ICPMS lab for analysis. Between 8-10 samples were prepared at a time.

Data Analysis:

During analysis, the Thermo ICPMS software yields a chromatogram of individual Hg isotopes. The method was written to maximize the number of data points collected within a period of time that corresponded to the chromatogram produced by the Tekran 2700. A .txt file of the counts per second (cps) of each of the 4-7 Hg isotopes measured at each time point was produced for each sample. The software allows users to manually integrate specific peak windows. However, for ease of data analysis in the presented analyses, MATLAB files (written by C. H. Lamborg) were used to extract peak integrations from .txt files of the chromatographs of the peak intensity produced by the ICPMS. These MATLAB files consisted of:

chromcrunch.m

chromint.m

These operations yielded integrations of the separated Hg species Hg(0), methylethylHg, and diethylHg that correspond to 4-7 isotopes of Hg(0), CH_3Hg^+, and Hg^{2+}. Four isotopes (198, 199, 200, and 202) were monitored for most measurements (Chapter 4, excluding +B12 treatments), while all 7 Hg isotopes were monitored for later measurements (Chapter 5).

The output of the Matlab files were .txt files containing sample peak integrations that were adapted into .xlsx spreadsheets for calculations. Peak areas for each isotope were corrected for reagent contributions from daily reagent blanks. For methylation rate measurements, the blank corrected Hg isotope abundances from the separated CH_3Hg^+ peak were used to measure changes in MMHg from demethylation and methylation. The integrated ^{202}Hg in the Hg^{2+} peak was monitored to determine changes in Hg^{2+} substrate availability over the course of the incubation (see below).

Once peak integrations were determined, we input the following mathematical calculations into the integrations spreadsheets to yield transformation rates:

According to Hintelmann and Evans, 1997, the total concentration of a specified isotope is the sum of that isotope in ambient solutions plus concentrations of that isotope in tracer solutions.

$$\Sigma^1 I = {}^1a + {}^1b \ldots + {}^1n$$

$$\Sigma^2 I = {}^2a + {}^2b \ldots + {}^2n$$

$$\Sigma^i I = {}^ia + {}^ib \ldots + {}^in$$

where a-n denote different solutions and 1-i represent different isotopes. Thus for our experiments, the sum of all contributions of $^{202}CH_3Hg^+$ to our bulk measurement:

$$\Sigma^{202}I = {}^{202}sw + {}^{202}meth + {}^{292}inorg$$

where

$^{202}\Sigma I$ is the sum of ^{202}Hg

sw is the ambient seawater in each incubation bottle to which isotope solutions are added

meth is the solution of enriched $CH_3{}^{198}Hg^+$ from which the $CH_3{}^{198}Hg^+$ spike is added

inorg is the solution of enriched $^{202}Hg^{2+}$ from which the $^{202}Hg^{2+}$ spike is added

This allows for full consideration of any contribution of rare isotopes in enriched solutions (such as the small % of $^{202}CH_3Hg^+$ in the enriched $^{198}CH_3Hg^+$ solution).

The relative contribution of each isotope is expressed as relative abundance in each source (sw, meth, inorg) to the most abundant isotope:

$^{200}sw/^{200}sw = R_{11} = 1$ $\quad$ $^{200}meth/^{198}meth = R_{21}$ $\quad$ $^{200}inorg/^{202}inorg = R_{13}$

$^{198}sw/^{200}sw = R_{21}$ $\quad$ $^{198}meth/^{198}meth = R_{22} = 1$ $\quad$ $^{198}inorg/^{202}inorg = R_{23}$

$^{202}sw/^{200}sw = R_{31}$ $\quad$ $^{202}meth/^{198}meth = R_{32}$ $\quad$ $^{202}inorg/^{202}inorg = R_{33} = 1$

As a result, equation X can be rewritten after substitution with the ratio notation:

$$\Sigma^1 I = {}^1a + R_{12}{}^2b + R_{1i}{}^in$$

Or for our example in equation X:

$$\Sigma^{202}I = R_{31}{}^{200}sw + R_{32}{}^{198}meth + {}^{292}inorg$$

As a result, by knowing the well-defined Hg isotope ratios of ambient seawater solution (sw: assumed natural abundance of Hg isotopes) and of the CH_3Hg^+ spike solution (meth; defined by the enriched isotopes in the starting enriched HgO species and altered by any changes due to pre-equilibration), we can calculate the $^{202}CH_3Hg^+$ produced from the Hg(II) spike solution (inorg) by measuring the total ^{202}Hg ($\Sigma^{202}I$) present in the separated CH_3Hg^+ peak determined by CVAFS-ICPMS.

Hintelmann and Evans (1997) and Hintelmann and Ogrinc (2003) use certified values of enriched HgO to determine the isotope ratios of spike solutions. In our experiments, both spike solutions, $^{198}CH_3Hg^+$ (meth) and ^{202}Hg(II) (inorg) were incubated in filtered seawater for 24-hours prior to addition to experimental bottle incubations in order to complex the Hg species to naturally occurring ligands in the seawater matrix. As a result, the isotope ratios of HgO certified by the manufacturer could not be used in our calculations. Instead, values for spike ratios were measured directly from the equilibrated spike solutions during sample analysis and used for calculations. IUPAC values were used for natural abundance ratios assumed for ambient seawater.

The matrix inversion approach [Hintelmann and Ogrinc, 2007] presents the contributions of isotope tracers using the following representation of the equations outlined above [Hintelmann and Evans, 1997]:

$$AX=B$$

With

$$A=\begin{bmatrix}1 & R_{12} & R_{13}\\ R_{21} & 1 & R_{23}\\ R_{31} & R_{32} & 1\end{bmatrix} \qquad X=\begin{bmatrix}1_{sw}\\ 2_{meth}\\ 3_{inorg}\end{bmatrix} \qquad B=\begin{bmatrix}\Sigma^{1}I\\ \Sigma^{2}I\\ \Sigma^{3}I\end{bmatrix}$$

Where the unknown contributions of the isotopes from various sources (sw, meth, inorg) that contribute to the total isotopic signal, I, of each isotope observed in the CH_3Hg^+ peak (ex: $\Sigma^{198}I$) can be solved for in the vector X using the inverse of A, as represented by the following:

$$X = A^{-1}B$$

The matrix calculation was entered into the spreadsheet to calculate resulting contributions of ^{200}Hg, ^{198}Hg, and ^{202}Hg from the solutions sw, meth, and inorg into the bulk CH_3Hg^+ pool.

Within the spreadsheet, the raw cps intensity values for ^{200}Hg, ^{198}Hg, ^{202}Hg from the CH_3Hg^+ peaks (and ^{199}Hg when used as a isotope dilution standard) were first corrected for contributions from reagent blanks measured daily. Blank corrected signals were then input as the vector B in equation X. After solving, the results of vector X were converted to concentrations of CH_3Hg^+ from standard curves of CH_3Hg^+ analyzed daily. These values represent the $CH_3{}^{202}Hg^+$ formed from methylation and the $CH_3{}^{198}Hg^+$ remaining after demethyaltion for each time point.

Potential methylation and demethylation rate constants were calculated using a variety of models of $^{202}Hg(II)$ substrate availability.

Initially, 202Hg(II) substrate availability was assumed to be constant over the course of the incubation, as was done by Monerrus et al, 2007. As a result, values for produced $MM^{202}Hg$ were calculated and shown in units of (% d-1) referring to the percent of total 202Hg(II) spike added that was methylated over the course of the 24-hour incubation.

However, Lehnherrr et al, 2011 dispute the assumption that Hg(II) substrate concentrations are constant, despite the fact that he used significantly higher initial concentrations of Hg(II) substrate relative to ambient conditions. They therefore performed some experiments to determine how Hg(II) substrate availability changed over the course of their incubations. They found a decrease in Hg(II) added to filtered seawater over time in a series of separate experiments from their rate measurements. The values they present and use to calculate their potential rates correspond to their isotopically enriched MMHg relative to available enriched Hg(II). In order to calculate km values, they fit the Hg(II) substrate decay to a best fit line and also account for the "instantaneous" methylation observed in their t0 bottles. However, they do not indicate whether the source of the filtered water for their Hg(II) substrate availability determination was any of the stations where they measured potental rates nor do they indicate when these additional experiments were performed.

Because we have the simultaneous ability to measure MMHg and Hg(II) as methylethylHg and diethylHg, we wanted to improve on the calculations of Lehnherr et al, 2011 by calculating $MM^{202}Hg$ as a percentage of the $^{202}Hg(II)$ substrate. First, I attempted to do this by dividing the matrix transformed $MM^{202}Hg$ signal by the bulk $^{202}Hg(II)$ signal in the diethylHg peak for each bottle. However, the bulk $^{202}Hg(II)$ value includes any ambient $^{202}Hg(II)$ in those waters. Therefore, I took the integrations of the diethylHg peaks and used the same setup for the linear matrix calculations outlined above for MMHg and calculated the $MM^{202}Hg$ as a percent of the $^{202}Hg(II)$ spike substrate. For most stations, 18N, 0, 12S, and BATS site, this resulted ~25% increases in values of $MM^{202}Hg/Hg(II)$ substrate (%) but did little to change the trends observed when the calculation included all $^{202}Hg(II)$ including ambient. However, for the 8N station, where the highest concentrations of ambient Hg(II) were measured, the values for km went from being below detection to being the highest measured along the entire cruise track. This makes sense. With more Hg(II) available, the denominator of $MM^{202}Hg/Hg(II)$ substrate (%) when it included all available $^{202}Hg(II)$ was quite large, and overwhelmed any signal specific to the added isotope spikes. After using the linear matrix transformation to differentiate between the $^{202}Hg(II)$ contributed by the spike and that from ambient Hg(II) in seawater, the value of MM202Hg/Hg(II) substrate (%) decreased correspondingly.

In all cases, the calculation of k_d, the potential demethylation rate constant, was much simpler. For this calculation, we used a similar assumption as that made by Lehnherr et al, 2011 and approximate demethylation as a first-order reaction.

References

DeWild, J., M. Olson, and S. Olund (2002) Determination of methylmercury by aqueous phase ethylation, followed by gas chromatographic separation with cold vapor atomic fluorescence detection, U. S. Geol. Surv. Open File Rep. 01-445, 19 pp.

Hintelmann, H., and R. D. Evans (1997) Application of stable isotopes in environmental tracer studies—measurement of monomethylmercury (CH3Hg+) by isotope dilution ICP-MS and detection of species transformation. Fresnius J. Anal. Chem., 358, 378-385.

Hintelmann and Orgrinc (2003) Determination of stable mercury isotopes by ICP/MS and their application in environmental studies. In Biogeochemistry of Environmentally Important Trace Elements (eds Cai, Y. and C. O. Braids) Ch 21 (ACS, 2003).

Lehnherr, I., V. L. St. Louis, H. Hintelmann, and J. Kirk (2011) Methylation of inorganic mercury in polar waters. Nat. Geosci., 4, 298-302.

Monperrus, M., E. Tessier, D. Amouroux, A. Leynaert, P. Huonnic, and O. F. X. Donard (2007) Mercury methylation, demethylation and reduction rates in coastal and marine surface waters of the Mediterranean Sea. Mar. Chem. 107, 49-63.

chromcrunch.m

```
%function chromcrunch
%this version meant for use with an ICP method that looks for Hg-
198, -199,
%-200 and -202.
% chl july 2012
%launch user interface to get the file names for data to process.
%downloaded from matlab exchange 12/2011
filelist=uigetfile_n_dir;

% get ready to write file later
filename = 'icpresults.txt';
fid = fopen(filename, 'w');


%loop to process each of the selected files
for w=1:length(filelist)

%import the data from an icp txt file. creates a structure with
the first 5
%header lines stored in field "textdata" and the counts for each
isotope in
%the field "data".
%filename
    A=importdata(filelist{w},'\t',5);

%start writing the output file line-by-line
%first with the filename and isotope...does it 4 times for each
of the 4
%isotopes.
%then, extracts the isotopes from the "data" field and prints
them to the
%file, isotope by isotope in the transposed direction (from left
to right,
%instead of top to bottom.
    for i=1:4
        fprintf(fid, '%s', filelist{w});
        if i==1
            fprintf(fid, '\t%d', 198);
        elseif i==2
            fprintf(fid, '\t%d', 199);
        elseif i==3
            fprintf(fid, '\t%d', 200);
        else
            fprintf(fid, '\t%d', 202);
        end

        x=i+1;
        fprintf(fid, '\t%d', A.data(:,x)');
```

```
        fprintf(fid, '\n');
    end

end

%when done, closes the file.
fclose(fid);
```

chromint.m

```
%chromint
%chl july 2012

clear all;

%set the start and endpoints for integration here
srtpts=[28 47 62];
endpts=[45 61 90];

%determine peak widths
wdth=endpts-srtpts+1;

%import the combined results file
filename=uigetfile('*.txt');
A=importdata(filename);

% get ready to write file later
filename = 'icpintegrations.txt';
fid = fopen(filename, 'w');


fprintf(fid, 'Sample \t Isotope \t Hg(0) Area \t MMHg Area \t
Hg(II) Area \t\n');

%smooth the data before integration
Asmooth=[];
windowSize=5;
for j=1:length(A.textdata)

Asmooth(j,:)=filter(ones(1,windowSize)/windowSize,1,A.data(j,2:en
d));
end


for i=1:length(A.textdata)
    fprintf(fid, '%s', A.textdata{i});
    fprintf(fid, '\t%d', A.data(i,1));

    hgoarea=sum(Asmooth(i,srtpts(1):endpts(1)))-
mean([Asmooth(i,srtpts(1)) Asmooth(i,endpts(1))])*wdth(1);
    mmhgarea=sum(Asmooth(i,srtpts(2):endpts(2)))-
mean([Asmooth(i,srtpts(2)) Asmooth(i,endpts(2))])*wdth(2);
    hg2area=sum(Asmooth(i,srtpts(3):endpts(3)))-
mean([Asmooth(i,srtpts(3)) Asmooth(i,endpts(3))])*wdth(3);

    fprintf(fid, '\t%d', hgoarea);
    fprintf(fid, '\t%d', mmhgarea);
    fprintf(fid, '\t%d', hg2area);
```

```
    fprintf(fid, '\n');
end
```